IMPAIRED CARDIAC CAMP-SPECIFIC PDE4, β_1-AR, AND NE IN AN ISCHEMIA-REPERFUSION RAT MODEL

By

Jonas Vaskas

Submitted July 22, 2014, Ottawa, Ontario.

This thesis is submitted as a partial fulfillment of the M.Sc. program
in the Graduate Department of Cellular and Molecular Medicine
University of Ottawa

Abstract

Ischemic injury in the heart is followed by an increase in SNS activity and the higher this activity, the poorer patient outcomes. An index of SNS activity in models of ischemia can be achieved by measuring NE, β-AR, and perhaps indirectly PDE4 to give an intracellular aspect on SNS signaling. A 20 minute ischemia-reperfusion was induced in a rat model with physiological measurements at 2-5 weeks post IR. At 3 weeks post IR, rats displayed increased PDE4 expression, decreased β_1-AR expression, increased plasma NE, decreased tissue NE storage, increased Doppler E/A ratio and unchanged LV ejection fraction. PET analysis with FDG revealed no infarct at 2 weeks, while analysis with $[^{13}N]NH_3$ displayed no resting flow defect but revealed trends in flow reserve impairment as early as 2.5 weeks with recovery at 5 weeks post-surgery. Applications of this model could be non-invasive imaging of PDE4 with (*R*)-$[^{11}C]$Rolipram PET at early time points for development towards prognostic and therapy guidance in humans.

Table of Contents

CHAPTER 2

Methods

CHAPTER 3

Results

List of Figures and Tables

List of Abbreviations

^{11}C	Carbon-11
^{18}F	Fluorine-18
^{3}H	Hydrogen-3
^{125}I	Iodine-125
^{13}N	Nitrogen-13
^{15}O	Oxygen-15
^{82}R	Rubidium-82
AMP	Adenosine monophosphate
ANP	Atrial natriuretic peptide
ATP	Adenosine triphosphate
AUC	Area under curve
β-AR	Beta adrenergic receptor
BCA	Bicinchoninic acid
BSA	Bovine serum albumin
CaMK2	Ca2+/calmodulin-dependent protein kinase
cAMP	Cyclic adenosine monophosphate
cGMP	Cyclic guanosine monophosphate
cMyBP-C	Cardiac myosin binding protein C
CP	Creatine phosphate
CRE	cAMP responsive element
CREB	cAMP responsive element binding protein
CVD	Cardiovascular disease
DA	Dopamine
DD	Diastolic dysfunction
DHF	Diastolic heart failure
DOPA	Dihydroxyphenylalanine
DV	Distribution volume

ECD	Electrochemical detector
EDTA	Ethylenediaminetetraacetic acid
EF	Ejection fraction
EKV	ECG-based kilohertz visualization
ePAC	Exchange proteins activated by cAMP
eNOS	Endothelin nitric oxide synthase
ERK	Extracellular signal regulated kinase
FAK	Focal adhesion kinase
FDG	2-Deoxy-2-[^{18}F]Fluoroglucose
FS	Fractional shortening
FSH	Follicle stimulating hormone
GAPDH	Glyceraldehyde-3-phosphate dehydrogenase
GLUT1	Glucose transporter 1
GLUT4	Glucose transporter 4
GPCR	G protein coupled receptor
GRK	G protein coupled receptor kinase
HED	^{11}C-hydroxyephedrine
HF	Heart failure
HPLC	High performance liquid chromatography
IR	Ischemia-reperfusion
K_m	Michalis-Menten Constant
LA	Left atrium
LAD	Left anterior descending [coronary artery]
LH	Luteinizing hormone
LV	Left ventricle
mAKAP	Muscle a kinase anchoring protein
MAP	Mitogen-activated protein
MDM2	Murine double minute
MI	Myocardial infarction
MPTP	Mitochondrial permeability transition pore

NE	Norepinephrine
NET	Norepinephrine transporter
NO	Nitric oxide
NYHA	New York Heart Association
PA	Phosphatidic acid
PDE	Phosphodiesterase
PET	Positron emission tomography
PKA	Protein kinase A
PNS	Parasympathetic nervous system
PVDF	Polyvinylidene fluoride
RAAS	Renin-angiotensin-aldosterone system
RACK1	Receptor for activated C kinase 1
RyR2	Ryanodine receptor 2
SD	Standard deviation
SDS	Sodium dodecyl sulfate
SDS-PAGE	Sodium dodecyl sulfate polyacrylamide gel electrophoresis
SERCA2a	Sarcoplasmic/endoplasmic reticulum Ca^{2+} ATPase 2a
SNS	Sympathetic nervous system
SR	Sarcoplasmic reticulum
SV	Stroke volume
TBST	Tris buffered saline with Tween 20©
TSH	Thyroid stimulating hormone
UCR	Upstream conserved region
UV	Ultraviolet
V_{max}	Maximal velocity

Acknowledgements

First and foremost my gratitude is directed towards my supervisor Dr. Jean DaSilva. It seems like such a long, long time ago when I approached you meekly if you had a master's project in mind. That moment began a journey of learning, success, and discovery of great value to me. To my committee, Dr. Beanlands and Dr. Suuronen, you both provided me with everything I needed in the necessary and farsighted committee, a diverse and intelligent conversation about all the facets of my project, both in and out of official meetings.

So many friends of the heart institute, Marika Kolajova, Kasia Drozd,Rick Seymour, Christine Archer, Julia Petryk, Stephanie Thorn, James Haley, Hélène Redfern, Ehsen Tayyabi, Taybeh Hadizad and all radiochem staff, Aleks Ostojic, Dan de Vette and all ACVS staff, I greatly enjoyed our relationships, long hours together, and the enormous help you provided me with my project. Everyone, my friends and family, contributed to my success in graduate research.

Contributions to Thesis Results

This thesis would not be possible without the selfless hard work of many collaborators. No experiment in this work was conducted without the training, guidance, and/or verification by others. Initial surgery was conducted by Dr. Stephanie Thorn and the majority of animal surgery was completed by Rick Seymour. I was present for each and every surgery making detailed notes and preparing animals for surgery with anaesthesia, fluid injection and post-surgery recovery. All radiotracers were produced in the University of Ottawa Heart Institute Radiochemistry Lab, picked up by myself and administered to rats for µPET studies by Marika Kolajova, Julia Petryk, Dr. Etienne Croteau or Dr. Stephanie Thorn. During µPET scanning I was present to deliver the tracer, make detailed notes, record vital signs, start and stop the camera. PET image reconstruction was done by Dr. Etienne Croteau and all PET image analysis was conducted by myself with the supervision of Dr. Rob de Kemp and technical support from Dr. Ran Klein and Jennifer Renaud.

Echocardiography and Doppler was performed by Marika Kolajova but all data was analyzed by myself with the verification of Dr. Basma Ismail and James Haley. Animal euthanasia, tissue collection, tissue lysis, protein content measurement and Western blot were performed by myself with training from Marika Kolajova. All Western blots were verified from tissue homogenate to protein band analysis by Marika Kolajova. Despite many efforts, I was unable to obtain reproducible results with the PDE4 activity enzyme assay and results

presented were obtained by Marika Kolajova using tissues that I had collected and homogenated. Plasma collection was done by myself with the instruction of Rick Seymour, while plasma NE ELISA was conducted by myself. Cardiac NE was done in equal collaboration with my 4th year honours student Ehsen Tayyabi. Approximately half of the samples were done by Ehsen, but all were eventually rerun by myself with the same results. All statistical analyses were conducted by myself.

CHAPTER 1

Introduction

1.1 Heart Disease

1.1.1 Heart Failure

Heart failure (HF) is the development of cardiac structural abnormalities that prevent the adequate delivery of oxygen to the body's metabolizing tissues (Dickstein et al. 2008). The etiology of HF is complex, involving diet, genetics, and lifestyle (Yusuf et al. 2001) and will be only briefly described here (for an extensive review, see Blair et al. (2013) and McMurray et al. (2012)). Clinically HF is defined by symptoms of dyspnea (breathlessness), edema in extremities, and fatigue. Signs of HF include increased jugular venous pressure, abnormal cardiac apex beat and pulmonary crackles, and in 50% of cases, a depressed left ventricle (LV) ejection fraction (EF). Approximately two thirds of all HF cases are caused by coronary artery disease however hypertension, diabetes, viral infection, alcohol abuse, chemotherapy and idiopathic (probable genetic basis) are also contributing factors (McMurray et al. 2012; Ackerman et al. 2011). In patients with systolic dysfunction from myocardial infarction (MI), maladaptive remodeling occurs. The surviving myocardium and surrounding extracellular matrix eventually lead to a dilated LV and reduced contractility (McMurray 2010, Shah et al. 2011). If untreated, systolic dysfunction progressively worsens because of additional myocyte death by repeated MI as well as increasingly harmful compensatory mechanisms by neurohormonal activation. The two neurohormonal systems at play are the renin-angiotensin-aldosterone system (RAAS) and the sympathetic nervous system (SNS). Together these systems may cause additional myocyte death while attempting to correct depressed LV output.

The blockade of these systems is the basis of HF treatment (McMurray 2010; Shah et al. 2011).

The compensatory mechanisms mentioned above combat low pump function but produce hemodynamic overload in the heart. Changes in cell size and protein expression eventually become maladaptive and the heart becomes unable to sustain sufficient cardiac output (Kuwahara et al. 2012; Barry et al. 2008; Thum et al. 2007). The LV may experience systolic dysfunction, diastolic dysfunction, or both in the progression from compensating to decompensating HF. Systolic dysfunction involves an EF of less than 40% in humans (Levy & Linker 2008) and increased end-diastolic LV volume (Hess 1993). The etiology of systolic dysfunction, which is prevalent in HF, stems from coronary artery disease, hypertensive cardiovascular disease, and less frequently, from dilated cardiomyopathy and myocarditis (Dougherty et al. 1984; Cohn et al. 1990). These pathologies incur loss of cardiac muscle cells and replacement with interstitial fibrosis (Federmann & Hess 1994). Reduced pump function is compensated by the Frank-Starling phenomenon and increased SNS activity (Packer 1992). Primary compensation is increased diastolic filling causing increased stroke volume, producing an enlarged LV with higher end-diastolic pressure. Primary compensation also includes enhanced SNS activity, increasing stroke volume, chronotropy and ionotropy. These primary compensatory mechanisms produce high wall stress and greater oxygen demands on the heart and thus primary compensation side-effects must be compensated with secondary compensations: development of hypertrophy, inhibition of SNS by baroreceptor reflex, and

release of atrial natriuretic peptide (ANP; diuretic and vasodilator). As systolic dysfunction progresses, both primary and secondary compensatory strategies become maladaptive as Beta-adrenoceptor (β-AR) signal transduction and baroreceptor reflex lose their vital function. Eventually the heart is unable to achieve adequate cardiac output (Federmann & Hess 1994).

Cardiovascular diseases are a major cause of mortality and morbidity worldwide (Garjarsa & Kloner 2010), accounting for 1 in every 3 deaths in the United States and an estimated cost of $312.6 billion in 2009 (Go et al. 2012). Approximately 23 million people worldwide (McMurray et al. 1998) and 400,000 people in Canada are living with symptomatic HF with 33% mortality in the first year of diagnosis (Liu et al. 2001) and 50% mortality in the fifth year (Levy et al. 2002; Roger et al. 2004).

1.1.2 Diastolic Dysfunction

Diastolic dysfunction (DD) involves resistant filling and higher filling pressures in the LV (Hess 1993). Many patients with DD are asymptomatic in regards to HF as well as preserved EF (Nagarakanti & Ezekowitz 2008). DD may progress into diastolic heart failure (DHF) which displays many signs and symptoms of HF (dyspnea, edema, low exercise capacity), but with preserved EF (Nagarakanti & Ezekowitz 2008). A percentage of 30-55% of HF patients have DHF, without systolic dysfunction (Redfield et al. 2003; Senni et al. 1998; Vasan 1995). The diagnosis of DD can be made with invasive catheterization to measure cavity pressures or with mitral valve (between left atria (LA) and LV velocity

measurements such as the E/A ratio. Both E and A occur during diastole. E refers to the peak blood flow velocity wave during the rapid filling of the LV while the A is a later wave resulting from atrial contraction. This is a measure of diastolic filling, not function, and an E/A ratio from 1 to 1.5 is normal in humans. Early in DD, the E/A ratio is < 1. Atrial contraction increases and early velocity decreases because early mitral velocity filling (E) is slowed and the atrial contraction (A) is compensating. As DD progresses and LA pressure increases, causing E/A ratio > 1, and impaired atrial contraction representing a transition in diastolic filling from poor relaxation to impaired filling. When DD becomes severe, the LV compliance is low and the LA pressure increases producing a large E wave and small A wave. Thus an E/A ratio > 2 is observed (Nagarakanti & Ezekowitz 2008).

1.1.3 Fetal Gene Program

HF induces a new type of protein expression to help compensate for pump function. As the heart attempts to compensate with hemodynamic overload, genes that are abundantly expressed during fetal development become upregulated (Olson 2004) though are usually silent during adulthood (Barry et al. 2008; Thum et al. 2007; Li et al. 1996). These genes include fetal isoforms of α-actin, β-actin, ventricular calcium channels and smooth muscle α-actin as well as the hormones ANP and brain natriuretic peptide (Kuwahara et al. 2012). There is a close relationship between fetal gene expression program and the adult failing heart gene program (Thum et al. 2007). The activation of this program initially increases contractility and maintains cardiac output but sustained stress and

protein isoform alterations, may eventually lead to cardiac dysfunction (Kuwahara et al. 2012).

1.1.4 Ischemia Reperfusion Injury and Myocardial Stunning

MI is a result of myocardial ischemia, yet the extent of infarction depends on both ischemia and reperfusion phases of injury (Black 2000). Unlike the fibrosis in HF, ischemic myocardium that has blood flow re-established is reversible if ischemia lasts for 20 minutes or less (Braunwald & Kloner 1982). A complete coronary occlusion causes MI slowly over hours but ischemia followed by reperfusion creates a damaging inflammatory response (Park & Lucchesi 1999). After a brief ischemic episode a phenomenon called stunning occurs when the heart receives adequate perfusion but not contracting normally. (Heyndrickx et al. 1978). Braunwald & Kloner (1982) described this phenomenon as a slow recovery after an ischemic episode, involving the reestablishment of adenosine triphosphate (ATP) and creatine phosphate (CP) stores. More recent evidence has implicated oxygen, calcium, pH, inflammation and the mitochondria in stunned myocardium (Yellon et al. 2007) (Figure 1.2).

Oxygen is thought to play a role by means of increased oxygen free radicals (Zweier 1988) and the reduced availability of nitric oxide (NO) because of hypoxic conditions prior to reperfusion (Zweier & Talukder 2006), but animal and human studies have shown contradictory results. Numerous clinical trials in mitigating IR injury have been largely disappointing despite promising animal study results (Yellon & Hausenloy 2007). Reperfusion causes a sudden increase

in intracellular calcium causing sarcolemma mitochondrial overload and lethal hypercontraction of cardiac cells (Piper et al. 1998). The pH of ischemic tissue is acidic, and the fast alkalinisation during reperfusion damages myofibrils (Lemasters et al. 1996). Inflammation is caused by chemical attractants released during ischemia, clogging the vasculature with leukocytes that release harmful reactive oxygen species and catabolic enzymes (Winten-Johansen 2004). Finally, the non-selective mitochondrial surface PTP channel has a role in causing stunned myocardium as it opens during the calcium overload caused by ischemia-reperfusion, depolarizing the membrane and preventing oxidative phosphorylation from occurring. Cells affected by ischemia lose their stores of ATP, causing cell death (Hausenloy, D.J., & Yellon, D.M. 2003; Kim et al. 2006; Griffiths & Halestrap 1995). Ischemic episodes may or may not develop into HF so the study of mechanism, diagnostics and treatments are of great interest (Yellon & Hausenloy 2007).

1.1.5 IR Rat Model Characteristics

Rat models of IR injury are explored in the hopes of understanding the counter-intuitive mechanism of severe myocardial injury despite the reestablishment of blood flow during thrombolysis, stenting, and angiography (Klocke et al. 2007). Unlike chronic occlusion resulting in MI, IR is accomplished by placing a protective piece of 0.5 mm PE-10 tubing atop the coronary artery prior to ligation to protect artery integrity (Klocke et al. 2007). Animal models of IR aide in the development of clinical damage mitigation techniques such as

ischemic preconditioning, post conditioning, immunosuppression, and redirecting of cardiac metabolism (Frank et al. 2012).

In the rat heart, oxygen free radicals are thought to be directly responsible for post IR ventricular dysfunction (Ambrosio et al. 1991; Zweier et al. 1987), further shown by the efficacy of anti-oxidant superoxide dismutase (Petty et al. 1994). Oxygen free radicals were known to be produced by neutrophils, and the initial finding of the complement system as a major inflammatory and exacerbater of IR injury in rat myocardium (Hill & Ward 1969). Lastly, as ischemic myocardium is reperfused, the abundance of hydrogen ions produced from anaerobic glycolysis are anti-ported out of the cell as Na+ is imported. High intracellular $Na+/Ca^{2+}$ exchanger on the sarcoplasmic reticulum releases high amounts of Ca^{2+} into the cell causing hyper-contracture and damage to the myocardium (Lemasters et al. 1996). In an attempt to correct this, inhibition of the Na+/H+ exchanger was first shown with amiloride and improved ventricular function in Langendorff perfused rat hearts (Karmazyn 1988). Rat models of IR injury are continually being explored for pre-clinical studies to determine the mechanism and drug targets for alleviating IR injury.

1.1.6 MI Rat Model Characteristics

The rat model of MI is commonly used by means of coronary artery ligation, first described by Pfeffer et al. (1979). Under anaesthesia, the heart is externalized and the proximal coronary artery ligated, resulting in visible cyanosis distal to the ligature. A period of high mortality occurs within 48 hours after

surgery (Tucci 2009). In Sprague-Dawley rats, the rat model used in this work, the mortality after surgery is 36% (Liu et al. 1997). The necrosis of cardiomyocytes from MI reduces EF and causes LV dilation and the size of infarction in rat correlates well increased LV volume and diastolic pressure (Tucci 2009). Increased LVDP can be detected by E/A ratio (>1.5) to provide insight on diastolic dysfunction 1 week after MI (Saraiva et al. 2007) while neurohormonal markers diverge from normal values (Francis et al. 2001). With a large MI (>40% of LV mass), rats will experience pulmonary congestion as early as one week post-surgery (Antonio et al. 2009). Rats with MIs causing necrosis in 46% of the LV mass develop HF at 3 weeks with reduced cardiac output and inability to increase cardiac output during stress and exercise (cardiac reserve) (Pfeffer et al. 1979).

1.2 Sympathetic Mechanisms of Action in the Heart

The nervous system of vertebrates is divided into central (brain and spinal cord) and peripheral (somatic and autonomic) nervous systems. The autonomic nervous system (ANS), a branch of the peripheral nervous system, consists of the SNS and parasympathetic nervous systems (PNS) (Figure 1.1) both of which facilitate efferent signalling to the body (Hildreth et al. 2009). The hypothalamus integrates outgoing information (Forster 1998) and centrally regulates the SNS output to the body (Snitker et al. 2000). Most organs receive both SNS and PNS inputs. Cardiac ventricles are innervated by the SNS and PNS (Pierpont et al., 1985). SNS activation results in the release of norepinephrine (NE) at sympathetic nerve terminals and increases cardiac chronotopy and ionotropy while

epinephrine (EPI), released from the kidney's adrenal medulla into the circulation acts on blood vessels and the heart muscle (Lymperopoulos et al. 2007; 2012). These neurotransmitters are important in the development of cardiovascular disease. Research in the past decades have established that the compensatory over activity of the SNS after an ischemic insult is detrimental to the heart and thus SNS inhibitors (β-Blockers, angiotensinogen converting enzyme inhibitors, aldosterone receptor blockers) are also a benefit to cardiac disease patients (Lymperopoulos 2013).

1.2.1 Myocardial NE Function and Distribution

The sympathetic nervous system is vital to heart function (Malpas 2010). NE was discovered in 1946 (Von Euler 1946) within sympathetic nerve terminals and is a neurotransmitter and hormone that regulates vital bodily functions, but also important in the pathophysiology of many cardiovascular, neural, psychiatric and endocrine disorders (Eisenhofer et al. 2004). Part of the catecholamine family, NE influences nearly all tissues and regulates and/or is essential in the synthesis of certain hormones, especially during stress (Kvetnansky et al. 2009).

NE is synthesized from the amino acid tyrosine (Figure 1.4). Within post-ganglionic sympathetic neurons that innervate the heart, tyrosine enters the neuron and undergoes the first and rate limiting step of NE synthesis: hydroxylation by tyrosine hydroxylase to dihydroxyphenylalanine (DOPA) (Kaufman & Kaufman 1985; Nagatsu et al. 1964). DOPA is decarboxylated to

dopamine (DA) by aromatic L-amino acid decarboxylase. In the cardiac neurons that utilize NE, DA-β-hydroxylase produces NE (Fernstrom & Fernstrom 2007).

SNS activation leads to NE release from neuronal storage vesicles (Brodde & Michael 1999). NE is able to activate nine adrenergic receptors in the vasculature and synapse region: three α_1 adrenoceptors (α_{1A}, α_{1B}, α_{1D}), three α_2 adrenoceptors (α_{2A}, α_{2B}, α_{2C}), and three β-adrenoceptors (β_1, β_2, β_3) (Bylund et al., 1994). Upon release, approximately 80% of the NE is recycled back to the sympathetic neuron by the NE transporter (NET) (Leineweber et al. 2002). The remaining NE activates one or more of the 9 adrenergic receptors or spills over into the surrounding circulation (Leineweber et al., 2002). When NE binds to a β-AR and through signal transduction the dissociation of the intracellular G-protein complex occurs (Rockman et al. 2002).

1.2.2 Myocardial β-Adrenoceptor Function, Expression, and Regulation

Cardiac contractility is mediated through β-ARs (Barbuti & DiFrancesco 2008). Many species have β-ARs with the same seven transmembrane structure, suggesting their importance (Dessy & Balligand 2010). β_1-ARs are coupled to stimulatory G_s proteins while myocardial β_2-ARs are coupled to G_s proteins (Hausdorff et al. 1989; Strulovici et al. 1984) as well as the inhibitory G_i (Abramson et al. 1988; Xiao et al. 1995). First cloned by Emorine et al. (1989), β_3-ARs are present in most cardiac cells and have a different coupling profile than β_1 and β_2 (Dessy & Balligand 2010). In the human ventricle, β_3-AR appears to preferentially couple to G_i (Gauthier et al., 1996) however, G_s coupling was

observed (Gauthier et al. 1998). In the human heart, β_1-AR and β_2-AR comprise about 95-98% of the β-AR population on myocytes (Brodde 1993) with 3-5% β_3-AR (Liang & Mills 2002; Myslivecek & Trojan 2003). β_1-AR to β_2-AR are respectively expressed in atria at an approximately 70%:30% ratio, while in the ventricles at a ratio of 80%:20% (Brodde 1991).

NE increases myocardial contractility largely through β_1-AR in both atria and ventricles while β_2-AR stimulation causes only sub-maximal contractile force (Kaumann et al., 1989; Motomura et al. 1990). Myocardial β-AR activation stimulates adenylyl cyclase (AC) localized in the plasma membrane and G proteins located within the cell (Figure 1.6) (Dupre et al. 2007). Activation or inhibition of AC occurs based on the G protein subunit (Gsα activation or Giα inhibition) (Gilman 1987). All nine members of ACs catalyze adenosine triphosphate (ATP) into the second messenger, cyclic adenosine monophosphate (cAMP) ACs type V and VI predominate in the cardiac tissue of mammals (Tang et al. 2010). AC activation increases cAMP which activates protein kinase A (PKA) and phosphorylates a number of targets to increase contractility (discussed below) (Walsh & Van Patten, 1994; Kaumann & Molenaar, 1997). While all β-ARs have the ability to stimulate AC, β_3-ARs appear to preferentially stimulate endothelial nitric oxide synthase (eNOS) (Brixius et al. 2006). β_3-AR agonists do not decrease or increase contractility (Cohen et al., 1999; Kaumann & Molenaar, 1996; Skeberdis et al.2008) likely due to their distinct coupling to NOS signalling (Kirstein et al., 1995) causing peripheral vasodilation with subsequent SNS

activation, tachycardia (Berlan et al., 1994; Shen et al., 1994; Tavernier et al., 1992) and ionotropy (Donckier et al., 2001; Shen et al., 1996).

β-ARs are susceptible to internalization and degradation (Lefkowitz & Shenoy 2005; Pitcher et al. 1998; Freedman & Leftowitz 1996). Excessive stimulation of G-protein coupled receptors (GPCR) causes phosphorylation by a GPCR kinase (GRK). This event makes the receptor a high affinity target for β-arrestin, which blocks the cytoplasmic site from activation (Wilden, 1995; Krupnick et al., 1997). The β-arrestins interact with clathrin and other endocytotic proteins to internalize the receptors, leading to three outcomes: dephosphorylation, resensitization and return to plasma membrane, degradation by lysosomes, or activation of different cell pathways (Reiter and Lefkowitz 2006).

β_1-ARs are found on the surface of fibroblasts, myocytes and lymphocytes. β_1-AR are distributed uniformly on the myocyte surface while active β_2-AR are only found within transverse tubules (Nikolaev et al. 2010). Brodde et al. (1986) reported approximately 10 times higher β-AR density in circulating lymphocytes than atrial appendage, however, a linear relation between densities was found. Density of β-AR in dermal fibroblasts (Kotanko et al. 1992) was similar to results found by Brodde et al. (1996) in the atrial appendage. To my knowledge, β-AR levels have not been measured post-IR.

1.2.3 cAMP/PKA Intracellular Signalling

Cyclic adenosine monophosphate (cAMP) is an important 2nd messenger for numerous cellular functions and its levels increase with β-AR stimulation (Beavo & Brunton 2002; Houslay & Milligan 1997) (Figure 1.6). Intracellular cAMP is synthesized at the cellular membrane by AC and its action results in cellular responses through the activation of PKA (Colledge & Scott 1999; Rubin 1994). PKA signalling is considered to be a fine-tuned molecular switch instead of a catalyst (Taylor et al. 2012). Unlike metabolic enzymes, designed to produce a product from a reactant, PKA is a switch that turns on and off a cascade of events (Taylor et al. 2013) by interacting with cAMP. The external structure of PKA consists of two catalytic subunits and two regulatory subunits (Taylor et al. 1990; Bauman & Scott 2002). Binding of cAMP to PKA disassembles PKA's regulatory units from its catalytic subunits, enabling the phosphorylation of target proteins. PKA's internal structure consists of an N-terminal lobe with a β-sheet and a C-terminal helical lobe (C-lobe), features conserved in all protein kinases. ATP binds to a glycine rich loop on PKA, distinct from ATP binding sites in other ATPases (Ramakrishnan et al. 2002). PKA positions the adenine ring at the base of a large hydrophobic pocket between the N and C lobes. The phosphate group is wedged between the glycine and catalytic loops before it moves to the active site to be added to the target protein (Taylor et al. 2013). cAMP is eventually degraded into 5'-AMP by phosphodiesterases (PDEs) (Conti & Jin 1999; Manganiello & Degerman 1999) and PKA joins back with its regulatory subunits to become inactive (Taylor et al. 2013).

1.2.4 PKA-Stimulated Cardiac Effector Proteins

Heart rate contraction is mediated by a rise in intracellular Ca^{2+} due to cellular membrane depolarization. Ca^{2+} binds to troponin C, facilitating the production of actin-myosin cross-bridging and sliding thick and thin muscle filaments (Marks 2013). This event occurs rapidly during each heartbeat. The process is facilitated by a number of receptors that are influenced by cAMP-PKA signalling, generally increasing strength and rate of contraction in the heart. L-type Ca^{2+} channels are located on the cell surface and allow Ca^{2+} movement to and from the sarcoplasmic reticulum, a major store of calcium in the cell (Bodi et al. 2005). The channel is regulated by sympathetic signalling which thus influences the rate and strength of myocyte contraction (Keef et al. 2001; Van der Hayden 2005). PKA phosphorylates L-type Ca^{2+} channels on Ser-1928, increasing its responsiveness to agonists (Perets et al 1996; Gao et al 1997; Hulme 2003). PKA phosphorylation opens the ryanodine receptor 2 (RyR2) which is an intracellular Ca^{2+} channel on the sarcoplasmic reticulum (SR), responsible for releasing and sequestering calcium with each heartbeat. Ca^{2+} is pumped back into the SR by sarcoplasmic/endoplasmic reticulum Ca^{2+} ATPase 2a (SERCA2a). Phospholamban regulates the Ca^{2+} affinity of SERCA2a and its phosphorylation by PKA results in increased Ca^{2+} uptake, enhancing lusitropy (Marks 2013). Ca^{2+}/calmodulin dependent kinase 2 (CaMK2) is also activated by β-AR stimulation (Baltas et al. 1997). Further studies implicated sympathetic-induced CaMK2 phosphorylation with Ca^{2+} handling proteins (Kuschel et al. 1999; Ferrero 2007; Said 2002). Phospholamban can be directly phosphorylated by

CaMK2 (Simmerman et al. 1986) resulting in lusitropic effects of SERCA2A (Marks 2013). Cardiac myosin binding protein C (cMyBP-C) can be phosphorylated by PKA resulting in decreased Ca^{2+} sensitivity and increased cross bridge formation (Gordon et al. 2000; Solaro & Rarick 1998) although studies of these effects have been inconsistent (de Tombe & Stienen 1995; Janssen & Tombe 1997; Johns et al. 1997). Stelzer et al. (2006) sought to clarify the contradictions by using transgenic mice deficient in cMyBP-C. The authors discovered that PKA phosphorylation of cMyBP-C increased the acceleration of force after beta-adrenergic stimulation (Stelzer et al. 2006). Indeed, cAMP/PKA signalling has far reaching implications on cardiac function and its study in respect to SNS signalling requires more exploration.

1.2.5 NE & β-AR in heart failure

The SNS had been implicated in the pathophysiology of cardiac dysfunction and remodelling. An ischemic episode causing significant cell death results in compensatory increases in NE release from subcortical (Aggarwal et al. 2002) and cardiac sympathetic nerve terminals (Lymperopoulos et al. 2007;2012). Over time, excessive NE causes β_1-AR to be downregulated, shifting the β_1-AR:β_2-AR ratio from 80%:20% to 50%:50% in the failing heart (Bristow et al. 1982;1986). This β_1-AR downregulation has been confirmed numerous times in HF models and in humans (Hadcock & Malbon 1988; Ungerer et al. 1993; Ahmed 2003).

While β_2-AR is not downregulated in HF, it is dysfunctional in a manner termed "uncoupling" (Bristow et al. 1982; 1986; Rockman et al. 2002).β_2-AR stimulation appears to improve cardiac function and reduce apoptosis (Dorn et al. 1999; Liggett et al. 2000), but this coupling mechanism is disrupted in HF (Nikolaev et al. 2010). "Coupling" refers to the G proteins that interact with each β-ARs to produce a signal cascade. After prolonged stimulation by a β_2-AR agonist, signal transduction is disrupted (Sibley et al. 1987, Hausdorff et al. 1990, Benovic et al. 1987). Phosphorylation events on tertiary protein structure reduce Gs activity thus attenuating AC production of cAMP (Strader et al. 1989, Hausdorff et al. 1990).

While β_3-AR agonists decrease contractile force (Gauthier 1996; Gauthier 1998), they are upregulated in human HF patients (Moniotte 2001) and thought to be a "brake" on β_1 and β_2 signalling by acting through G_i and eNOS producing vasodilation (Moens 2010). Most attention is paid to the status of β-ARs because of the benefits of β-blocker therapy, however, changes in NE storage and cycling are also important.

Increased plasma NE (spill over from the heart tissue) is observed in the failing heart (Schlaich et al. 2003; Brunner-La Rocca et al. 2001). There is a significant negative relationship between interstitial NE concentration and β-AR density (Delehanty et al. 1994), confirming NE as the source of desensitization. Increased plasma NE is a predictor of progressive heart disease and worsening HF causing death (Brunner-La Rocca et al. 2001). Tissue NE, or NE storage, is

decreased in failing hearts (Chidsey et al. 1964; Chidsey 1963; Brunner-La Rocca et al. 2001), nearly eliminated from infarcted zones of the myocardium, while a 50% decrease post-infarction and full recovery is observed in non-infarcted myocardium (Mathes et al. 1971). NE spillover is thought to be mediated in part by decreased NE reuptake (Petch & Nayer 1979) and enhanced by loss of NE nerve terminals as seen in rapid pacing and NE infusion in canines (Qin 2002). The excess NE is excreted in urine, as demonstrated by HF patients. Increased NE urine levels were observed according to worsening NYHA class (Chidsev et al. 1965). The above explanation applies to HF as well, where HF heart rate and myocardial contractile force are impaired even when electrically stimulated (Covell et al. 1966). Increased cardiac output (L/min) during exercise (cardiac reserve) is impaired in HF patients, correlating with poor survival outcomes (Williams 2005). These results have been well studied in animal models of MI however their physiology post-IR has not been documented.

1.3 Phosphodiesterases

1.3.1 PDE Characteristics

Within the cell and important to β-AR signal transduction are a super family of proteins called phosphodiesterases (PDEs). PDEs are largely responsible for degrading the second messenger cyclic adenosine monophosphate (cAMP) and cyclic guanosine monophosphate (cGMP) (Beavo 1995; Soderling & Beavo 2000; Corbin & Francis 1999). There are eleven families, PDE1-PDE11, three are cAMP specific (4, 7 & 8), three are cGMP specific (3,6 & 9), and five

hydrolyze both (1,2,3,10 & 11) (Cameron & Baillie 2012). All eleven families share a common catalytic domain, but the rest of the enzyme can vary greatly (Francis et al. 2011). Some PDE genes contain multiple promoter regions, regulatory and transcription factors that result in alternative splicing and a large molecular diversity (Bender & Beavo 2006; Conti & Beavo 2007). The families of PDE1-4 are widely expressed whereas PDE5-11 are more tissue specific (Francis et al. 2011).

PDE1 is expressed in the brain, heart, lung, and smooth muscle (Reneerkens et al. 2009; Dent et al. 1998; Sonnenburg et al. 1998; Yan et al. 1994; Kostic et al. 1997) and has a role in vascular remodelling (Chan & Yan 2011). PDE2 expression is widespread including brain, heart, adrenal cortex and platelets (Reneerkens et al. 2009; Ito et al. 1996; Martins et al. 1982) and has a function in cardiovascular remodelling and therapies (Mehel et al. 2013). PDE3 and PDE4 provide most of the cAMP hydrolyzing activity in most cardiovascular cells (Francis et al. 2011). PDE3 is involved in many tissues and a player in myocardial contractility, clot formation, vascular smooth muscle, and immunology (Beavo & Reifsnyder 1990; Thompson 1991; Weishaar 1985; Komas et al. 1996; Manganiello et al. 1995). A review of PDE4 literature will follow.

PDEs 5-11 are more tissue specific than PDEs 1-4 but hold great potential for therapeutics and drug discovery (Francis et al. 2011). PDE5 is found to be important within the vascular and respiratory smooth muscle (Francis et al. 2006),

cerebral Purkinje cells (Shimizu-Albergine 2003), endothelial cells (Zhu et al. 2005) and gastrointestinal epithelial cells (Sopory et al. 2004).The PDE6 family is required for light perception and found in the eye relatively abundantly (~20 um) compared to other tissues (Burns & Arshavksy 2005; Cote 2006). PDE7 are present in high amounts within the cells of the immune system (Bloom & Beavo 1996). PDE8 is found in the testis, spermatozoa (Baxendale & Fraser 2005; Vasta et al. 2006) and Leydig cells, the producers of leutizing hormone (LH) (Vasta et al. 2006). PDE8 is found in adrenal glands, where steroids are produced (Tsai et al. 2011) and also with thyroid stimulating hormone (TSH) in adrenocortical disease (Horvath et al. 2010). PDE9 is present in the mammalian brain and seen as a potential target for Alzheimer's disease (van Staveren et al. 2002; Remeerlems et al. 2009; Reyes-Irisarri et al. 2007). PDE10 is present in neural cells and a target for psychiatric disorders (Francis et al. 2011). PDE11 protein and mRNA are found in abundance in the hippocampus and are responsible for a large part of the cAMP regulation there (Kelly et al. 2010). Despite the same conserved catalytic domain, PDEs vary widely in their function and distribution.

1.3.2 Phosphodiesterase 4

In rat cardiomyocytes, PDE3 and PDE4 are responsible for 90% of cAMP-hydrolysis (Kaasik & Ohisalo 1996; Mongillo et al. 2004). PDE4 is a potent regulator of cAMP, distinctly classified because of its unique inhibition by the drug Rolipram (Wachtel 1982). K_m values of PDE4-cAMP interaction are approximately 25 fold lower than PDE4-cGMP (Reeves et al. 1987). There are

three isoforms PDE4 in the rat heart, PDE4A, PDE4B, PDE4D, totalling approximately 24 isoforms (Kenk 2010). PDE4C mRNA is not found in the rat heart (Kostic et al. 1997). PDE4 alone accounts for 30-60% of cAMP hydrolysis in the rat heart (Mongillo et al. 2004; Richter et al. 2011; Kaasick & Ohisalo 1996). 60% of PDE4 cAMP-hydrolyzing activity is accomplished by PDE4D, while 30% and 10% is done by PDE4B and A, respectively (Kostic et al. 1997; Mongillo et al. 2004; Richter et al. 2005). Localization of rat cardiac PDE4 isoforms has been reported on the sarcolemma (Okruhlicova et al. 1996) the Z-line of sarcomeres (Mongillo et al. 2004) while also shown to be an integral component of the ryanodine receptor in mice and humans (Lehnart 2005) and mainly cytosolic in dogs (Weishaar et al. 1987, Smith et al. 1997).

1.3.3 PDE4 Structure

PDE4s are 1,039 amino acid long proteins with a molecular weight of 119 kDa (Eichinger et al. 2005) though these characteristics vary based on the isoform. All PDEs contain the same three domains, a conserved catalytic domain and regulatory N and C termini (Thompson 1991; Boldger 1994). The catalytic domain of the 11 PDE families is approximately 300 amino acids long (Ke 2004) and looped into 17 alpha helices (Xu et al. 2000). Three subsets of these 300 amino acids form the only pocket large enough (~450 $\underline{\text{Å}}^3$) to fit cAMP (Ke 2004). Biochemical studies have also shown that PDE4s require a divalent metal, usually Mg^{2+} or Zn^{2+}, for catalytic activity (Hardman et al. 1971). The biochemical role of

these metals is still a source of debate, though stability of the protein with cAMP (Ke 2004) and a catalytic role (Huai et al. 2003) are well supported.

The proposed mechanism of cAMP catalysis by PDEs (Ke 2004) begins with the entrance of cAMP into the catalytic pocket where two divalent metals hold the phosphate group, polarizing the phosphate-oxygen bond, and making it positively charged. A histidine residue protonates the phosphate group causing further polarization and a site for a nucleophilic attack. A water molecule held by one of the divalent metals attacks the phosphate as a nucleophile causing a break between one of the phosphor-oxygen bonds.

1.3.4 PDE4 Compartmentalization

The diffusion of cAMP is estimated at a rapid 700 um^2/s (Oliveira et al. 2010). If cAMP was unhindered, PKA would activate all of its targets rapidly and indiscriminately instead of activation at specific subcellular sites important for cell function (Stangherlin & Zaccolo 2012). PDE4 isoforms are found throughout the cell, localized in the cytoplasm and attached to proteins to control cAMP pools. Both PDE4A1 and A5 are associated with the cell membrane (Baillie et al. 2002; Beard et al. 2002). In rat myocytes, isoforms of PDE4B and D are localized on the Z line of sarcomeres (Mongillo et al. 2004) and L-type calcium channels (Leroy et al. 2011). PDE4D3 has been found to form complexes with the ryanodine receptor, PKA and muscle a kinase anchoring protein (mAKAP) (Marx et al. 2000). Other protein interactions include PDE4D3 and myomegalin (Verde et al. 2001), PDE4D5 and activated C-kinase 1 (Bolger et al. 2002, Yarwood et al.

1999), PDE4D5 and β-arrestin (Ballie et al. 2007; Perry et al. 2002), PDE4D and gravin (Willoughby et al. 2006), PDE4D5 the receptor for activated C kinase 1 (RACK1), focal adhesion kinase (FAK) (Serrels et al. 2010), and PDE4D4 with exchange proteins activated by cAMP (Epac) and mAKAP (Dodge-Kafka et al. 2005). In summary, PDE4 isoforms are distributed widely throughout the myocyte and interact with cellular components to control cAMP pools and signaling.

1.3.5 PDE4 Regulation

PDEs are regulated both in the long and short term (Figure 1.8), by hormones, neurotransmitters, light, and oxygen derivatives (Francis et al. 2011). PDE4s functional role is determined by cellular location, modifying proteins and post-translational splicing (Cameron & Ballie 2012). Each PDE4 isoform has the same catalytic subunit, but they differ in their N-terminal domain (McCahill et al. 2008) which affects their protein-protein interaction and protein-lipid anchoring (Cameron & Ballie 2012). Within this N-terminal domain are the upstream conserved regions (UCR) 1 and 2. These are not present in all PDE4 subtypes but are the key functional modulators of PDE4 activity due to their phosphorylation site by ERK, MAP kinase and PKA. UCR1 has a PKA phosphorylation site (MacKenzie et al. 2002) while ERK phosphorylation of the catalytic subunit occurs (Ballie et al. 2000) but UCRs usually determine activity regulation afterwards (Houslay & Ballie 2003). Phosphorylation by PKA increases PDE4 activity, increasing its ability to hydrolyze cAMP (Cameron & Ballie 2012).

Phosphorylation by ERK as no effect on isoforms without UCRs, but it inhibits PDE4 isoforms with UCRs, which is then countered by the activation of PKA with large cAMP levels (Hoffman et al. 1999). These mechanisms occur quickly, since treatments increasing cAMP synthesis, also increase PDE4 activity in a matter of hours (Verghese et al. 1995).

Long term regulators of PDE4 include ubiquitination, caspase modification and phosphatidic acid. PDE4D5 ubiquination occurs on the C-terminus by murine double minute (MDM2) after β-adrenergic activation (Li et al. 2009) and initial ubiquination primes the enzyme for further ubiquination leading to inactivated PDE4D5 by arrestin molecules (Cameron & Ballie 2012). PDE4A5 can be cleaved by caspase 3 (Huston et al. 2000). Huston et al. (2000) found caspase 3-specific cleavage sites that remove 10 kDa from the N-terminus of the enzyme, a region containing SH3 binding domain for tyrosine kinase. The removal of this key site affects its activity, inhibitor sensitivity and anchoring ability. Finally, long PDE4 isoforms, those containing one or more UCRs, have binding sites for phosphatidic acid (PA) (Nemoz et al. 1997). Long PDE4 isoforms bind PA within the N-terminus region, increasing V_{max} without affecting K_m (Grange et al. 2000) and cAMP levels decrease (El Bawab et al. 1997).

Apart from the above regulatory factors, PDE4 is also transcriptionally modulated. Vicini & Conti (1997) discovered an intronic PDE4D promoter region that is responsive to follicle stimulating hormone (FSH), increasing subtype expression of some isoforms, but not others. This group also found the promoter was responsive to cAMP, increasing PDE4D expression which in turn will

stabilize cAMP levels (Conti et al. 1995). In PDE4A, several interesting promoter regions were found including a TATA box, CREB binding site (Olsen & Bolger 2000; Sassone-Corsi 1988; Montminy 1997) and AP1-binding sites (Olsen & Bolger 2000). PDE4D5 has also been shown to have two CRE sites (Le Jeune et al. 2002). Indeed, there is a variance of promoter sites between isoforms. D'Sa et al. (2002) showed that neurons utilized different PDE4 isozymes based on their activity at a given time. PDE4 enzymes share a common catalytic domain, but their promoter regions and interactions with modifiers differ greatly.

1.3.6 PDE4 Regulation of cAMP

Cardiac PDE4 is the most important controller of cAMP pools produced by NE stimulation in rats. In rat myocytes, PDE4 inhibition produces a larger increase in cAMP compared to PDE3 inhibition during β-AR stimulation by isoproterenol (Mongillo et al. 2004). In contrast, when stimulating AC with forskolin, PDE3 inhibition produces a larger cAMP pool than PDE4 inhibition (Mongillo et al. 2004). cAMP is generated at the interior cell surface by adenylyl cyclase (Beavo & Brunton 2002; Conti et al. 2007) and translates into many cellular responses by activating PKA (Colledge & Scott 1999; Rubin 1994). All PDE4 subtypes are in turn regulated by PKA phosphorylation (Sette & Conti 1996) on a single serine residue (Sette & Conti 1996). This phosphorylation disrupts a hydrogen bond, creating a negative charge and changing the entire PDE4 enzyme to a high activity state (Sette & Conti, 1996; Hoffman et al., 1998; Torphy, 1998; Liu & Maurice, 1999). PDE4 activity (ρmol cAMP hydrolyzed per min per gram of tissue) is increased by 60% by PKA phosphorylation (Mackenzie

et al. 2002) and 100-200% for the longer PDE4 subtypes PDE4A4 and PDE4D3 (Houslay & Adams 2003).

1.3.7 PDE4 in Cardiovascular Disease

PDE activity is preserved in compensated cardiac disease, but impaired in animal models of HF and consistent clinical observation has not been conducted on PDE function in human heart disease (Osadchii 2007). A study by Richter et al. (2011) demonstrated that PDE4A and D activity is reduced in humans with idiopathic dilated cardiomyopathy. A number of isoform specific knockouts have been developed in regards to PDE4 to reveal their function. A PDE4A knockout model has been developed, thus far no overt phenotypes have been discovered (Jin et al. 2005). Leroy et al. (2011) investigated PDE4B knockout in mice and concluded its importance with respect to intracellular calcium cycling by the notable improvement in cardiac contractility and response to β-AR stimulation. While these changes were not seen in PDE4D knockout, these mice exhibit progressive cardiac dysfunction and worsening outcomes with induced MI (Lehnart 2005). This is thought to be caused primarily by increased PKA phosphorylation of RyR receptor, making the sarcolemma "leaky", thus producing progressive HF and arrhythmia (Lehnart 2005, Wehrens 2003). The role of PDEs [and PDE4] in cardiac disease is an ongoing field of investigation (Osadachii et al. 2007).

1.4 PET Imaging

1.4.1 Basis of PET

A method of diagnosis and monitoring CVD is positron imaging tomography (PET), a technique that employs the venous injection of a radioactive tracer, measurement of its biodistribution, and three-dimensional quantification for analysis of molecular physiology (Figure 1.3). PET is able to non-invasively detect pathologies when no major lesions are present (Frey 1989; Herscovitch 1990; Sedvall et al. 1988). This modality has been implemented in cancer, cardiac, and neurologic diagnostic imaging. A molecule/drug of interest is labelled with a neutron-deficient radioisotope such as ^{13}N, ^{11}C, ^{15}O and ^{18}F produced from a cyclotron. The tracer travels through the body and emits positrons as it decays. Positrons travel less than 1-8 mm in the body, depending on the isotope, before annihilating with the subject's electrons (Zhang et al. 2008), producing two anti-parallel gamma rays of 511 keV. The circular PET camera that surrounds the subject contains scintillation crystals, detecting the γ-rays. After randoms, decay, attenuation, and scatter corrections, a three-dimensional PET image of the target organ is produced from the numerous camera slices. Different tracers provide unique information and clinical utility that can quickly and non-invasively distinguish normal and disease physiology (Wahl 2009). Most compounds or drugs have the potential to be chemically radio-labelled, making PET imaging a modality with tremendous potential for

pathophysiological investigation, thus the investigation into new animal models and tracers is of great research interest.

1.4.2 PET in Cardiac Disease

Myocardial perfusion imaging is the most used PET modality for cardiovascular disease (CVD) patients (Hendel et al. 2009). ^{82}Rb, ^{13}N, ^{18}F and ^{15}O water are available PET tracers for myocardial perfusion imaging (Higuchi & Bengel 2008; Heller et al. 2009). These tracers reliably detect perfusion defects caused by stenosis or microvascular dysfunction that may lead to tissue necrosis and fibrosis (Rischpler et al. 2013). Another tracer, [^{11}C]-hydroxyephedrine (HED), is an analogue of NE that can be used to image the sympathetic innervations of the heart (Munch et al. 2000; Schwaiger et al. 1991). Aside from blood flow and viability, novel tracers are being explored to assess risk stratification, therapy guidance and response to therapy (Rischpler et al. 2013). Collectively, the development and study of PET tracers enable enhanced understanding of cardiovascular disease physiology and future diagnostics and treatments.

1.4.3 FDG and Rest/Stress [^{13}N]NH_3 PET Utility in Cardiovascular Assessment

Both 2-Deoxy-2-[^{18}F]Fluoroglucose (FDG) and [^{13}N]NH_3 are cyclotron produced tracers used routinely in clinical cardiac PET imaging. An analogue of glucose, FDG, is used to detect myocardial viability. FDG is transported into myocytes by GLUT1 and GLUT4 transporters where it is metabolised by

hexokinase V to FDG-phosphate. No further metabolism occurs nor is the tracer able to leave the cell (Kearfott et al. 1984). This uptake is only observed in viable myocardium and the size of a FDG uptake defect provides prognostic value in humans (Ghosh et al. 2010).

$[^{13}N]NH_3$ is a PET tracer commonly used for perfusion assessment of the heart. Injected $[^{13}N]NH_3$ diffuses freely across the capillary and cell membranes (rate constant k1), where it is metabolized into $[^{13}N]$-glutamine by α-ketoglutarate-glutamate reactions and bound (k3), or washed back out of the cellular space (rate constant k2). The metabolized tracer is trapped within the myocardial muscle cells so the subsequent washout (rate constant k4) is assumed to be zero during estimation of myocardial blood flow (Choi et al. 1993). $[^{13}N]NH_3$ PET has been shown to be an excellent predictor of future cardiac events (Fiechter et al. 2013). Physiological cardiac reserve, the ability to increase cardiac output, is a considerable indicator of exercise capacity, and thus cardiovascular health (Cooke et al. 1998). Analysis of the difference between rest myocardial perfusion and pharmacologically induced stress perfusion (myocardial flow reserve) improves the detection of coronary stenosis (Fiechter et al. 2013). One such stress perfusion protocol is with step-wise infusion of β-AR agonist dobutamine in rats (Croteau et al. 2004) for applications in coronary stenosis disease modeling. To date many models of cardiac dysfunction have been investigated with PET tracers leading to clinical applications. To date, few studies have investigated cardiac ischemia reperfusion injury with PET.

1.5 Imaging PDE4 with PET

1.5.1 (*R*)-[^{11}C]Rolipram

Rolipram ((R/S)-4(3-cyclopentyloxy-4-methoxyphenyl)-2-pyrrolidone) (Figure 1.9) is a drug that inhibits all PDE4 isozymes. Originally tested as an antidepressant (Wachtel, 1983; Zeller et al. 1984; Bertolino et al. 1988) it was soon retracted because of nausea side effects (Zeller et al. 1984). Rolipram is still widely utilized in cancer, cardiac, and neurologic disease research. (*R*) and (*S*) Rolipram was originally labelled with C-11 by DaSilva et al. (1997) in order to non-invasively quantify PDE4 levels in brain and cardiac tissue as an index of cAMP and sympathetic nervous system activity. PET imaging of the SNS in cardiac diseases could provide important information, notably risk stratification and therapy guidance (Rischpler et al. 2013).

1.5.2 Previous Cardiac Results with (*R*)-[^{11}C]Rolipram

(*R*)-[^{11}C]Rolipram was found to selectively bind all PDE4 subtypes in rat myocardium with fast clearance and kinetics that match blood flow (Lourenco et al. 2001; Kenk et al. 2007). Labelled metabolites of (*R*)-[^{11}C]Rolipram were not found to bind PDE4, and were categorized into the non-specific binding compartment in kinetic modelling (Kenk et al. 2008). (*R*)-[^{11}C]Rolipram binding was dose-dependently increased by treatments that increase NE, histamine and serotonin, but not dopamine (Lourenco et al. 2006). Using CGP12177, a β-AR antagonist, the elevated (*R*)-[^{11}C]Rolipram binding with treatments elevating NE was blocked (unpublished results), confirming that (*R*)-[^{11}C]Rolipram binding is

mediated by β-AR receptors (Lourenco et al. 2006). Using desipramine (DMI), a NET blocker, to elevate synaptic NE, (*R*)-[^{11}C]Rolipram uptake can test PDE4 responsiveness. This method is similar to how Cooke et al. (1998) tested cardiac reserve, the ability of the heart to respond appropriately to stress. Cardiac reserve is impaired in cardiac dysfunction (Cooke et al. 1998). Increased (*R*)-[^{11}C]Rolipram uptake after DMI treatment indicated PDE4 expression after sustained SNS activity, thus PDE4 was deemed "responsive" in Sham animals. PDE4 non-responsiveness was observed in obese rats and rats following the anti-cancer treatment, adriamycin, a known cardiotoxic drug (Greene et al. 2009; Kenk et al. 2010, respectively). (*R*)-[^{11}C]Rolipram in rats demonstrates high myocardial uptake, specific PDE4 binding, and reproducible uptake measurements (Logan distribution volume (DV)) all obtained at low receptor occupancy and dose (<10%, <0.2 ug/kg, respectively) (Thomas et al. 2011). The above results indicate (*R*)-[^{11}C]Rolipram provides high LV contrast, reliably detects changes in cardiac PDE4, and provides insight into several disease models, providing support for exploration of (*R*)-[^{11}C]Rolipram in animal models of cardiac dysfunction for the study of cAMP/PDE4 with PET.

1.5.3 Study Rationale

To date much research focus is on animal models of permanent MI that produce reduced EF though nearly 50% of patients with HF symptoms show normal EF (Sharma & Kass 2014). Furthermore, approximately 20% of HF patients have unrecognized MI, a phenomenon of having an MI without

symptoms (Pride et al. 2013). In addition, the study of infarcted myocardium and remodelling is not possible using PET, as shown by Kenk et al. (unpublished) with (*R*)-[^{11}C]Rolipram, since the total ligation of the left anterior descending (LAD) coronary artery prevents the tracer to go in the infarcted area. A model of cardiac dysfunction with flow to the area at risk and preserved EF has yet to be extensively explored to assess these shortcomings of MI animal models. A rodent model of IR injury could provide insight into clinical situations such as unstable angina, percutaneous intervention, and coronary artery bypass grafting.

The exploration of 20 min and 45 min IR models in the thesis sought to explore this with the use of PET tracers and other measurements of SNS activation and cardiac dysfunction. This thesis continues the work of Kumiko McKasey, who in a 20 min IR model at 2 weeks post-surgery observed no resting flow defect using [^{13}N]NH_3 PET and a 60% increase in angiotensin II type 1 receptor in area at risk and a 115% increase in the infarct of MI model (McKasey 2012). Blockade of this receptor minimizes LV hypertrophy suggesting its role in cardiac dysfunction and renal failure (Amann et al. 1998; Dickhout et al. 2011). This supported the 20 min IR as a model of cardiac dysfunction with flow to the area at risk for investigation of remodelling pathophysiology with PET tracers.

Next this thesis sought to understand PDE4 physiology post-cardiac dysfunction in the remodelling phase (2-5 weeks) post-surgery as much research focuses on the early and late stages (less than 72 hours or 8 or more weeks, respectively). During 2-5 weeks post-surgery there are significant changes in

cardiac physiology including systolic pressure, end diastolic volume, (Gaudron et al. 1990), BNP levels (Choi et al. 2013) and development of fibrotic scar (Sanchez-Mas et al. 2014). If timepoints of changes PDE4 expression are found between 2-5 weeks post-surgery, this timepoint will be further analyzed with markers of cardiac dysfunction and SNS signalling. The long term goal of this thesis is to enhance understanding of PDE4 as a potential biomarker of SNS activity post ischemic injury, as this has not been extensively documented.

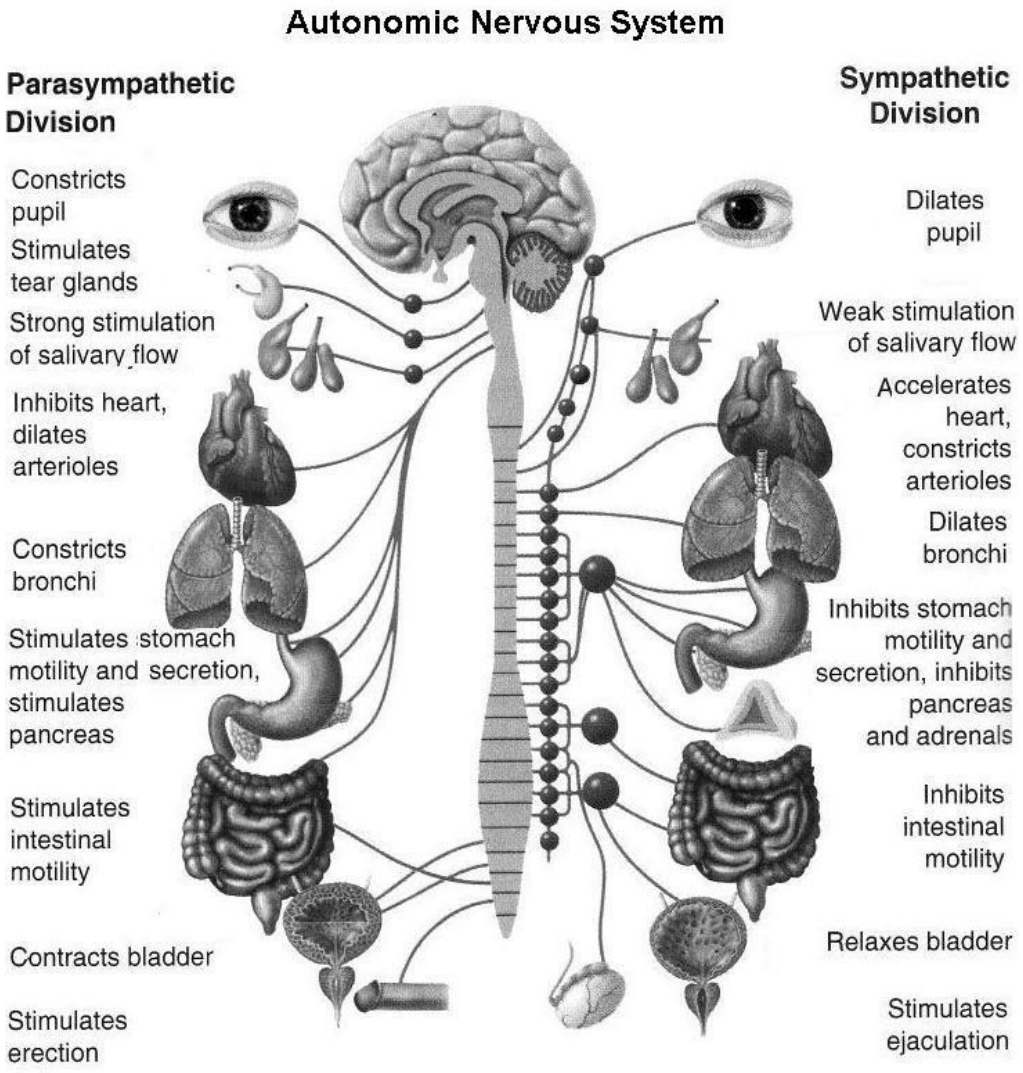

Figure 1.1: Parasympathetic and Sympathetic anatomical divisions, innervated organs and physiological consequences. Reproduced from http://www.yesselman.com/ans.jpg.

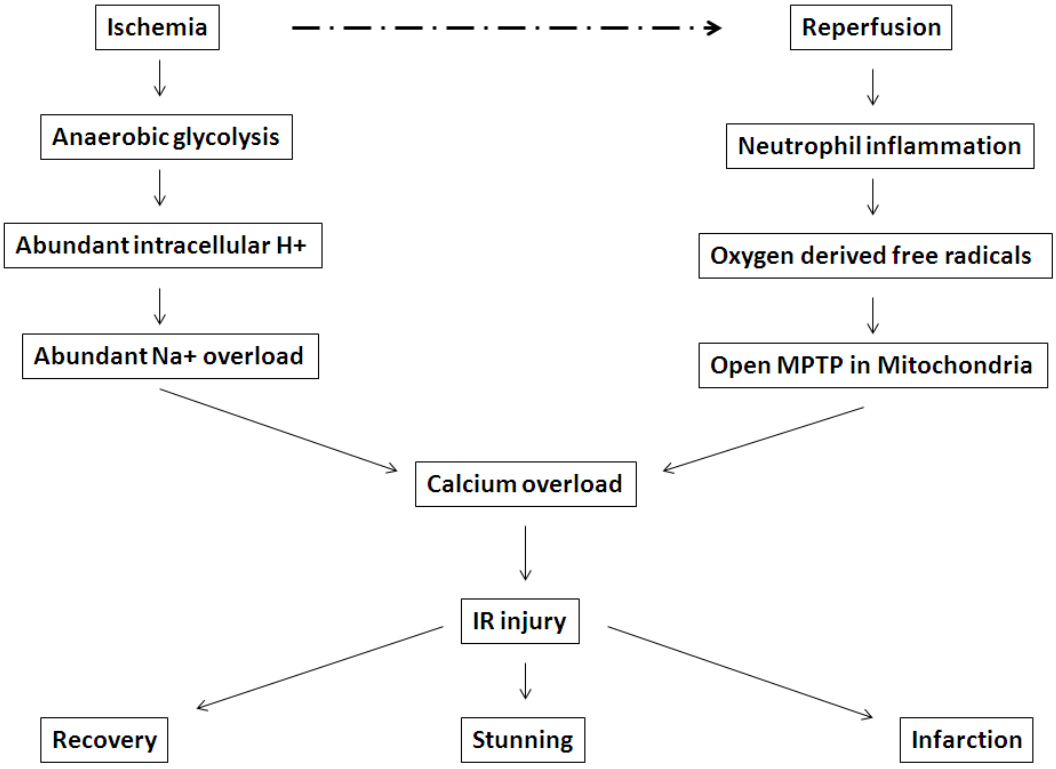

Figure 1.2: Cellular mechanisms of ischemia-reperfusion injury. Cellular pathways during both ischemia and reperfusion contribute to produce calcium overload. Ischemia produces excess protons by means of anaerobic glycolysis, activating H+/Na+ exchanger. Excess intracellular Na+ stimulates Na+/Ca2+ exchange at the sarcoplasmic reticulum. Reperfusion produces cytokine attractants that cause neutrophil accumulation, vascular plugging, release of degrative enzymes, oxygen free radicals and the opening of the MPTP, depolarizing mitochondria and preventing oxidative phosphorylation from occurring. Calcium overload damages myofibrils and their ability to contract normally. Ischemic episodes of 20 min or less may produce transient LV dysfunction but no lasting blood flow defect while episodes 20 min or more produce permanent infarction. Adapted from Yellon & Hausenloy 2007. Abbreviations; IR, ischemia reperfusion, MPTP, mitochondrial permeability transition pore.

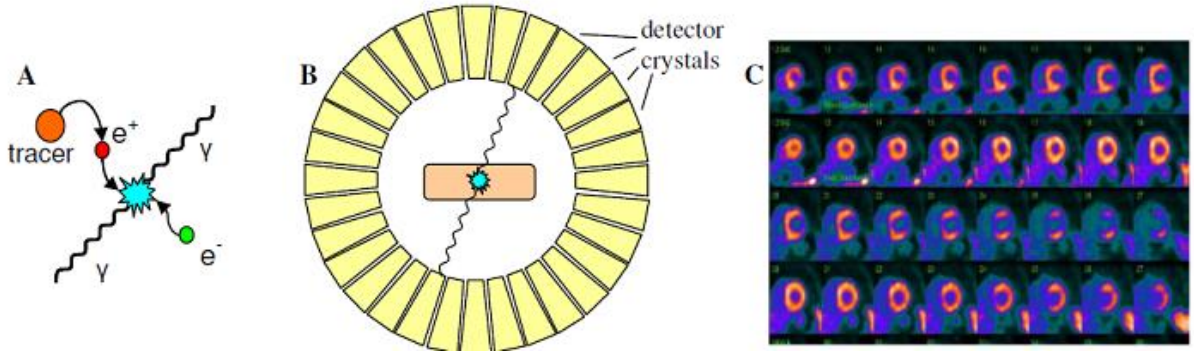

Figure 1.3: A pharmacological molecule of interest that is labelled with a neutron deficient isotope is injected in vivo, is distributed through tissues and decays over time with positron (e^+) emissions. Positrons annilate with naturally occurring electrons (e^-) (A) to produce to antiparallel (180^o from each other) gamma rays (γ) that are detected on a circular scintillation crystal module (B) providing location, frequency and time of annilation events to be recorded and processed into slices (C). PET image slices are corrected for scatter and attenuation before a three-dimensional PET image is obtained.

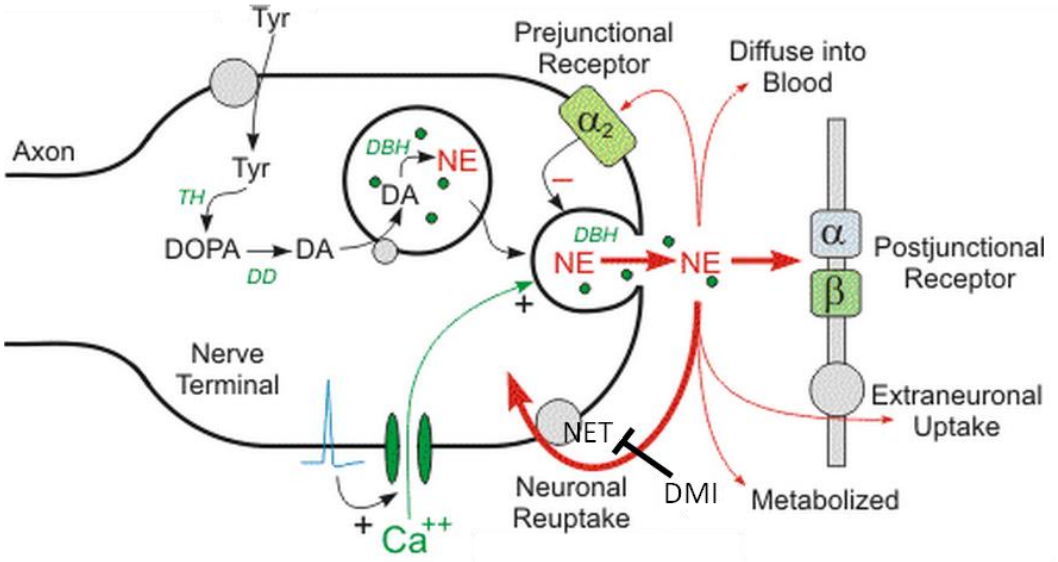

Figure 1.4: Schematic of sympathetic neuronal norepinephrine (NE) synthesis and release into synaptic space. The amino acid L-Tyrosine (Tyr) enters the neuron and is converted to L-dihydroxyphenalanine (DOPA) by tyrosine hydroxylase (TH). Next DOPA is converted to dopamine (DA) by Dopamine decarboxylase (DD) and finally Dopamine is converted to NE by Dopamine β-Hydroxylase (DBH). An action potential on the neuron triggers the influx of calcium (Ca++) caused vesicles of NE to be released into the synapse where most is recycled back to the neuron by NE transporter (NET) which can be blocked by desipramine (DMI). Figure modified from: http://www.cvpharmacology.com/NE%20syn-release.gif.

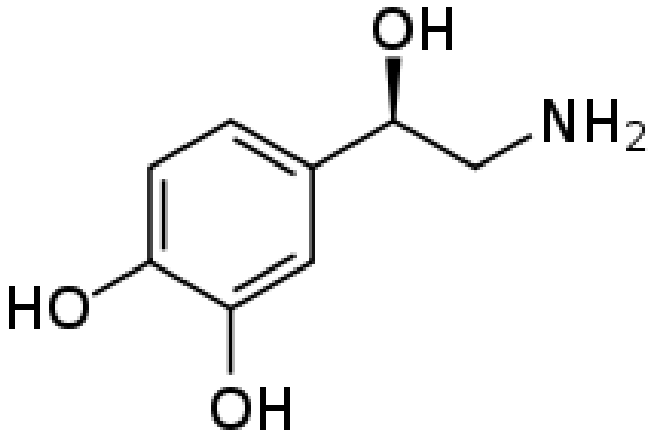

Figure 1.5: Chemical structure of the sympathetic nervous system neurotransmitter norepinephrine.

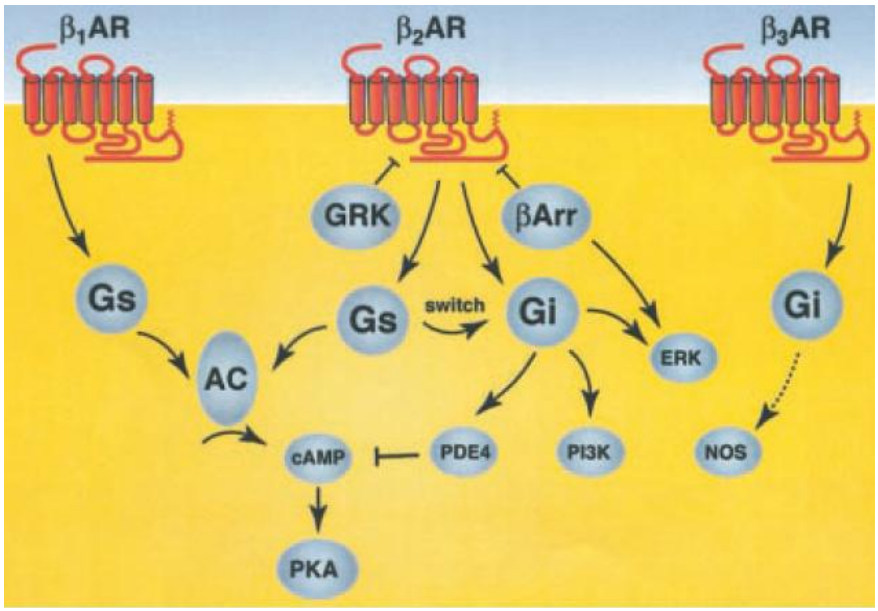

Figure 1.6: Intracellular consequences of NE stimulation of β1, β2 and β3-adrenergic receptors. Dissociation of G-subunits (Gs and Gi) activates adenylyl cyclase (AC), Extracellular signal-related kinase (ERK) or nitric oxide synthase (NOS). AC converts adenosine triphosphate (ATP) into cyclic adenosine monophosphate (cAMP) which removes the regulatory subunit of phosphokinase A (PKA) freeing it to phosphorylate targets. Most cardiac cAMP is metabolized by phosphodiesterase 4 (PDE4) but PDE3 is also an important metabolizer. G-protein related kinase (GRK) and β-arrestin (β-Arr) inhibit β2-AR function while Phosphoinositide 3-kinase is another 2nd messenger important in insulin signalling. Figure modified from Lohse et al., 2003.

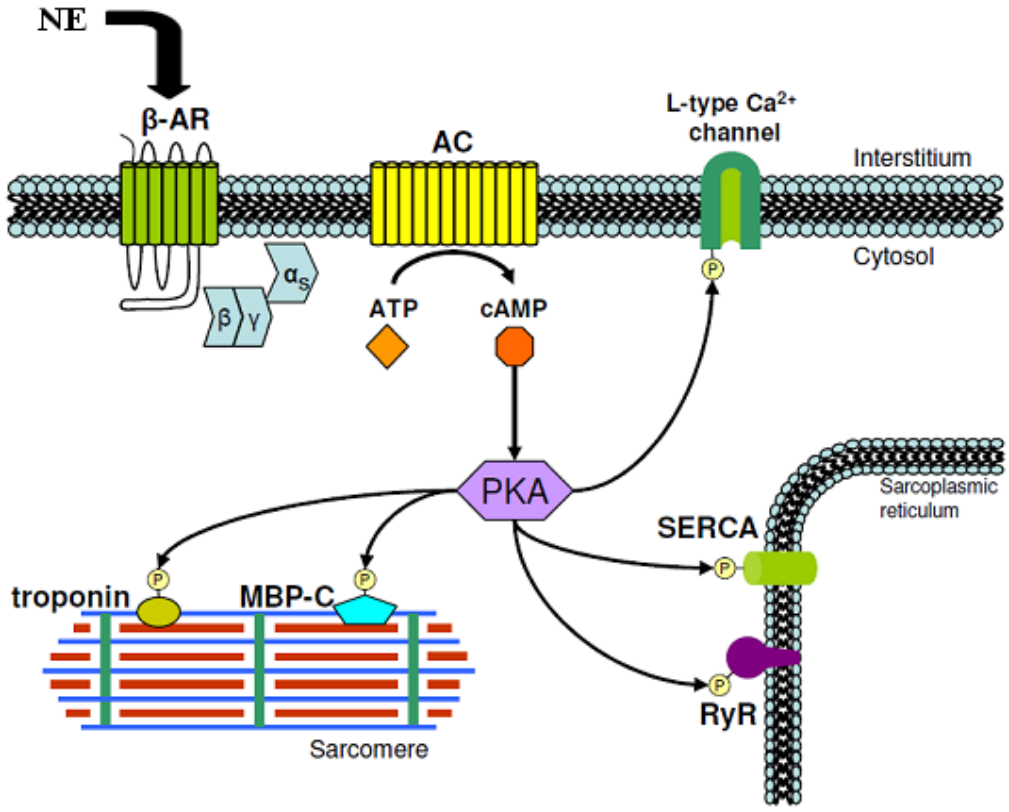

Figure 1.7: cAMP-specific PKA signalling and its effect on intracellular calcium and contractility. NE stimulation to β-ARs stimulates the G protein dissociation and activating adenylyl cyclase (AC). AC converts adenosine triphosphate (ATP) to cyclic adenosine monophosphate (cAMP). cAMP activates phosphokinase A (PKA) that phosphorylates a number of targets to increase intracellular Ca++, increasing strength and speed of contraction. PKA phosphorylates troponins, removing the inhibition on actin. Phosphorylation of the Ryanodine receptor (RyR) and sarcoplasmic reticulum Ca^{2+}-ATPase (SERCA) releases the internal stores of calcium. PKA phosphorylation of the L-type Ca^{2+} channel allows entry of extracellular calcium while phosphorylation of myosin binding protein C (MBP-C) increases sensitivity of the sarcomere to Ca^{2+}. Figure modified from the thesis of Miran Kenk 2010.

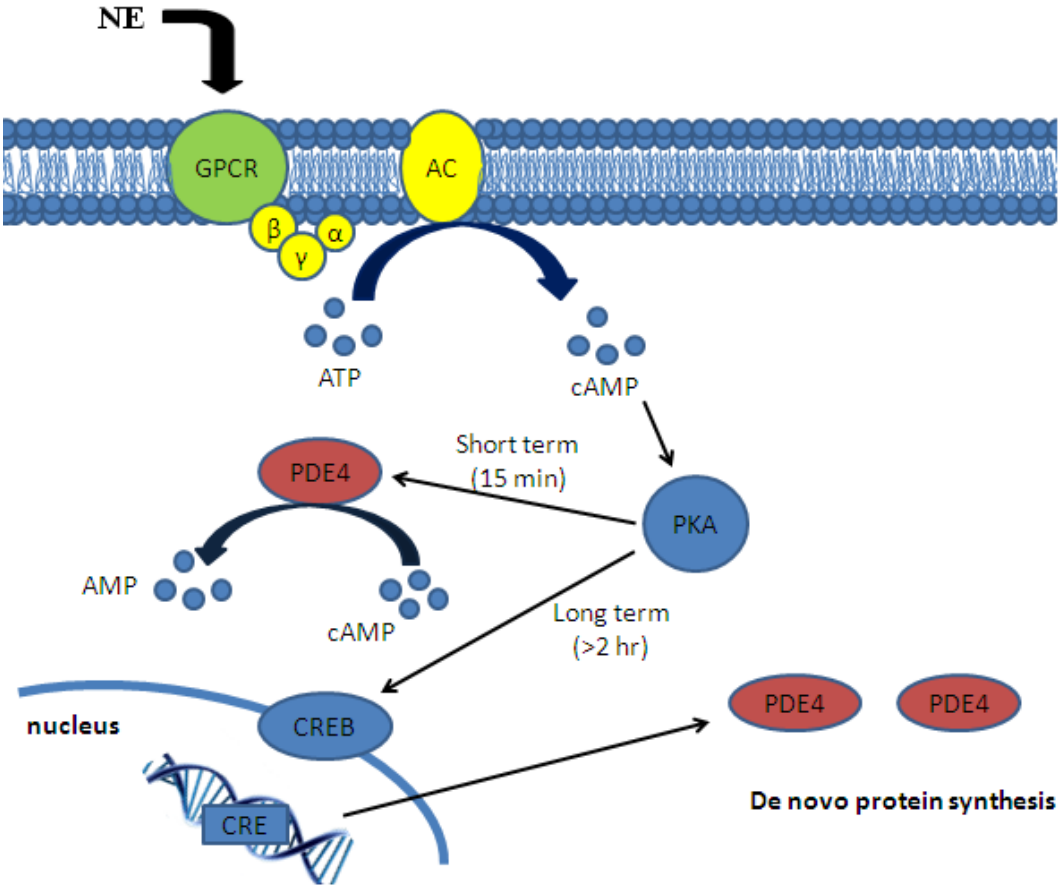

Figure 1.8: cAMP-specific PKA signalling and its regulation on PDE4. NE stimulation to β-ARs stimulates the G protein dissociation and activating adenylyl cyclase (AC). AC converts adenosine triphosphate (ATP) to cyclic adenosine monophosphate (cAMP). cAMP activates phosphokinase A (PKA). Phosphodiesterase 4 (PDE4) catalyzes the hydrolysis of cyclic adenosine monophosphate (cAMP) to adenosine monophosphate (AMP). PKA regulates PDE4 by phosphorylated, increasing its activity in the short term (15 min) and in the long term (>2 hr) by binding to cAMP-responsive element binding protein (CREB) that binds to cAMP responsive element (CRE) in DNA promoter region, resulting in *de novo* protein synthesis.

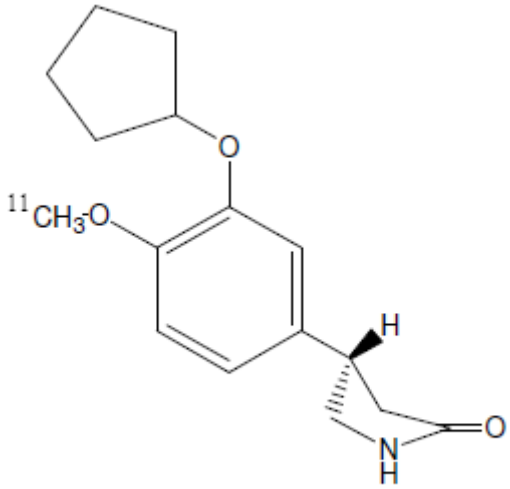

Figure 1.9: Chemical structure of the PDE4-specific inhibitor (*R*)-[^{11}C]Rolipram.

1.6.0 Hypothesis

1) Dysfunctional cAMP-mediated signalling measured at the PDE4 level is observed at early time points 2-5 weeks post-surgery in rats with myocardial reperfusion injury and MI that accompany any changes in SNS activity and cardiac function

1.6.1 Objectives

1) To develop a model of IR injury that has no resting flow defect to permit future study of the area at risk with PET tracers.

2) Develop a timeline of PDE4 protein expression in the early healing phase of post IR and MI injury (2-5 weeks).

3) With the above aims explored, test timepoints with changed PDE4 protein expression and activity for correlation with multiple measurements of cardiac dysfunction and SNS activity.

1.6.2 Specific Aims

1) FDG and [^{13}N]NH_3 PET will be used to assess blood flow and myocardial viability in both 20 min and 45 min IR models.

2) Non-invasive echocardiography and Doppler will be used to assess systolic and diastolic function in both 20 min and 45 min IR models.

3) Western Blot of PDE4 in suitable rat model from 2-5 weeks post-surgery will be conducted.

At timepoint post-surgery when PDE4 protein expression is altered in appropriate model:

4) Western Blot of $\beta_{1\text{-}3}$-AR to assess alterations from ischemia.

5) Measurement of plasma and tissue NE levels using commercially available ELISA and custom designed high performance liquid chromatography (HPLC), respectively, to measure SNS activity.

6) PDE4 activity will be measured using commercially available kit.

CHAPTER 2

Methods

2.0 Study Design

The overall study protocol is shown in Figure 2.1. The first goal of this thesis was to produce a model of cardiac dysfunction with no resting flow defect. Kenk et al (unpublished) sought to investigate (*R*)-[^{11}C]Rolipram PET in a model of MI, but none of the tracer entered the infarcted area. Here, two models were tested, 20 and 45 minute periods of ischemia by temporary ligation of the left anterior descending coronary artery. Through FDG, [^{13}N]$NH_{3,}$ and echocardiography it was shown that 45 minutes of ischemia produced a small scale fibrosis and resting flow defect. While this model may be beneficial for understanding small scale infarction by reperfusion injury, the differences between 45 min IR and MI may be too subtle for the scope of a Master's thesis. With no defect produced with FDG or [^{13}N]NH_3 PET as well as preserved ejection fraction in PET in the 20 min IR model, its investigation was extended to test for changes in PDE4 expression from 2-5 weeks. These timepoints were tested due to their importance in remodelling and healing. 3 weeks post 20 min IR was found to have increased PDE4 expression in all isoforms and investigation of SNS markers (Cardiac and NE levels), PDE4 activity as well as other measurements of cardiac dysfunction (echocardiography, mitral valve doppler, histology).

2.1 Animal Surgery

2.1.1 Animals

Male Sprague-Dawley rats (200-275 g) (Charles River, Montreal, Canada) were housed in pairs for 1 week with free access to food and water on a 12-hour light/dark cycle. All animal experiments within this work were conducted in adherence with the University of Ottawa Animal Care Committee and the Canadian Council on Animal Care for the use and care of laboratory animals.

2.1.2 IR Surgery

All Western Blots, NE analyses, Doppler's, and PDE4 activity assays were done on rats that underwent surgery performed by Mr. Rick Seymour. 2 week IR rats and MI rats that were imaged with FDG and rest/stress [^{13}N]NH_3 underwent surgery by Dr. Stephanie Thorn. All other rats that were imaged had IR or MI induced by Mr. Rick Seymour.

Male Sprague-Dawley rats were anesthetised with 2 mL/min isoflurane, quickly intubated, and attached to a ventilator prior to procedure described by Klocke et al. (2007). A cranial-caudal incision was made on the chest followed by blunt dissection of the pectoral muscle. The ribcage was then exposed, and the third or fourth intercostals space retracted based on where the heartbeat was felt. Silk suture was placed under the left anterior descending coronary artery with a small curved needle. A polypropylene (PE50) tube was placed between the suture knot and the artery for safe removal of the occlusion. The animal remained on the

ventilator with the ligation for 20 min or 45 min, at which point the suture was removed, blood flow re-established and the chest cavity was then closed. Animals were recovered on high oxygen and analgesics for 48 hrs. Sham animals underwent the same surgery with open chest cavity but no ligation was performed.

2.1.3 MI Surgery

All Western Blots were done on rats that underwent surgery performed by Mr. Rick Seymour. 2 week IR rats and MI rats that were imaged with FDG and rest/stress [^{13}N]NH_3 underwent surgery by Dr. Stephanie Thorn. All other rats that were imaged had IR or MI induced by Mr. Rick Seymour.

The same surgical method was employed as the above-mentioned surgery but without the PE50 tubing and as described by Higuchi et al. (2008). The ligation was permanently kept in place after the chest cavity was closed and sutured. Animals were recovered on high oxygen and analgesics. Sham animals underwent the same surgery with open chest cavity but no ligation was performed.

2.2 Echocardiography

Technical acquisition on echocardiography was performed by Marika Kolajova. Echocardiography was conducted using Vevo 770 high-resolution imaging system (VisualSonics, Toronto, Ontario). Rats were anesthetised with isoflurane (1-3%). Chest and stomach hair were removed. Parasternal long and

short axis views were recorded in B and M mode. Motion of the heart walls was recorded with summative cardiac cycles in ECG-based kilohertz visualization (EKV) mode (Cherin et al. 2006). A 716B scanhead was used with transducer frequency of 23.5 MHz, focal length of 17.5 mm and field of view at 32 mm. M-mode was used to inspect wall motion defects, if present. Analysis of B-mode EKV cine loops measured the dimensions of the myocardium during systole and diastole for calculations of ventricular volume. Measured dimensions allowed for the calculation of ejection fraction (EF), fractional shortening (FS), stroke volume (SV), and LV mass using manufacturer software (Vevo 770 3.0.0, Visual Sonics).

2.3 PET Imaging

All PET image acquisition was completed in collaboration with Dr. Stephanie Thorn, Marika Kolajova, Christine Archer, Julia Petyrk, Dr. Etienne Croteau and radiochemistry staff. PET image analysis was completed with the supervision of Dr. Rob de Kemp and Jennifer Renaud.

2.3.1 [^{13}N]NH_3 PET Imaging

Rats were anesthetised with isoflurane (1-2%) and placed on scanning bed of the Siemens Inveon™ small animal PET scanner (Siemens, Knoxville, TN; 12.7 cm axial field-of-view, spatial resolution < 1.4 mm). [^{13}N]NH_3 (44.4-74 MBq (1.2-2.0 mCi)) bolus injection was administered over 30 seconds (< 1.0 mL volume) via 26 G catheter inserted into the tail vein. List-mode data was gathered over 30 min followed by a 10 min transmission scan. PET data was acquired into 20 frames (12 x 10 sec, 3 x 60 sec and 5 x 300 sec), reconstructed on a 128 x 128

image matrix with 0.34 x 0.34 x 0.80 mm pixel size with expectation maximization 3D/maximum a posteriori (OSEM3D/MAP; β=1.0 OSEM3D iterations=2 MAP iterations=18). Corrections were applied for dead-time, isotope decay, detector efficiencies, randoms, scatter, and attenuation for image reconstruction. Data analysis and LV orientation was done with in-house software FlowQuant©. Myocardial blood flow (mL/min/g) polar maps were generated using the 0.5-2.5 min data and a one compartment model with constant distribution volume estimation.

2.3.2 Rest-Stress Dobutamine [^{13}N]NH_3 PET

Rats were anesthetised with 2% isoflurane and underwent a rest [^{13}N]NH_3 scan as described above. After a 1 hour washout of [^{13}N]NH_3 from the rest scan, the rats underwent dobutamine stress [^{13}N]NH_3 scan as previously described (Croteau et al. 2004). Dobutamine (Novophram) was administered in a 3 stepwise increase progression, 5 μg/kg/min for 2 min, 10 μg/kg/min for 2 min, 20 μg/kg/min for 9 min. [^{13}N]NH_3 bolus containing 44.4-125.8 MBq (1.2-3.4 mCi) was injected at the 9th minute of dobutamine infusion when the rat heart rate is at its peak.

Analysis of [^{13}N]NH_3 PET was conducted on IR rats 2.5, 4, and 5 weeks post-surgery in 20 min IR rats. Anterolateral flow [stress/rest] (ratio reserve) and [stress – rest] (delta reserve) were subtracted from contralateral LV wall of the same rat (Figure 2.4). With this methodology, Sham rats would theoretically have the same ratio and delta reserve values in anterolateral LV and contralateral LV

wall, as the healthy heart increases blood flow uniformly throughout the LV. Thus, subtracting anterolateral ratio and delta reserve from contralateral (inferoseptal) in shams would produce an expected value of zero. Stenosis in the anterolateral wall impairs flow during stress, making the ratio reserve and delta reserve values smaller compared to normal myocardium. Anterolateral wall ratio and delta reserves subtracted from the normal, remote myocardium of the contralateral (inferoseptal) wall of the same rat would theoretically produce a negative value. The greater the ischemia, the less blood flow to the anterolateral wall, thus the difference between anterolateral and contralateral reserves would be greater (more negative).

2.3.3 FDG PET Imaging

2-4 days post 45 min IR surgery, rats (n=4) underwent FDG PET to assess myocardial viability and potential of further model development. Rats were anesthetised with 2% isoflurane and injected via tail vein with 40.7-44.4 MBq (1.1-1.2 mCi) of activity. Tracer uptake was 1 hr prior to a 10 min static scan of the LV.

2.4 Histology

Hearts were dissected out following animal sacrifice while being perfused with the preservative paraformaldehyde (4%). Tissue slides were stained using standardized methods for Masson Trichrome and Hematoxylin/Eosin stains by technical services of the pathology and laboratory medicine department at the University of Ottawa. These procedures included fixation in 10% neutral buffered

formalin and a 20:1 fixative ratio. Automatic tissue processing into 5 μM slices was completed at room temperature. Imaging of slices was performed with Lecia microscope using Leica workstation software (Leica Microsystems Inc., Richmond Hill, Ontario).

2.5 Western Blot

All Western Blots were reproduced by Marika Kolajova. PDE4 and β-AR protein expression were assessed with immunoblotting techniques using Bio-Rad Western Blot system (Bio-Rad Laboratories, Ltd., Mississauga, Ontario) according to manufacturer's instructions. Hearts were excised, and the LV was separated into area at risk, border zone, or remote myocardium (Figure 2.2) for IR rats, and infarct, peri-infarct, and non-infarcted areas of MI rats. Areas at risk and infarct zones were determined as uniform in discoloration and consistency. Border zone and peri-infarcted areas were defined as the heterogeneous area surrounding the area at risk/infarct that separated it from visibly normal myocardium. Visibly normal myocardium was dissected and labeled as remote myocardium in IR rats and non-infarct in MI rats. Sham tissue was dissected from identical areas of LV and was of similar mass. Tissue samples were frozen and powdered with mortar and pestle in liquid N_2. 100-400 mg powdered tissue was homogenized (2 x 15 sec with polytron homogenizer) in approximately 500-700 μL of lysis buffer (25 mM Tris-HCl, 2% Triton X100, pH 7.8), complete protease inhibitor cocktail (Roche Canada, Mississauga, Ontario) and lysed for 20 min on ice. Sample lysates were centrifuged for 10 min at 12,000 g and aliquots

were taken for storage at -80^{o}C. Pierce Bicinchoninic acid (BCA; Novagen, San Diego, USA) was used to determine protein concentration of lysate. Sample lysates were diluted in 2x Sample Buffer (10% Sodium dodecyl sulfate (SDS), Glycerol, 1M Tris (pH 6.8), 1% bromphenol blue, 3.08% w/v DL-dithiothreitol), boiled for 3 min (except samples for PDE4D blotting, which were heated at 56^{o}C for 3 min) and pulse centrifuged at 9,500 x g. Lysates were injected onto 8% Tris-glycine reducing gel and underwent SDS-PAGE. After separation on gel at 150 V for ~65 min, protein was transferred to polyvinylidene fluoride (PVDF) membranes for ~20 hours at 43 V and 0.12 A. After transfer, protein was treated with blocking solution (150 mM NaCl, 10 mM Tris, 1% Tween 20 and 5% milk, pH 8) for 1 hr. Incubation with primary antibody was done at manufacturer-recommended dilutions and duration (listed below). Secondary antibody incubations (listed below) were administered at recommended dilutions for 1 hr. Absorbed antibodies were visualized with horseradish peroxidase-conjugated groups on the secondary antibodies with enhanced chemiluminescence substrate (Western Lighting® Plus-ECL, Perkin Elmer Inc., Waltham, MA, USA). Imaging was conducted with FluoroChem HD image station (Alpha Innotech, San Leandro, CA). Image analysis was conducted with AlphaEase FC IS-990 software (Alpha Innotech). Data was expressed as ratios of target protein to glyceraldehyde-3-phosphate dehydrogenase (GAPDH) protein band intensity, and normalized to mean sham control for each PVDF membrane.

Antibodies: all antibodies used were prepared in 2.5% milk/Tris buffered saline with Tween 20 (TBST, except β1-AR was in 2% bovine serum albumin

(BSA)) and at the following dilutions and sources: PDE4A, 1:1000, FabGennix International Inc., Product #PD4 112AP. PDE4B, 1:1000, Santa Cruz Biotechnology, Product #sc-25812. PDE4D, 1:200, Santa Cruz Biotechnology, Product #sc-25814. β_1-AR, 1:1000, Abcam, Product #ab3442. β_2-AR, 1:200, Santa Cruz Biotechnology, Product #sc-570.β_3-AR, 1:200, Santa Cruz Biotechnology, Product #sc-1473. GAPDH, 1:5000, Santa Cruz Biotechnology, Product #sc-25814. Goat anti-rabbit IgG-HRP, 1:5000, Santa Cruz Biotechnology Product #sc-2004. Donkey anti-goat IgG-HRP, 1:5000, Santa Cruz Biotechnology Product #sc-2020, Lot# F1212. Donkey anti-mouse IgG-HRP, 1:5000, Santa Cruz Biotechnology Product #sc-2314, Lot# C2012.

2.6 PDE4 Enzyme Assay

All PDE4 activity assay experiments were performed by Marika Kolajova. PDE4 activity, the rate of hydrolysis of cAMP (ρmol/min/g), in cardiac tissue was measured with PDE4 Enzymatic Assay Kit (PDEasy-200, FabGennix; Frisco, Texas) based on previously described methods (Thompson and Appleman, 1971). Tissue was excised from the rat after sacrifice, frozen and powdered with mortar and pestle in liquid N_2. Samples were stored at -80^{o}C. The same homogenization protocol was conducted with Western Blot as mentioned above but with SolO buffer (FabGennix) replacing lysis buffer. Sample protein was added to incubation buffers and blocked samples included 50 mM (R/S) Rolipram. [^{3}H]cAMP substrate at 1 µM final concentration was incubated 10 min with shaking at 34^{o}C. PDE4 hydrolysis of cAMP was terminated by boiling

samples for 3 minutes. The lysis reaction produces 5'-AMP and is then converted to [^{3}H]adenosine with western diamondback rattlesnake venom (*Crotalus Atrox*). [^{3}H]adenosine was separated from [^{3}H]AMP and [^{3}H]cAMP with pre-activated ion exchange resin (FabGennix). Ion exchange resin was added to each tube, vortexed and incubated on ice for 20 min. Tubes were then centrifuged at 13,000 x g for 2 min. The supernatant contained unbound [^{3}H]adenosine only and was removed, mixed with scintillation fluid (BCS-NA scintillation cocktail, Amersham), and quantified with β-scintillation counter (1219 RackBeta liquid scintillation counter, LKB Wallac, Perkin-Elmer). The separation of [^{3}H]AMP and [^{3}H]cAMP, and subsequent scintillation measurement provided the fractional amount of hydrolysed product, and thus total PDE activity. PDE4 activity was calculated as the fraction of PDE hydrolysis of cAMP inhibited by 50 μM Rolipram, and expressed as ρmol of cAMP hydrolyzed per minute per mg of protein.

2.7 Cardiac NE Concentration

Cardiac NE measurements (ng/mg of protein) were completed in equal collaboration with 4th year research student Ehsen Tayyabi. Samples of 100-400 mg of three LV regions were dissected out after sacrifice. Samples were separated into area at risk, border zone, or remote myocardium for IR animals and infarct, peri-infarct, and non-infarcted areas of MI rats. Areas at risk and infarct zones were determined as uniform in discoloration (fibrosis) and consistency. Borderzone and peri-infarcted areas were defined as the heterogeneous area

surrounding the area at risk/infarct that separated it from visibly normal myocardium (Figure 2.2). Visibly normal myocardium was dissected and labelled as remote myocardium in IR rats and non-infarct in MI rats. Sham tissues were dissected from identical areas of LV and were of similar mass. Samples were immediately placed on dry ice, later powdered with liquid N_2, homogenized in 1.5 mL 80/20 v/v ethanol and 0.1 M formic acid, then centrifuged at 14,000 x g. Supernatant was poured into conical flask and solvents removed with rotational evaporation at 60^{o}C. Residue on the walls of the flask was reconstituted with 1 mL 0.1 M formic acid, 1 mL 1.5 M Tris, 0.05 M Ethylenediaminetetraacetic acid (EDTA) (pH 8.5) and filtered (0.2 µM) prior to use with HPLC. Injection volume of sample was 100 µL with 250 µl of both 0.1 M formic acid and 1.5 M Tris, 0.05 M EDTA (pH 8.5).

Sample preparation was followed by injection onto column-switch HPLC static 1 mL loop as previously described by (Thackeray et al.2013). Pump 1 delivered 2 mL of 1.5 M Tris Base, 0.05 EDTA (1 mL/min) across capture column (Direct Connect refillable guard column, 2 × 20 mm, Alltech, Deerfield, IL, USA) packed with aluminum oxide (Type WA4, Sigma) to trap NE from sample, while removal of Tris, plasma proteins, and macromolecules was done with 10 mL of deionized water across the capture column at 1 mL/min. After rinsing, column flow was switched delivering NE sample towards the analytical column via mobile phase: 5/95 methanol / 50 mM ammonium formate, 0.27 mM EDTA, 0.346 mM octane sulfonic acid (pH 2.85, 1 mL/min). Elution from capture column to analytical column was terminated after 2 min. Eluents of both

columns were analyzed by two detectors: Ultraviolet (UV) absorbance detector and electrochemical detector (ECD). Signals from sample contents were integrated and converted to voltage using the PeakSimple 6-channel chromatography system. Chromatograms were then analyzed using PeakSimple 3.67 software. NE standards were run at varying concentrations (ng/mL) to create a standard curve and relationship ($r^2 > 0.999$) between NE concentration and area under curve (AUC) of ECD voltage peaks. Mass of NE obtained from AUC was corrected for dilutions, tissue mass, volume and mass lost from containers.

2.8 Plasma NE Concentrations

Blood samples were obtained from Sprague-Dawley rats by tail vein 26 gauge catheter under 2% isoflurane anaesthesia. Animals were under anaesthesia for no more than 5 minutes during total procedure as described by Popper et al. (1977). After collection, plasma was isolated by centrifugation at 1,600 x g for 4 minutes and kept at -80^{o}C. NE ELISA kit BA E-5200 (Labor Diagnostika Nord, Nodhorn, Germany) was used to measure NE in 50 uL of rat plasma. Briefly, NE was extracted using a cis-diol trapping gel, then acylated and enzymatically modified. The sample in suspension was removed from the extraction plate and incubated with primary antibody overnight at 4^{o}C. Samples were washed 4 x 5 min and then incubated with secondary antibody for 30 minutes. Next samples were washed 4 x 5 min and incubated with TMB to detect horseradish peroxidise on secondary antibody for 25 min. After incubation, absorbance was measured at 450 nm. Sample NE concentration was determined by referring to standard curve

absorbance and correcting for dilution. Concentrations calculated from the standard curve were multiplied by the correction factor of 0.2 because the volume of standards was 10 µL while volume of samples was 50 µL (10/50 = 0.2).

2.9 Statistical Analysis

All data are expressed as mean ± standard deviation (SD). Data was compared using unpaired two tailed student's t-test, or paired when appropriate. One-way ANOVA was used on all Western blot analysis (one per timepoint), followed by student's t-test when appropriate. Statistical analyses of the data presented in Fig 3.04 were done using one-way ANOVA with bonferonni post hoc. with $p < 0.05$ considered significant.

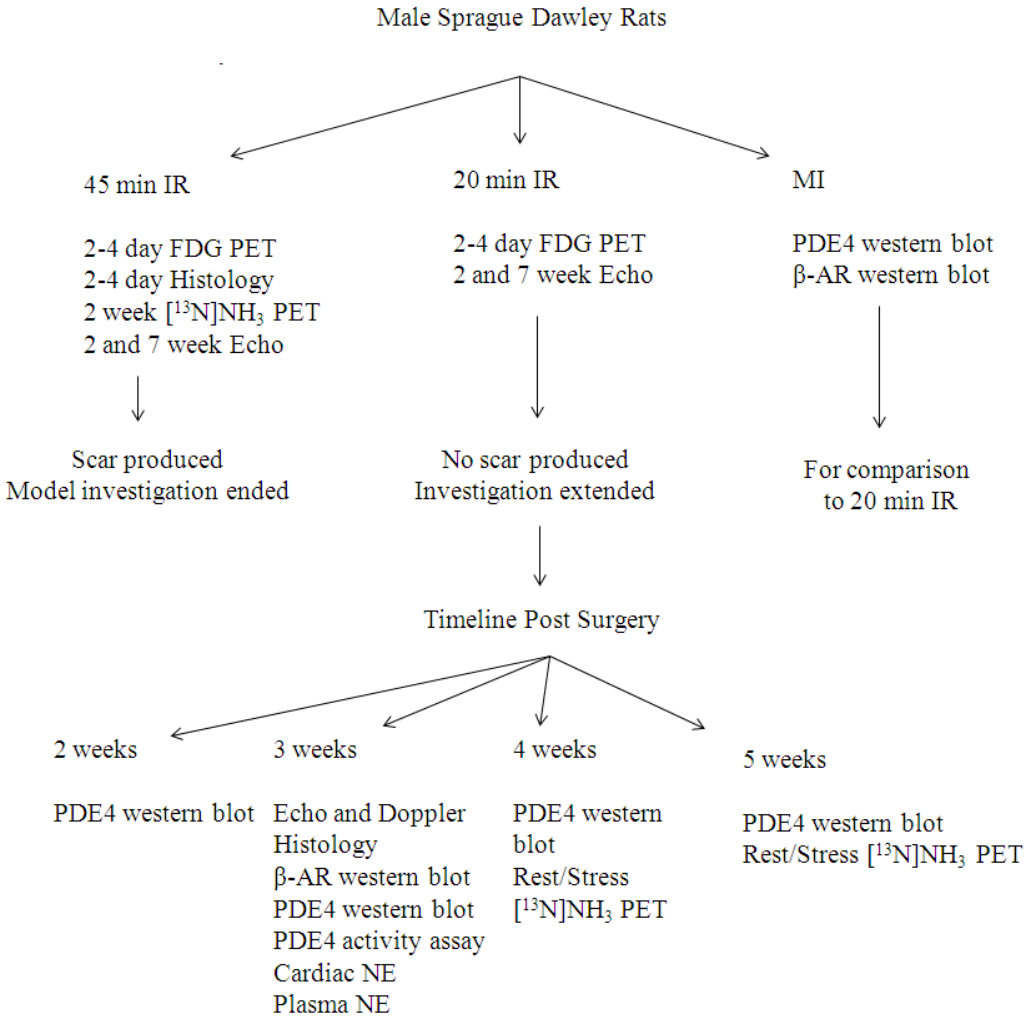

Figure 2.1: Experimental workflow throughout this thesis. The initial objective was to extend the work of McKasey (2012) with an IR rat model for the investigation of PET tracers that non-invasively measure SNS signalling. Both 20 min IR and 45 min IR models were investigated. 45 min IR rat displayed a small anterolateral infarct and was deemed too similar to MI for investigation within the scope of a master's thesis. 20 min IR rat model was observed to have no resting blood flow or glucose uptake defect and was selected for PDE4 protein level analysis from 2-5 weeks post-surgery. 3 weeks post-surgery displayed increased PDE4 protein expression and the investigation at this timepoint was extended to include the listed measurements of cardiac function and SNS activity. Abbreviations: β-AR , β-adrenergic receptor, FDG, 2-Deoxy-2-[^{18}F]Fluoroglucose, IR, ischemia reperfusion, MI, myocardial infarction, NE, norepinephrine, PDE4, phosphodiesterase 4, PET, positron emission tomography.

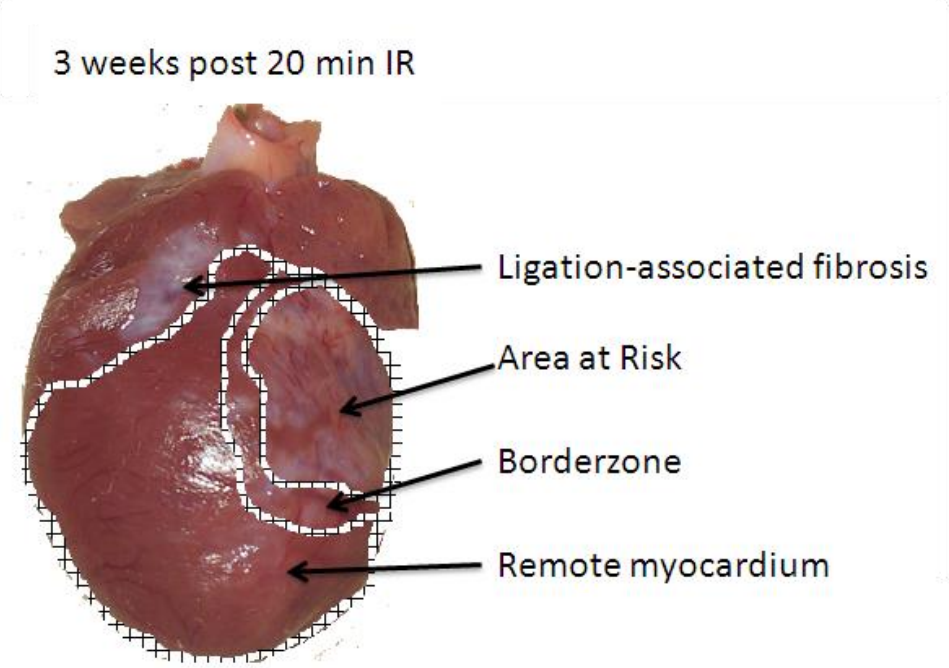

Figure 2.2: Representative photograph of 3 weeks post-surgery 20 minute ischemia-reperfusion rat post-mortem with area at risk, borderzone, and remote myocardium areas labelled for dissection. The suture is also labelled as it produces epicardial fibrosis by wound healing, not ischemia.

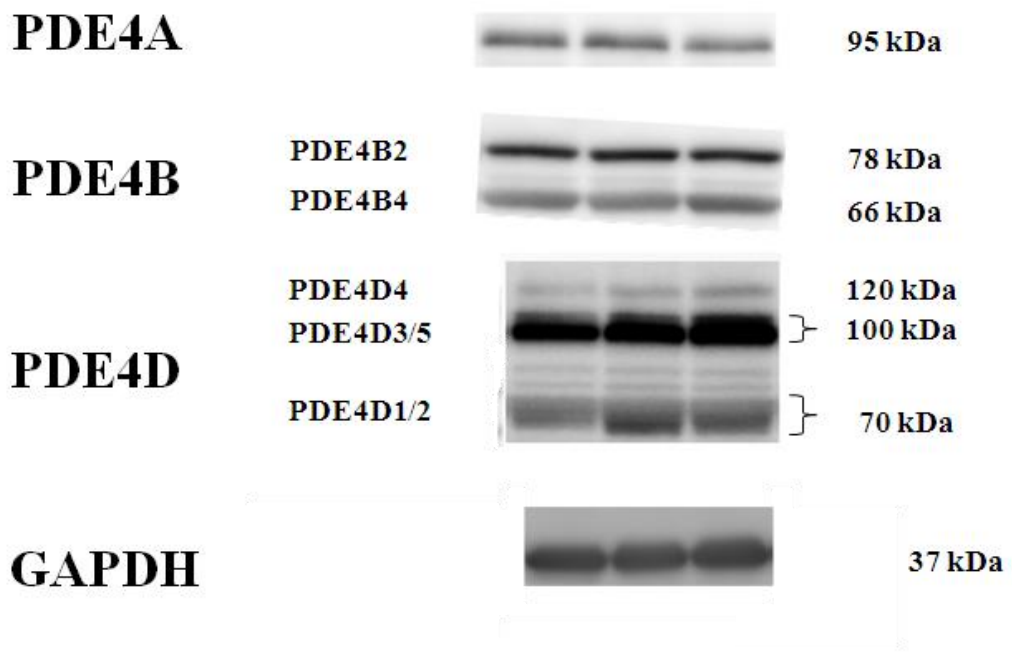

Figure 2.3: Representative Western blot, isoform, and molecular weight of PDE4A, PDE4B, PDE4D and GAPDH expression in rat LV homogenates. Molecular weights were determined from the literature, for review see Kenk (2010). Abbreviations: GAPDH, glyceraldehyde 3 phosphate dehydrogenase, kDa, kilodalton, LV, left ventricle, PDE4A, phosphodiesterase 4A, PDE4B, phosphodiesterase 4B, PDE4D, phosphodiesterase 4D.

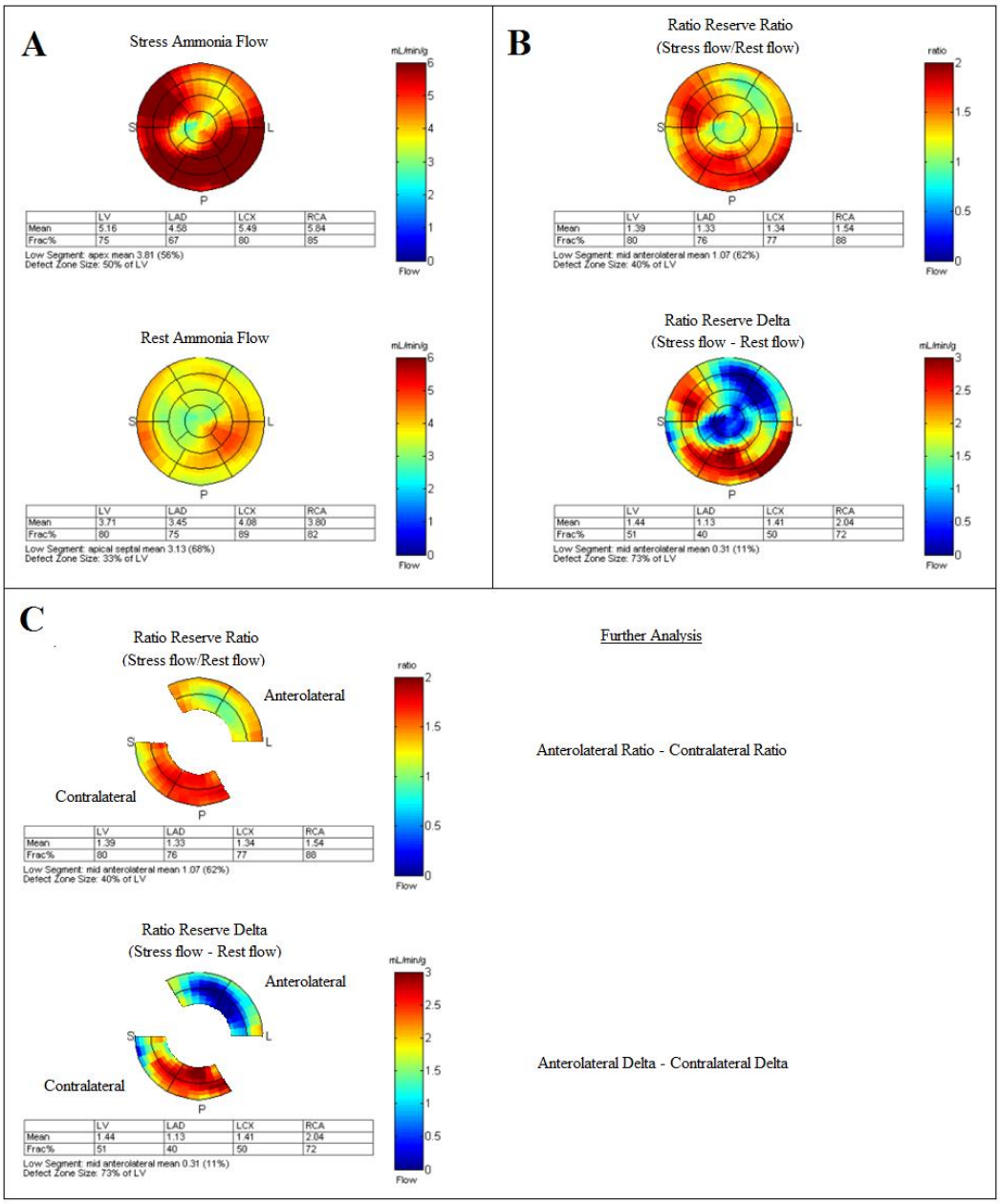

Figure 2.4: schematic of cardiac flow reserve analysis using [^{13}N]NH_3 PET example ischemic rat. 1 compartment model calculation of blood flow during [^{13}N]NH_3 PET was obtained in the first 2 minutes of scan time in both rest and stress, and flow (ml/min/g) data was exported into 17 segment model (A). Flow ratio reserve (Stress blood flow/Rest blood flow) was calculated in the anterolateral portion of the LV and subtracted from the flow ratio reserve in the contralateral LV zone while flow delta reserve (Stress blood flow – Rest blood flow) was calculated in the anterolateral portion (basal anterior, basal anterolateral, mid anterior, mid anterolateral zones of 17 segment) (B). Anterolateral ratio and delta flow reserve was subtracted from the respective contralateral LV portion from the same rat (C).

CHAPTER 3

Results

3.1 Imaging Models of IR with PET, Histology and Echocardiography to Assess Cardiac Dysfunction

Imaging was conducted on both 20 min IR and 45 min IR rat models to determine the extent of ischemia, viability, systolic and diastolic dysfunction present. The goal was to produce a model of cardiac dysfunction with no resting flow defect at rest for the future study of the area at risk with PET tracers.

3.1.1 Surgical Mortality and Contributions of Surgeons

During an initial pilot study (n=20), rats underwent 20 minute IR (n=3), 45 minute IR (n=4) and sham control (n=5). Mortality during the pilot study surgery performed by Dr. Stephanie Thorn, for 45 min IR rats was 7 out of 11 (63.6%) during the surgery. For 20 min IR rats in the pilot study mortality was 1 in 4 (25%) 2 weeks after surgery. Next a group (n=36) of 20 min ischemia-reperfusion (n=21), total ligation myocardial infarct (MI) (n=5) and sham (n=14) underwent surgery by Mr. Rick Seymour. Mortality was for MI rats was 1 out of 5 (20%) during the surgery, and 2 out of 21 (9.5%) for 20 min IR rats. All Western Blots, NE analyses, Doppler, and PDE4 activity assays were done on rats that underwent surgery performed by Mr. Rick Seymour. 2 week IR rats and MI rats that were imaged with FDG and rest/stress $[^{13}N]NH_3$ underwent surgery by Dr. Stephanie Thorn. All other rats that were imaged had IR or MI induced by Mr. Rick Seymour.

3.1.2 Echocardiography

Echocardiography was conducted on the LV to measure cavity dimensions during systole, diastole, cardiac output and mitral valve velocities, all

measurements of cardiovascular health. Within the pilot study, both 20 min (n=3) and 45 min IR (n=3) rat surgery (performed by Dr. Stephanie Thorn) produced anterolateral wall motion defect with significant left ventricle ejection fraction (LVEF) reduction ($p<0.05$) at 2 weeks and 7 weeks compared to Sham (Table 1). 20 min IR model was further investigated with Mr. Rick Seymour as surgeon. 20 min IR rats (n=12) showed no significant LVEF depression at 3 weeks (Table 2). There were no significant changes in stroke volume, diastolic or systolic volume (Figure 3.00). Mitral valve acceleration time in 20 min IR rats displayed a significant increase in E/A ratio compared to sham at 3 weeks (Figure 3.01) ($p<0.05$). These results indicate possible systolic dysfunction in 45 min IR rats and impaired diastolic filling in 20 min IR rats.

3.1.3 FDG and [^{13}N]NH_3 Positron Emission Tomography

FDG PET was performed on 45 min IR rats to analyze myocardial viability, 2-4 days post-surgery and exhibited consistent anterolateral infarct (Figure 3.02). This infarct zone was confirmed using FlowQuant© software at 2 weeks with both FDG and [^{13}N]NH_3 PET imaging (Figure 3.03). This was further analyzed and a myocardial blood flow and glucose defect match of 17% of the LV (n=4) in 45 min IR rats was observed (Figure 3.04). This region of poor uptake represents necrotic myocardium in 45 min IR rat LV.

3.1.4 Rest/Stress Dobutamine [^{13}N]NH_3 PET

Analysis of [^{13}N]NH_3 PET was conducted on IR rats 2.5, 4, and 5 weeks post-surgery in 20 min IR rats only to test myocardial reserve, an index of cardiovascular health (Table 3). Anterolateral flow stress/rest (ratio reserve) and

stress – rest (delta reserve) were subtracted from contralateral LV wall from the same rat. Sham exhibited close to zero difference in delta and ratio reserve, while IR rats had decreases in ratio and delta differences in anterolateral region compared to contralateral control (Figure 3.05). MI rats showed a very negative trend in both ratio reserve and delta reserve (Figure 3.05) and greater negative values than IR rats at every time point. For IR rats, 2.5 week IR had the most negative ratio and delta difference followed by 4 weeks and then 5 weeks though statistically these trends were not significant (ANOVA with $p>0.05$ considered significant)

3.1.5 Histology

Masson Trichrome histology is a stain that can image collagen *in vitro,* revealing the extent of fibrosis in the myocardium, if present. 3 weeks post-surgery, 20 min IR rats were dissected by area at risk, borderzone and remote myocardium (Figure 2.2). 45 min IR rat heart histology displayed non-transmural anterolateral infarcts with fibrotic scarring (Figure 3.06) confirming the infarct zone identified by PET imaging. Masson Trichome staining in 20 min IR rats at 3 weeks post-surgery display anterolateral epicardial fibrosis (Figures 3.07 and 3.08). Total ligation MI rats at 3 weeks post-surgery exhibit anterolateral transmural fibrosis and wall thinning (Figures 3.07 and 3.08).

		sham (n=5)	20 min (n=3)	45 min (n=4)
2 week	EF	75.324 ± 7.2%	*59.2 ± 4.9%	*56.9 ± 7.9%
	FS	58.632 ± 7.1%	40.9 ± 4.4%	40.59 ± 8.2%
7 week	EF	76.8 ± 10.0%	*60.3 ± 2.8%	*58.2 ± 8.7%
	FS	57.4 ± 10%	44.36 ± 2.9%	40.9 ± 10.4%

Table 1: Sham, 20 min IR, and 45 min IR EF and FS measured with echocardiography at 2 and 7 weeks post-surgery. All surgeries within this table were performed by Dr. Stephanie Thorn. Student's t-test was performed with $p < 0.05$ considered significant (*). Abbreviations: EF, ejection fraction, FS, fractional shortening, IR, ischemia reperfusion.

	Baseline			3 weeks post-surgery		
	EF	FS	E/A	EF	FS	E/A
n	6	6	3	6	6	3
Sham	77.5 ± 7.0%	59.53 ± 5.9%	1.07 ± 0.10%	75.7 ± 9.9%	56.7 ± 10.2%	1.14 ± 0.11
n	12	12	5	12	12	5
20 min IR	76.6 ± 5.7%	58.1 ± 6.0%	1.19 ± 0.14%	71.9 ± 13.8%	53.5 ± 13.1%	1.49 ± 0.20*

Table 2: Sham and 20 min IR rat model measurements of EF, FS and E/A ratio (mitral valve velocity at early (E) and atrial (A) peak flows) at baseline and 3 weeks post-surgery. All surgeries in the table were performed by Mr. Rick Seymour. Student's t-test was performed with $p < 0.05$ considered significant (*). Abbreviations: EF, ejection fraction, FS, fractional shortening, IR, ischemia reperfusion.

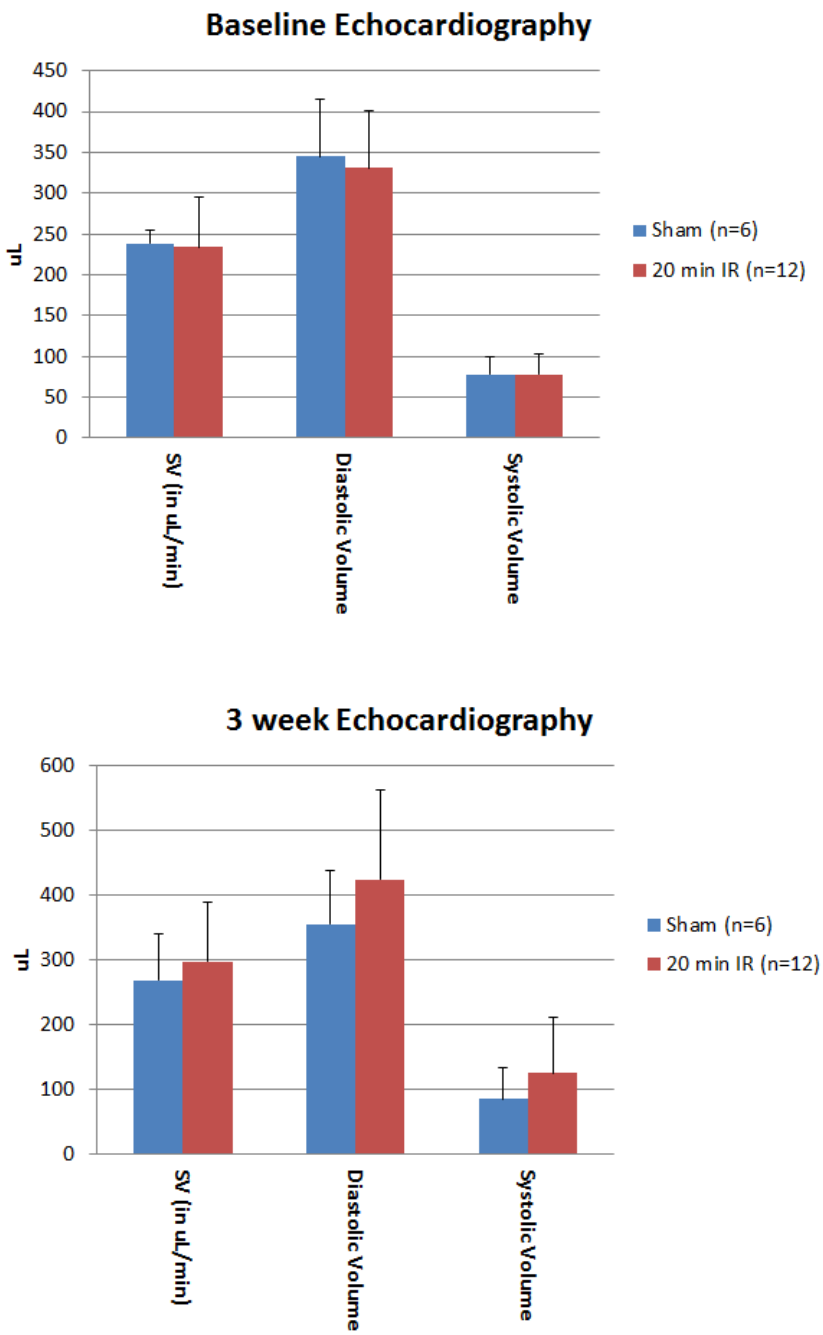

Figure 3.00: Echocardiography measurements of stroke volume (SV), diastolic volume and systolic volume at baseline and 3 weeks after surgery in sham and 20 min IR rat model. Abbreviations: IR, ischemia reperfusion, SV, stroke volume.

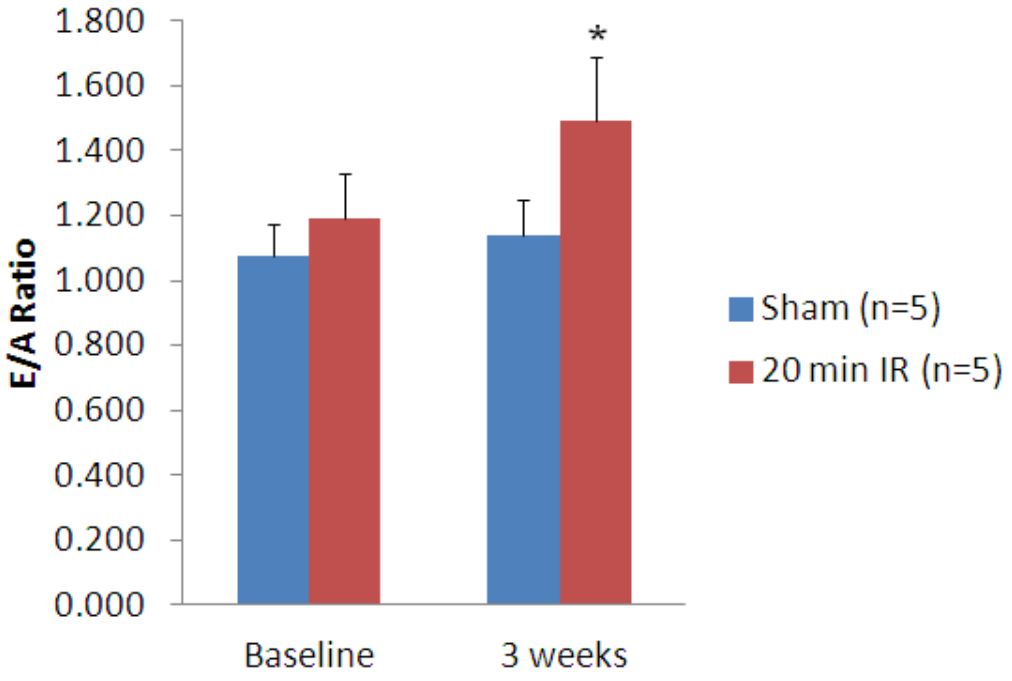

Figure 3.01: Sham and 20 min IR rat model measurement E/A ratio at baseline and 3 weeks post-surgery using Doppler echocardiography on the mitral valve in short axis view. E refers to the early peak flow velocity of blood through the mitral valve while A refers to the atrial or late peak flow velocity through the mitral valve. Student's t-test was performed with $p < 0.05$ considered significant (*). Abbreviations: IR, ischemia reperfusion.

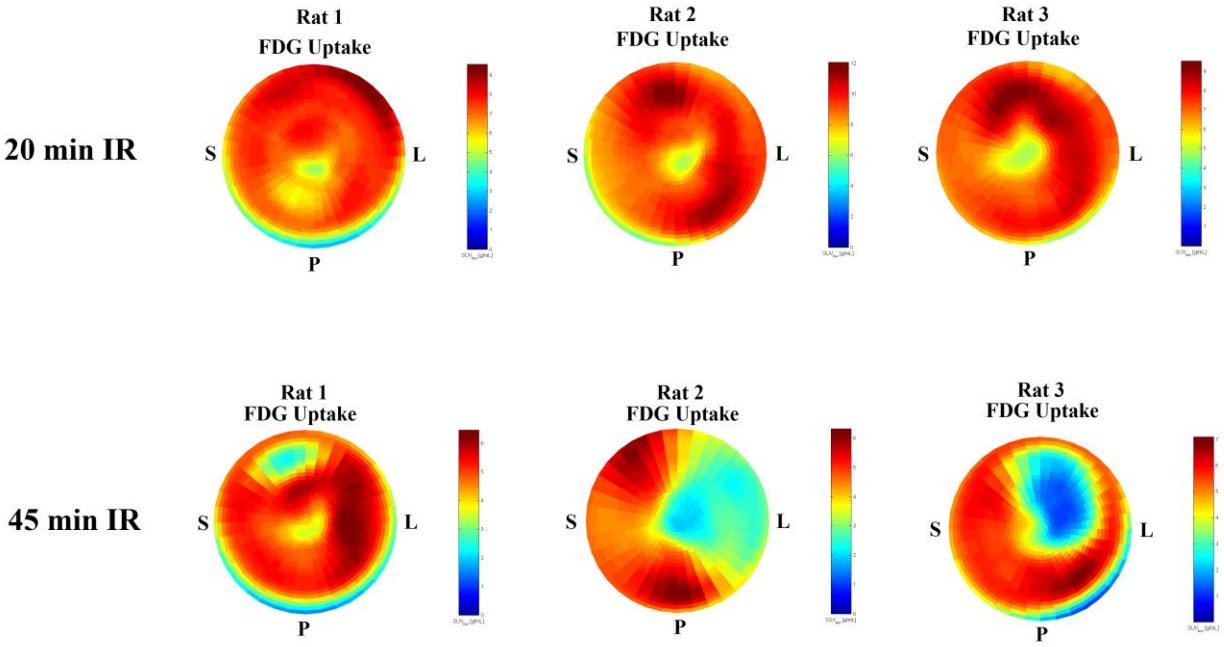

Figure 3.02: Left ventricle polar map uptake of [^{18}F]FDG measured by PET camera 2-4 days post 20 minute IR or 45 minutes IR surgery. S (septal wall), P (posterior wall), L (lateral wall). Abbreviations: IR, ischemia reperfusion, FDG, 2-Deoxy-2-[^{18}F]Fluoroglucose.

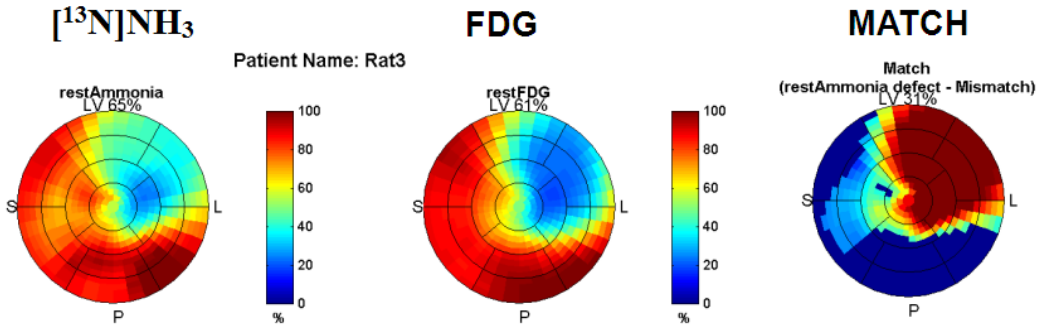

Figure 3.03: Polar map of LV [^{13}N]NH3 and [^{18}F]FDG uptake 2 weeks post-45 min LAD ischemia-reperfusion injury. Match polar map integration of the two tracers is also presented. Abbreviations: IR, ischemia reperfusion, LV, left ventricle, FDG, 2-Deoxy-2-[^{18}F]Fluoroglucose.

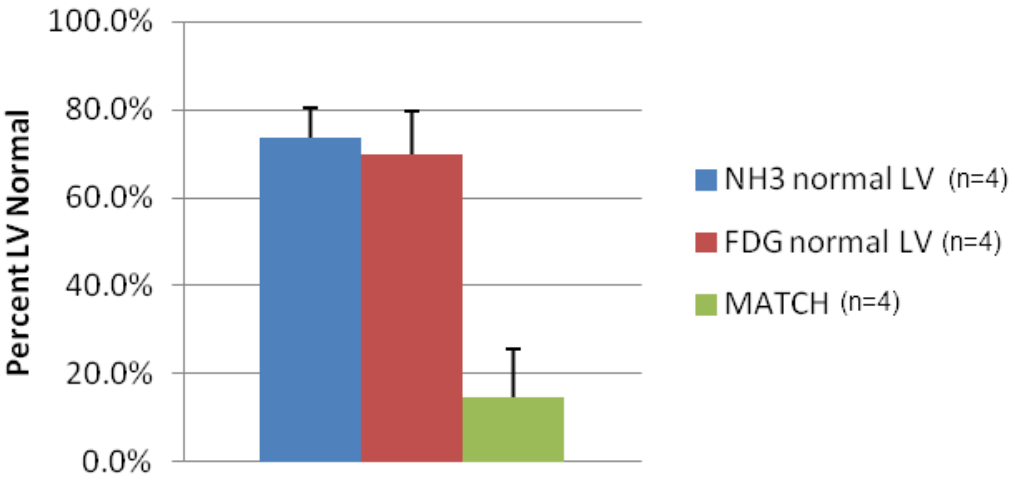

Figure 3.04: Quantification of % normal LV as measured by [^{13}N]NH_3 and FDG uptake 2 weeks post-45 min LAD ischemia-reperfusion injury. Abbreviations: LAD, left anterior descending [coronary artery], LV, left ventricle, FDG, 2-Deoxy-2-[^{18}F]Fluoroglucose.

	RATIO RESERVE			DELTA RESERVE		
	LAD	RCA	Δ	LAD	RCA	Δ
Sham						
Rat 12	2.02578	2.206501	-0.18072	3.180216	4.540846	-1.36063
Rat 14	1.674762	1.81352	-0.13876	2.080099	2.245749	-0.16565
Rat 19	1.270121	1.591623	-0.3215	0.963842	1.869578	-0.90574
Rat 22	1.808719	1.485085	0.323635	2.961849	1.648824	1.313025
Average	1.694846	1.774182	**-0.07934**	2.296501	2.576249	**-0.27975**
STDEV			0.279785			1.170486
MI						
Rat 1	0.959316	1.372154	-0.41284	0.107074	1.608561	-1.50149
Rat 3	1.236958	1.53336	-0.2964	0.13354	1.894454	-1.76091
Rat 6	1.682361	1.838592	-0.15623	2.175813	3.324596	-1.14878
Average	1.292878	1.581369	**-0.28849**	0.805476	2.27587	**-1.47039**
STDEV			0.128486			0.307248
2.5 week IR						
Rat 1	1.322412	1.565045	-0.24263	1.134173	1.891109	-0.75694
Rat 2	1.487657	1.706435	-0.21878	1.704521	2.669434	-0.96491
Rat 3	1.136416	1.164447	-0.02803	0.503427	0.711248	-0.20782
Rat 11	1.536919	1.632224	-0.09531	1.81416	2.398972	-0.58481
Average	1.370851	1.517038	**-0.14619**	1.28907	1.917691	**-0.62862**
STDEV			0.101851			0.320702
4 week IR						
Rat 11	1.246291	1.072706	0.173585	0.764242	0.215313	0.54893
Rat 12	1.658236	1.652384	0.005852	2.258247	2.500473	-0.24223
Rat 13	1.474365	1.559369	-0.085	1.407775	1.858671	-0.4509
Rat 14	1.489578	2.095406	-0.60583	1.38663	3.446032	-2.0594
Average	1.540726	1.769053	**-0.12785**	1.684217	2.601725	**-0.5509**
STDEV			0.336173			1.093996
5 week IR						
Rat 16	1.451799	1.463061	-0.01126	1.810852	1.812896	-0.00204
Rat 17	1.772814	1.824859	-0.05205	2.384839	2.302411	0.082428
Rat 18	1.121418	1.281461	-0.16004	0.165348	1.045808	-0.88046
Average	1.448677	1.523127	**-0.07445**	1.453679	1.720372	**-0.26669**
			0.076879			0.533214

Table 3: Raw data of Ratio and Delta reserve in the anterolateral LV, (LAD) and inferoseptal LV (RCA). Ratio reserve is the stress $[^{13}N]NH_3$ measured flow divided by the rest flow, and is unitless. Delta reserve is the $[^{13}N]NH_3$ measured flow is subtracted from the rest flow and is expressed in mL/min/g while ratio reserve is unitless. This data is graphed in Figure 3.04. Abbreviations: IR, ischemia-reperfusion, LAD, left anterior descending coronary artery, LV, left ventricle, MI, myocardial infarction, RCA, right coronary artery.

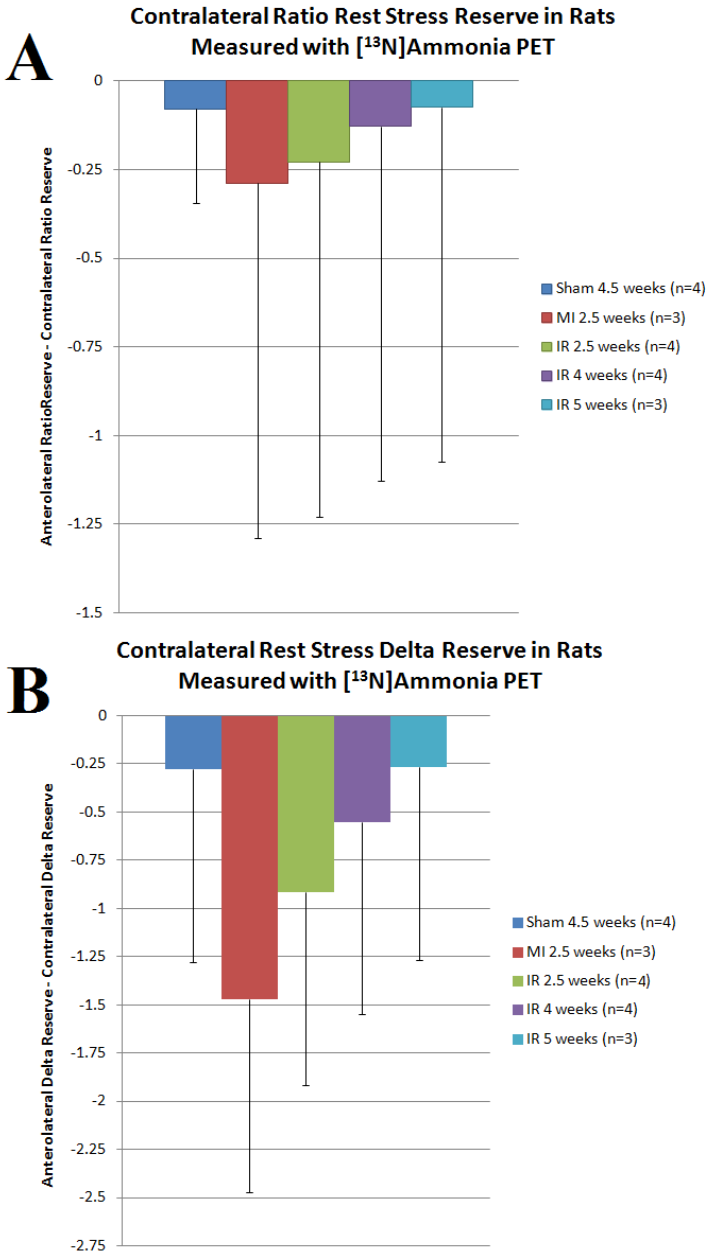

Figure 3.05: Cardiac flow reserve analysis using [^{13}N]NH_3 PET in 2.5, 4 and 5 week post IR rats. 1 compartment DV constant calculation of blood flow [^{13}N]NH_3 PET was obtained in the first 2 minutes of scan time, and flow (ml/min/g) data was exported into 17 segment model. (A) Flow ratio reserve (Stress blood flow/Rest blood flow) was calculated in the anterolateral portion of the LV and subtracted from the flow ratio reserve in the contralateral LV zone. (B) Flow delta reserve (Stress blood flow – Rest blood flow) was calculated in the anterolateral portion (basal anterior, basal anterolateral, mid anterior, mid anterolateral zones of 17 segment) of the LV and subtracted from the flow delta reserve in the contralateral. One way ANOVA was conducted with ($p<0.05$) considered significant. Abbreviations, IR, ischemia-reperfusion, LV, ischemia reperfusion, MI, myocardial infarction, PET, positron emission tomography.

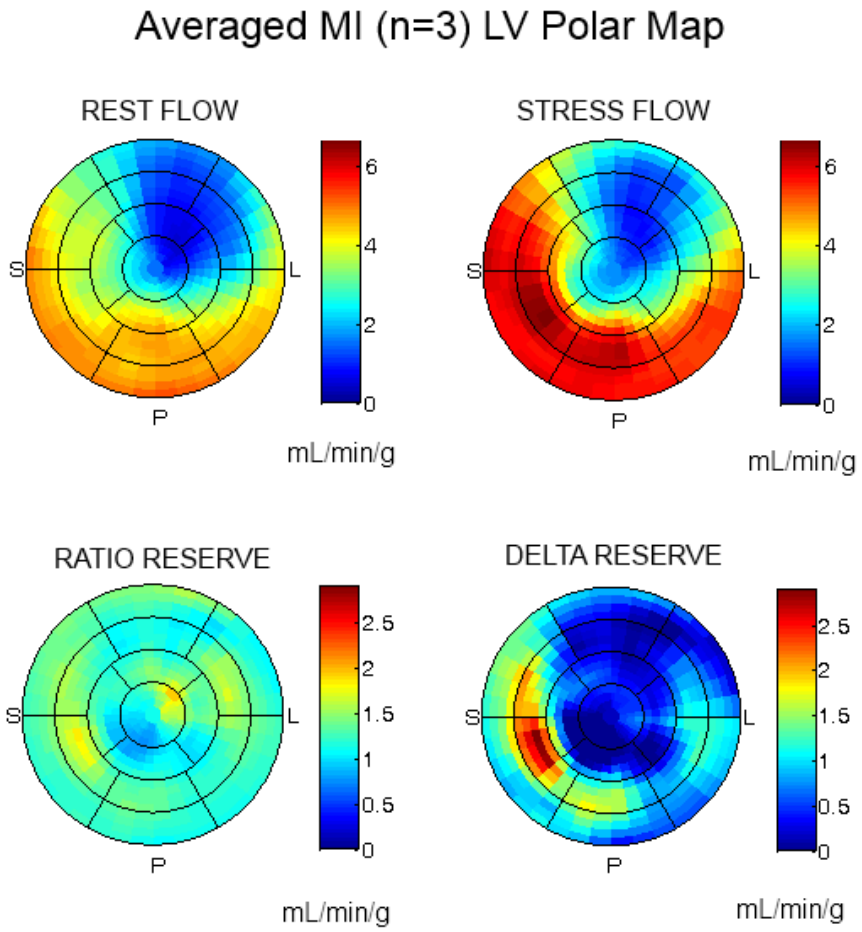

Figure 3.06: Compiled LV polar map of rats (n=3) using [^{13}N]NH_3 PET at 2.5 weeks post MI and analyzed with FlowQuant © software. Myocardial blood flow is expressed in mL/min/g of tissue. This data is part of Figure 3.04. Abbreviations: LV, left ventricle, MI, myocardial infarction.

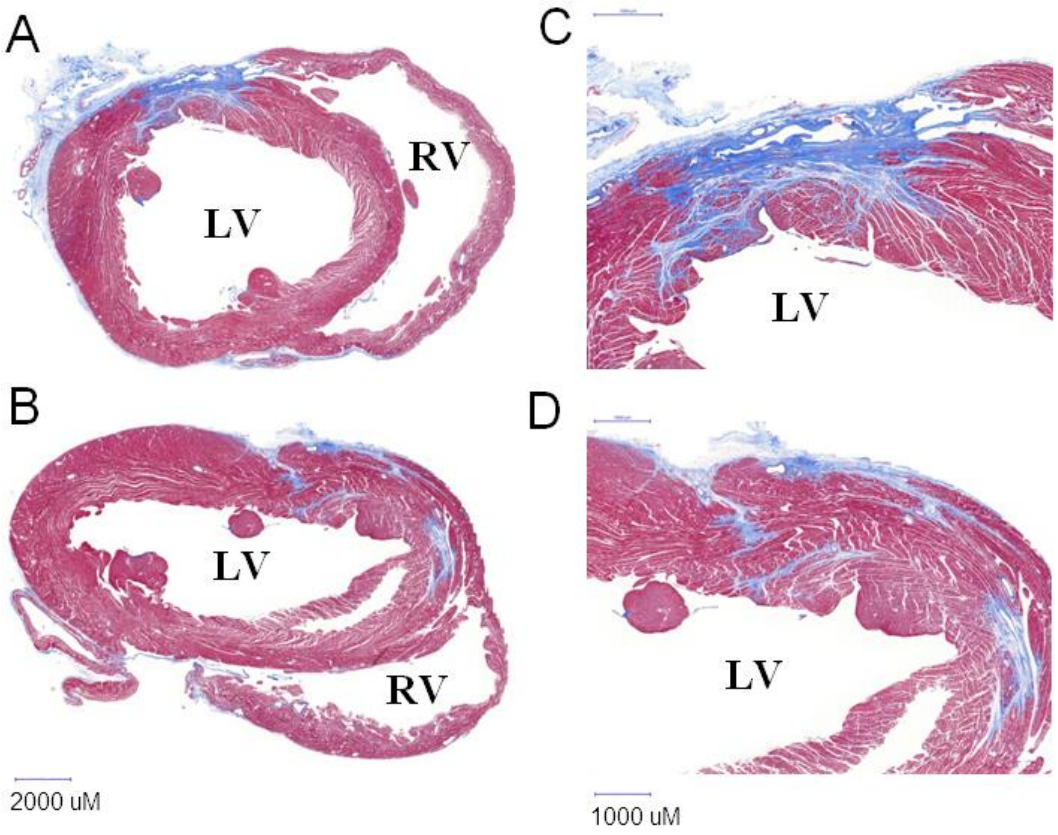

Figure 3.07: Masson Trichrome staining of 45 min IR rats, 2-4 days post-surgery, short axis rat cardiac slices (n=2). Panel A and B (1.0x magnification) and C and D (2.0x magnification) both show anterolateral fibrotic scarring in blue and normal myocardium in red. Abbreviations: LV, left ventricle, RV, right ventricle.

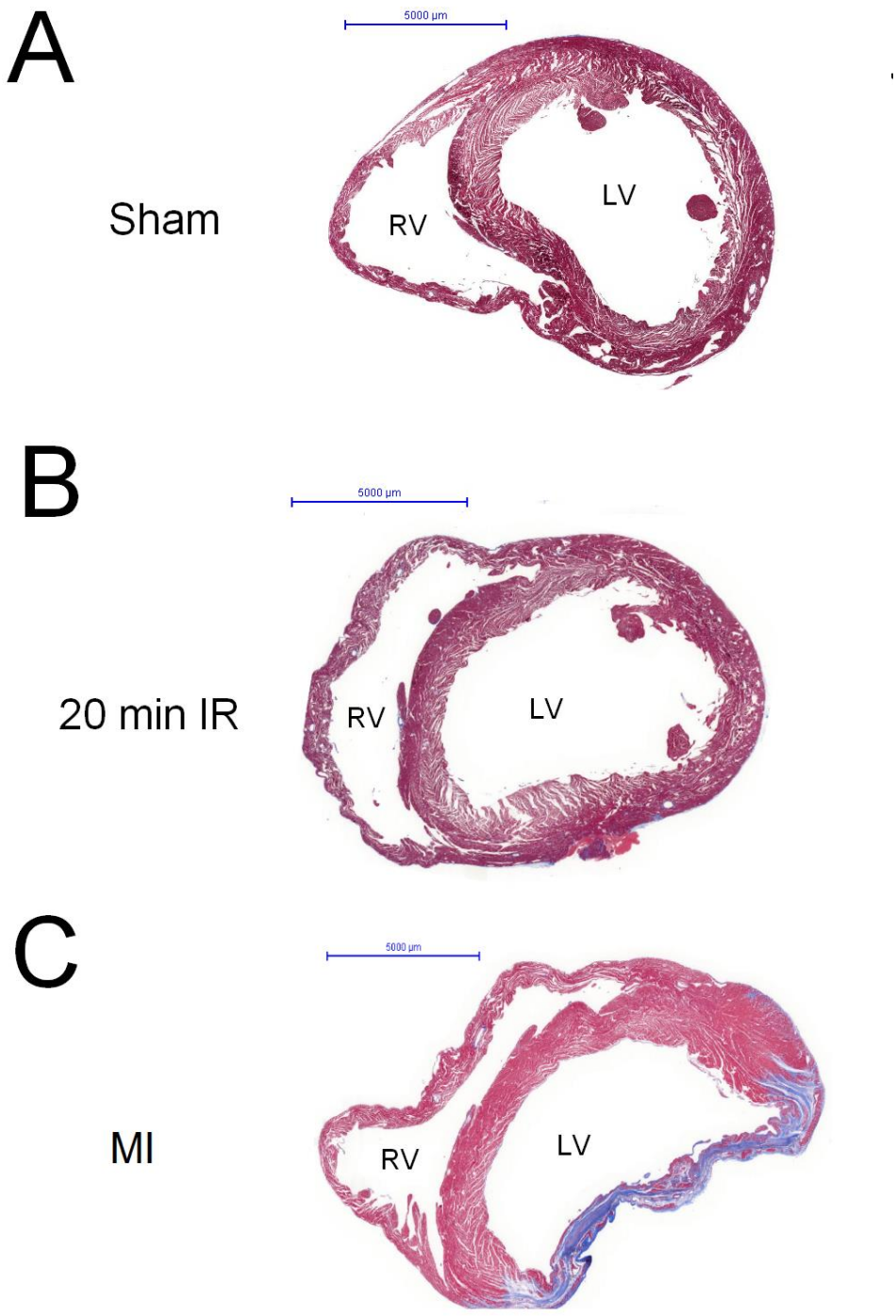

Figure 3.08: Masson Trichome staining of (A) Sham, (B) 20 minute ischemia-reperfusion, and (C) total ligation short axis rat cardiac slices (0.49x magnification) of left and right ventricle 3 weeks post-surgery. Anterolateral fibrotic scarring is shown in blue and normal myocardium in red Abbreviations: IR, ischemia reperfusion, LV, left ventricle, MI, myocardial infarction, RV, right ventricle.

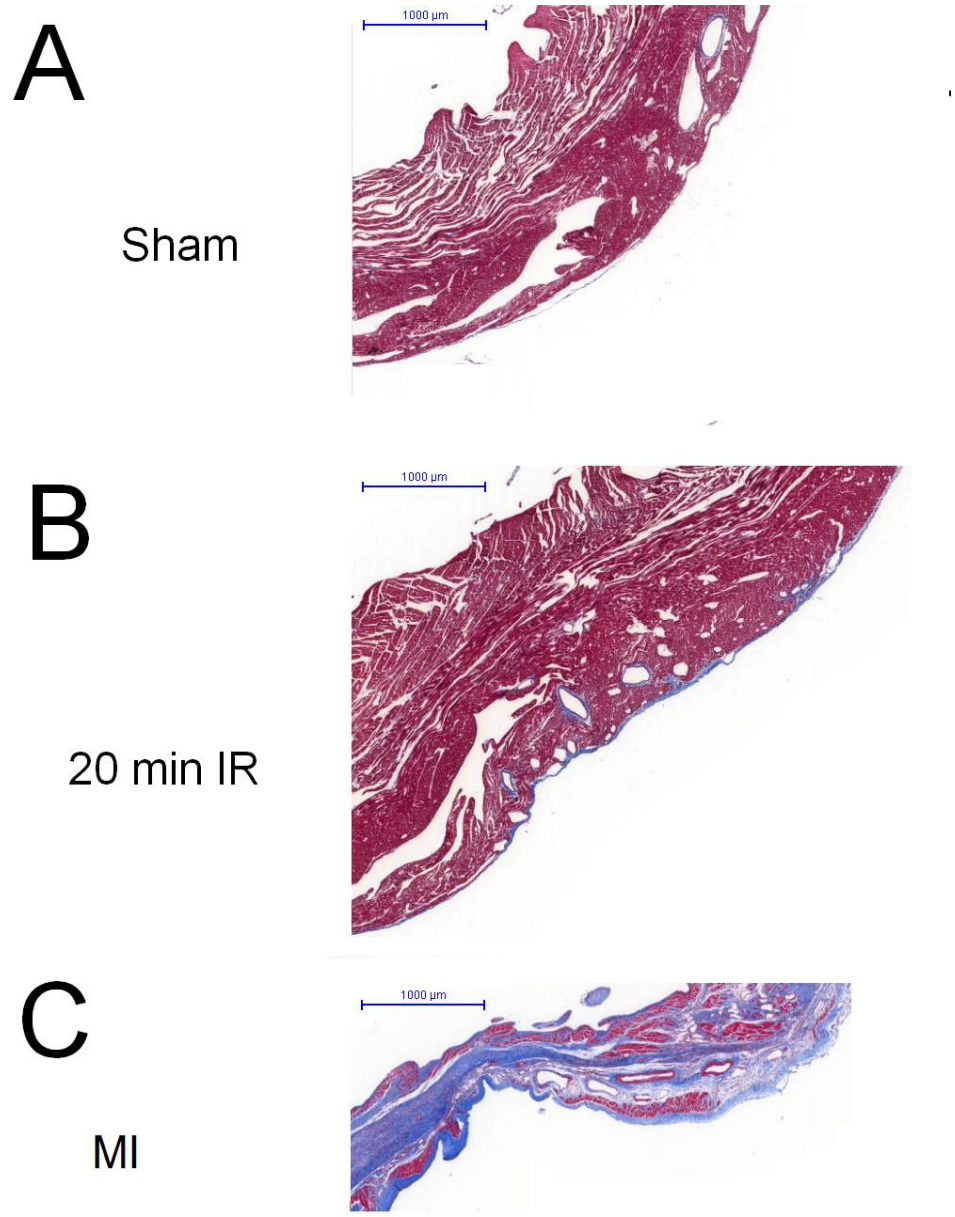

Figure 3.09: Masson Trichome staining of (A) Sham, (B) 20 minute ischemia-reperfusion, and (C) total ligation short axis rat cardiac slices (1.62x magnification) of anterolateral wall of left ventricle 3 weeks post-surgery. Anterolateral fibrotic scarring is shown in blue and normal myocardium in red. Abbreviations: IR, ischemia reperfusion, MI, myocardial infarction.

3.2 Western Blot of PDE4 20 min IR and MI 2-5 Weeks Post-Surgery

The 20 min IR rat model was selected for investigation of changes in PDE4 protein expression from 2-5 weeks, an important healing/remodelling phase after cardiac dysfunction. The heart was dissecting out into area at risk, border-zone and remote myocardium based on qualitative features shown in Figure 2.2. Differences in PDE4 protein expression may represent changes in cardiac health and/or SNS activity.

3.2.1 Representative Western Blots

PDE4 isoform identification was done by molecular weight in accordance with the literature (PDE4A: Abi-Gerges et al. 2009, Rena et al. 2001. PDE4B: Kostic et al., 1997, Richter et al., 2005, Shepherd et al. 2003. PDE4D: Bolger et al. 1997, Kostic et al. 1997, Richter et al. 2005) and all rats displayed unchanged GAPDH expression at all timepoints, shown by representative Western Blot (Figure 2.3).

3.2.2 Western Blot at 2 Weeks Post Surgery

At 2 weeks post-surgery, 20 min IR rats showed no significant downregulation of PDE4A, PDE4B or PDE4D in area of the myocardium (Figure 3.10, Figure 3.11).

3.2.3 Western Blot at 3 Weeks Post Surgery

PDE4A is significantly increased ($p<0.05$) in borderzone and remote myocardium, but not in the area at risk (Figure 3.12). 20 min IR rats showed significant increase ($p<0.05$) in the area at risk for PDE4B2, PDE4B4,

PDE4D1/2, PDE4D4, PDE4D3/5 isoforms (Figure 3.13). No significant changes in PDE4B or D expression were observed in the borderzone or remote myocardium 3 weeks post-surgery in 20 min IR rats (Figure 3.13).

MI surgery rats showed no change in PDE4A expression (Figure 3.14), PDE4B2 and PDEB4 expression significantly increased ($p<0.05$) in the infarct zone and PDE4B4 expression in the non-infarcted zone, PDE4D1/2 levels were significantly ($p<0.05$) increased in the infarct zone, while PDE4D3/5 was decreased in the peri-infarct zone ($p<0.05$) (Figure 3.15). All other PDE4D isoforms were unchanged.

3.2.4 Western Blot at 4 Weeks Post Surgery

20 min IR rats showed increased expression in PDE4A isoform in the remote myocardium only ($p<0.05$). No other significant differences were shown at 4 weeks post IR surgery compared to Sham (Figure 3.16, 3.17).

3.2.5 Western Blot at 5 Weeks Post Surgery

20 min IR rats displayed no changes in any PDE4 isoform expression at 5 weeks post-surgery compared to Sham (Figure 3.18, 3.19).

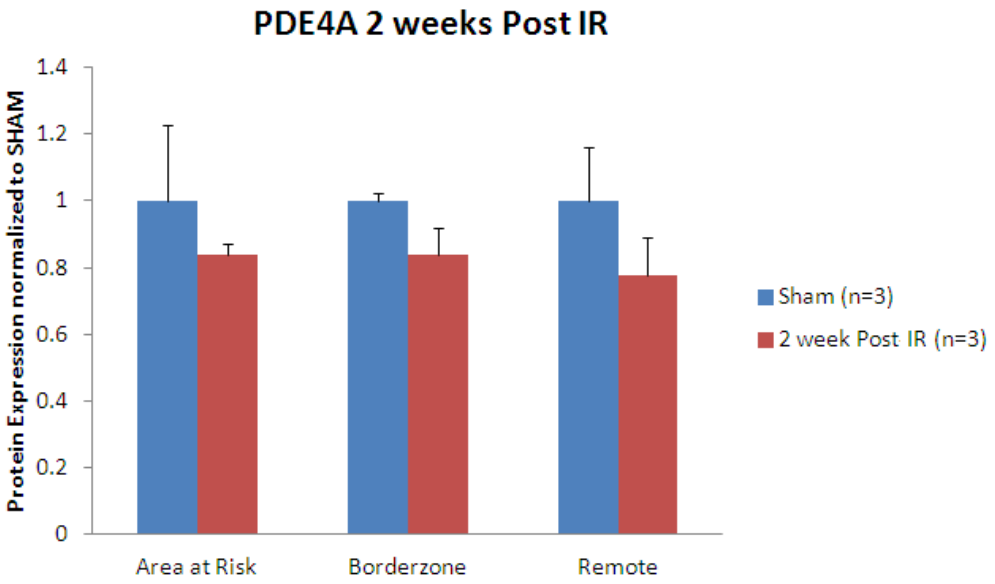

Figure 3.10: Western Blot quantification of PDE4A isoform expression in area at risk, borderzone, and remote left ventricle homogenates at 2 weeks post-20 min IR. Data is normalized to GAPDH, then expressed as a ratio to sham-treated controls. Student's t-test was performed with $p < 0.05$ considered significant (*). Abbreviations: GAPDH, glyceraldehyde 3 phosphate dehydrogenase, IR, ischemia reperfusion, PDE4A, phosphodiesterase 4A.

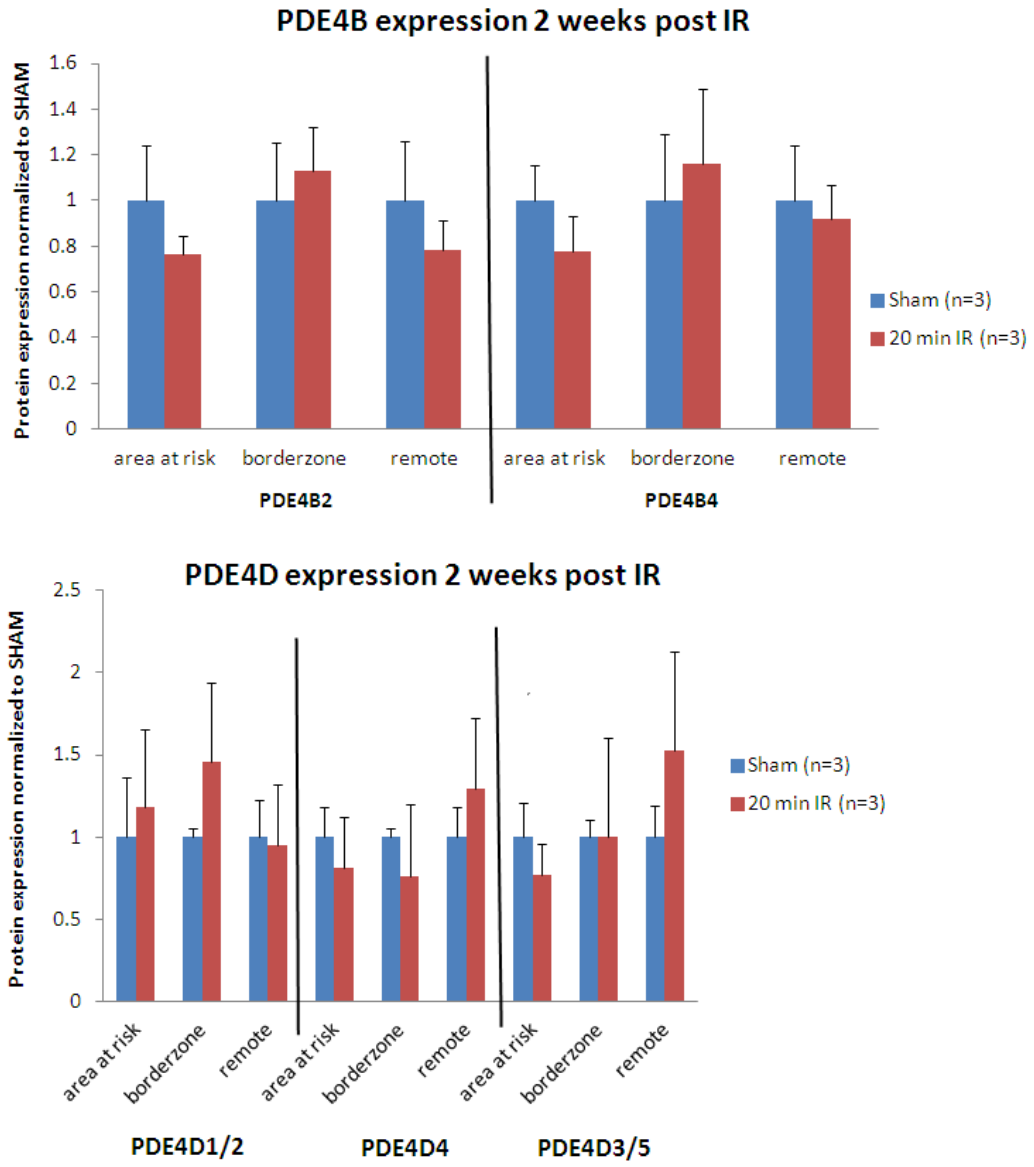

Figure 3.11: Western Blot quantification of PDE4B and PDE4D isoform expression in area at risk, borderzone, and remote left ventricle homogenates at 2 weeks post-20 min IR. Data is normalized to GAPDH, then expressed as a ratio to sham-treated controls. Student's t-test was performed with $p < 0.05$ considered significant (*). Abbreviations: GAPDH, glyceraldehyde 3 phosphate dehydrogenase, IR, ischemia reperfusion, PDE4B, phosphodiesterase B, PDE4D, phosphodiesterase 4D.

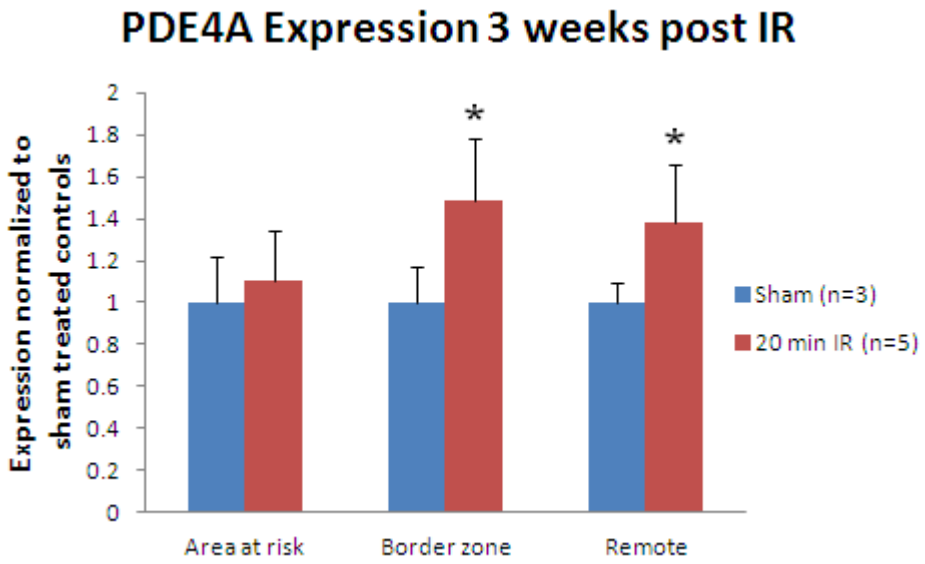

Figure 3.12: Western Blot quantification of PDE4A expression in infarcted, peri-infarcted and non-infarcted left ventricle homogenates at 3 weeks post-20 min IR. Data is normalized to GAPDH, then expressed as a ratio to sham-treated controls. Student's t-test was performed with $p < 0.05$ considered significant (*). Abbreviations: GAPDH, glyceraldehyde 3 phosphate dehydrogenase, IR, ischemia reperfusion, PDE4A, phosphodiesterase 4.

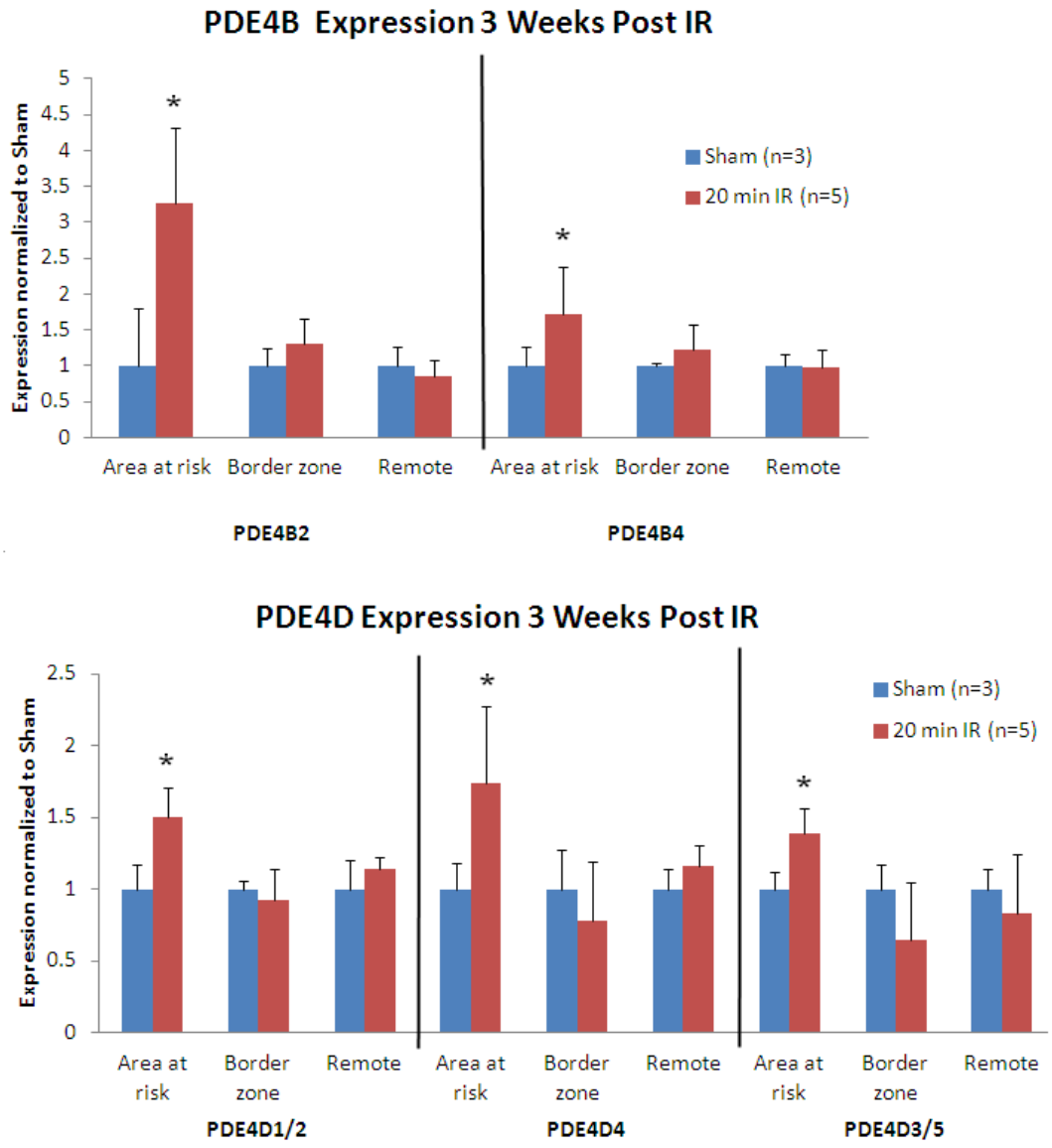

Figure 3.13: Western Blot quantification of PDE4B and PDE4D isoform expression in infarcted, peri-infarcted and non-infarcted left ventricle homogenates at 3 weeks post-20 min IR. Data is normalized to GAPDH, then expressed as a ratio to sham-treated controls. Student's t-test was performed with $p < 0.05$ considered significant (*). Abbreviations: GAPDH, glyceraldehyde 3 phosphate dehydrogenase, IR, ischemia reperfusion, PDE4B, phosphodiesterase 4B, PDE4D, phosphodiesterase 4D.

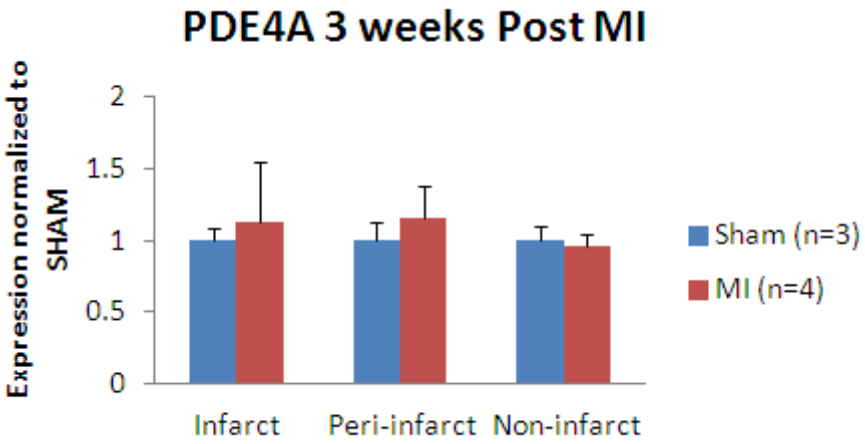

Figure 3.14: Western Blot quantification of PDE4A isoform expression in infarcted, peri-infarcted and non-infarcted left ventricle homogenates at 3 weeks post post LAD total ligation surgery. Data is normalized to GAPDH, then expressed as a ratio to sham-treated controls. Abbreviations; LAD, left anterior descending [coronary artery], GAPDH, glyceraldehyde 3 phosphate dehydrogenase, MI, myocardial infarction, PDE4A, phosphodiestase 4A.

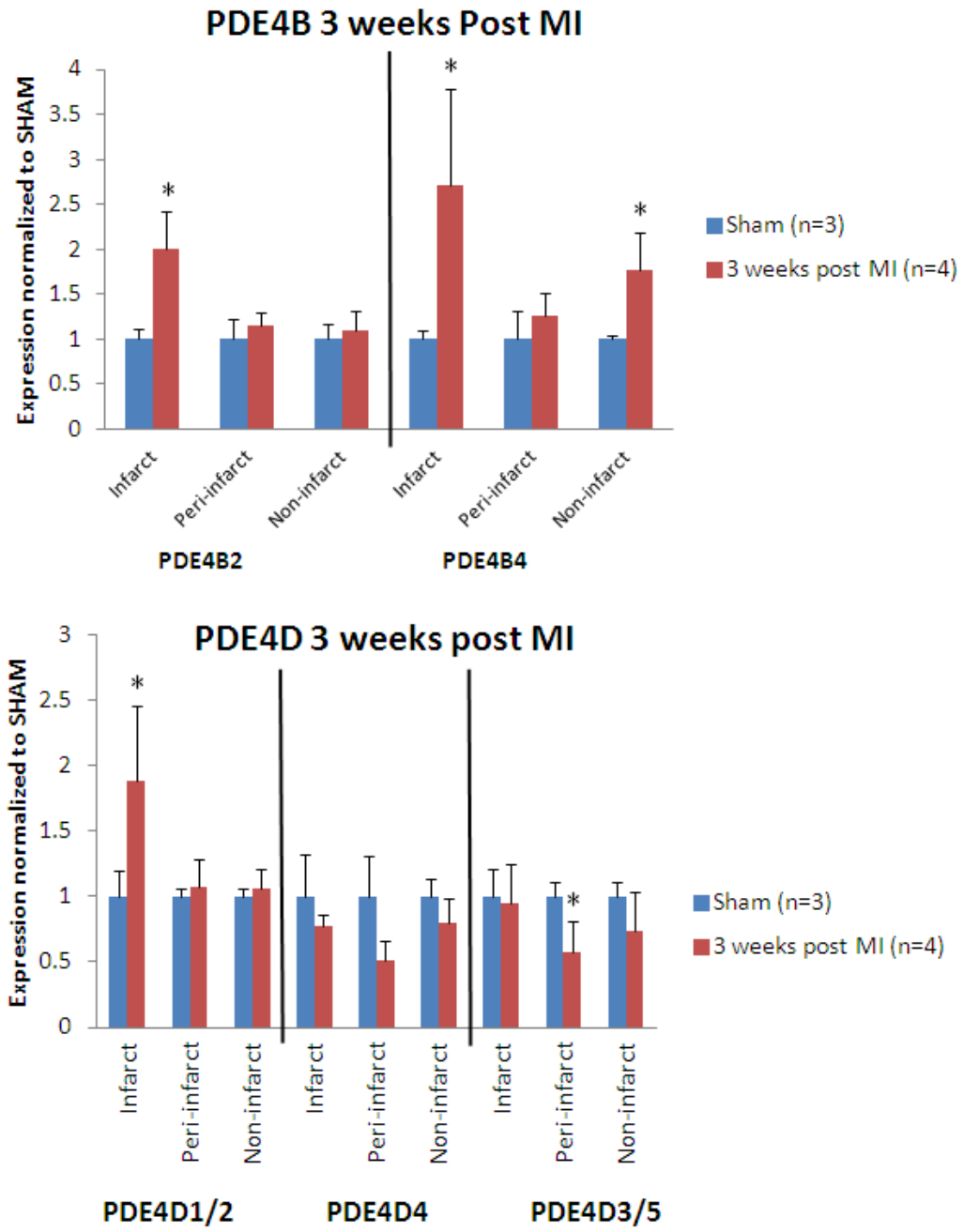

Figure 3.15: Western Blot quantification of PDE4B and PDE4D isoform expression in infarcted, peri-infarcted and non-infarcted left ventricle homogenates at 3 weeks post post LAD total ligation surgery. Data is normalized to GAPDH, then expressed as a ratio to sham-treated controls. Student's t-test was performed with $p < 0.05$ considered significant (*). Abbreviations; LAD, left anterior descending [coronary artery], GAPDH, glyceraldehyde 3 phosphate dehydrogenase, MI, myocardial infarction, PDEB, phosphodiesterase B, PDE4D, phosphodiesterase D.

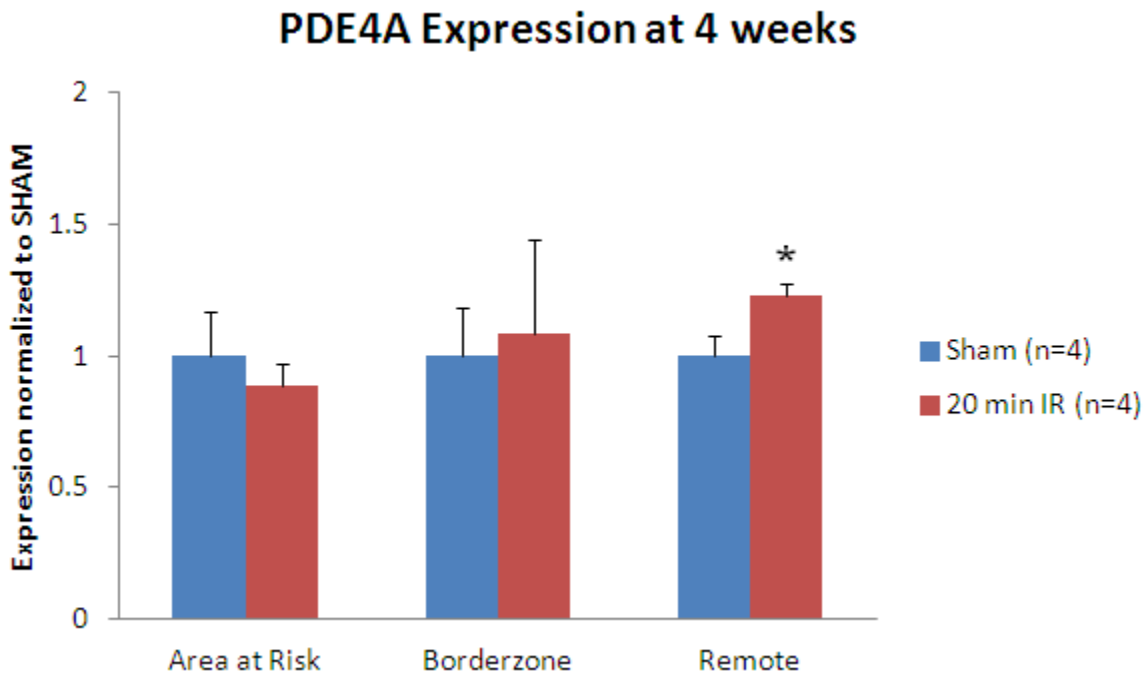

Figure 3.16: Western Blot quantification of PDE4A expression in area at risk, borderzone, and remote left ventricle homogenates at 4 weeks post-20 min IR. Data is normalized to GAPDH, then expressed as a ratio to sham-treated controls. Student's t-test was performed with $p < 0.05$ considered significant (*). Abbreviations; GAPDH, glyceraldehyde 3 phosphate dehydrogenase, IR, ischemia reperfusion, PDE4A, phosphodiestase 4A.

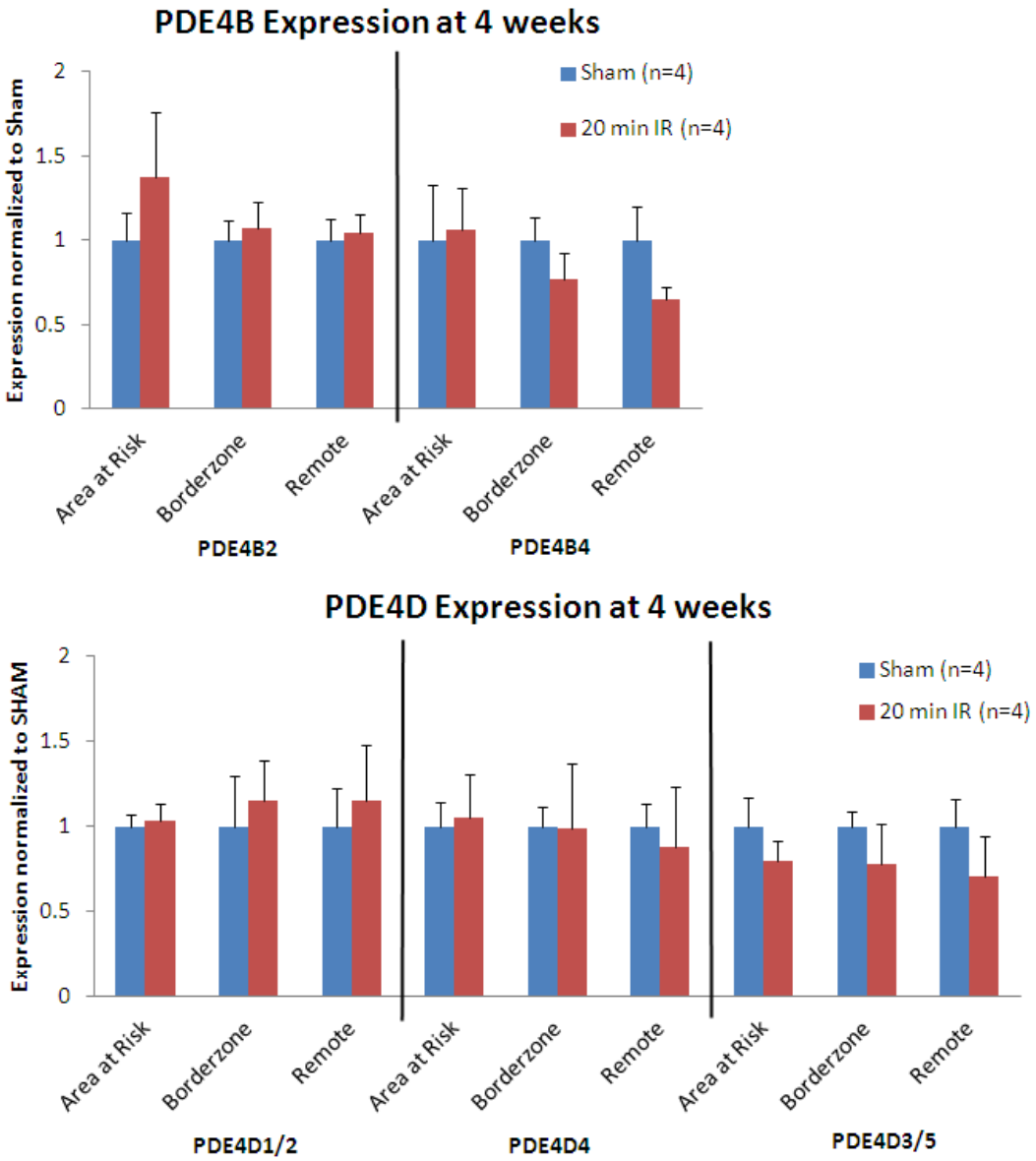

Figure 3.17: Western Blot quantification of PDE4B and PDE4D isoform expression in area at risk, borderzone, and remote left ventricle homogenates at 4 weeks post-20 min IR. Data is normalized to GAPDH, then expressed as a ratio to sham-treated controls. Abbreviations; GAPDH, glyceraldehyde 3 phosphate dehydrogenase, PDEB, phosphodiesterase B, PDE4D, phosphodiesterase 4D.

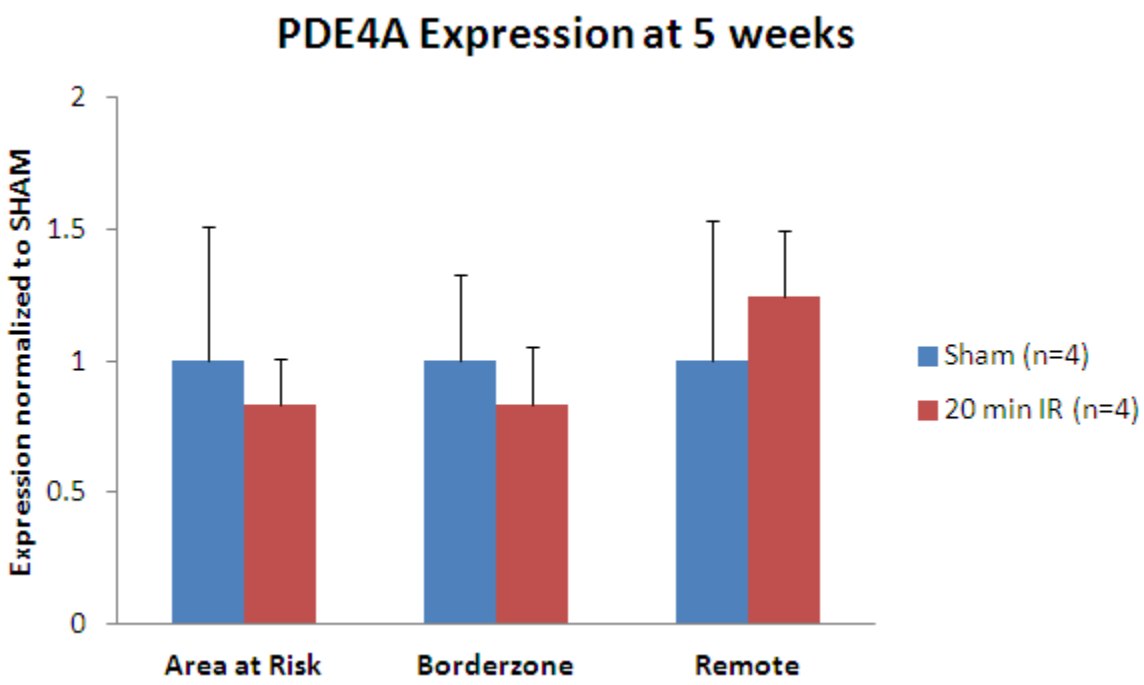

Figure 3.18: Western Blot quantification of PDE4A expression in area at risk, borderzone, and remote left ventricle homogenates at 5 weeks post-20 min IR. Data is normalized to GAPDH, then expressed as a ratio to sham-treated controls. Abbreviations: GAPDH, glyceraldehyde 3 phosphate dehydrogenase, IR, ischemia reperfusion, PDE4A, phosphodiestase 4A.

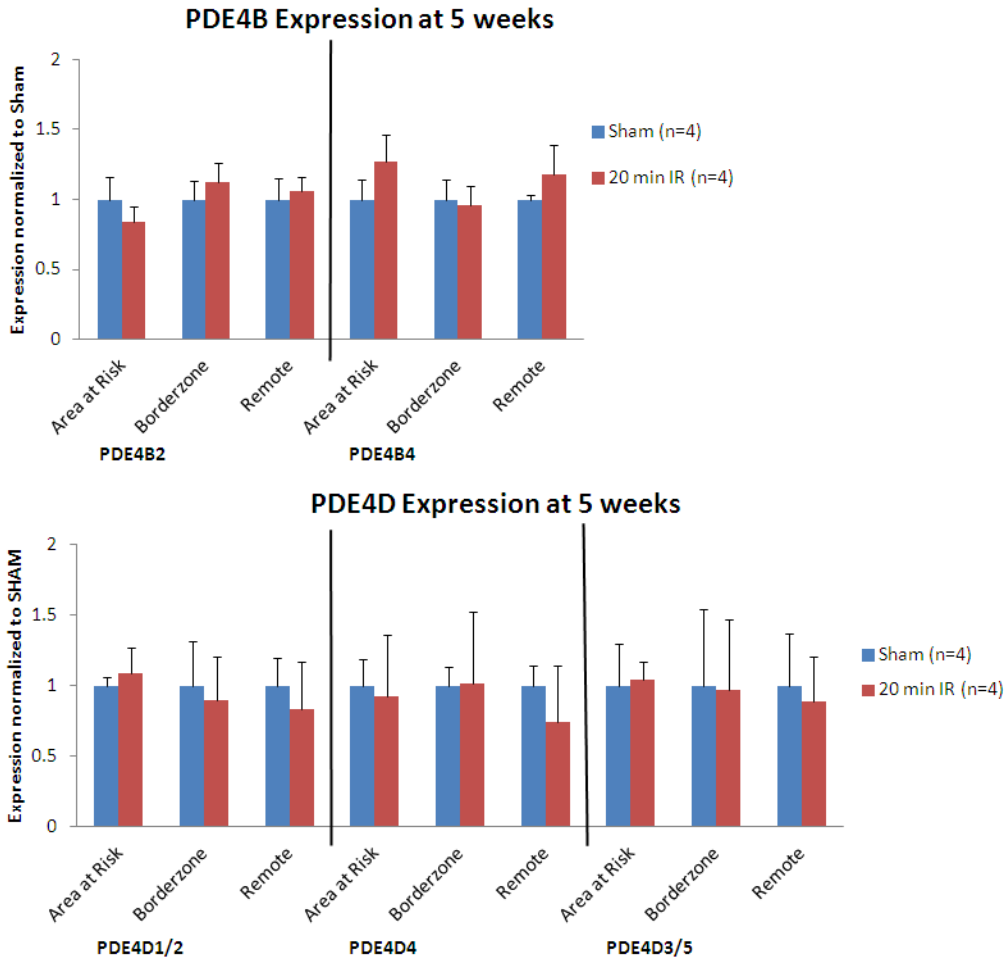

Figure 3.19: Western Blot quantification of PDE4B and PDE4D isoform expression in area at risk, borderzone, and remote left ventricle homogenates at 5 weeks post-20 min ischemia-reperfusion. Data is normalized to GAPDH, then expressed as a ratio to sham-treated controls. Abbreviations; GAPDH, glyceraldehyde 3 phosphate dehydrogenase, IR, ischemia reperfusion, PDEB, phosphodiestase B, PDE4D, phosphodiesterase D.

3.3 Physiological Measurements of SNS Signalling at 3 Weeks Post IR

As described above, 20 min IR rats were selected for investigation and during the 2-5 weeks screen for alterations in PDE4 protein expression, 3 weeks was found to have multiple isoform upregulation. The investigation of this timepoint was extended to include measurements of cardiac dysfunction and SNS activity to test if an association with PDE4 expression was present.

3.3.1 β-AR protein expression

At 3 weeks post-surgery, 20 min IR rats exhibited a significant 20% decrease ($p<0.05$) in β_1 adrenoceptors in the area at risk, but no other changes in β_1, β_2, or β_3 adrenoceptor expression in area at risk, borderzone, or remote myocardium (Figure 3.20). In MI rats, a significant 30% reduction ($p<0.05$) in β_1 adrenoceptor expression in the infarcted zone at 3 weeks post-surgery was observed, but no change in peri-infarcted or non-infarcted zones. No other changes were observed in any part of the myocardium with β_2 or β_3 adrenoceptors (Figure 3.21).

3.3.2 PDE4 activity assay

PDE4 activity is the rate at which PDE4 can hydrolyze cAMP into 5'AMP. This can be increased by phosphorylation from PKA. Highly active PDE4 is an indicator of high cAMP, and perhaps SNS signalling. No difference was detected in overall PDE enzyme activity or PDE4 enzyme activity at 3 weeks post-surgery in the area at risk, borderzone and remote myocardium (Figure 3.22).

This result suggests no change in PDE4 activity between 20 min IR model and Sham.

3.3.3 Cardiac NE

Cardiac NE is the NE that is synthesized, stored and used in the heart. 3 weeks post-surgery, 20 min IR rats displayed an 80% reduction in NE levels in the area at risk compared to Sham ($p<0.05$) while a 44% decrease was observed in borderzone compared to sham. In the remote myocardium zone, tissue NE was not significantly changed in 20 min IR rats compared to sham (Figure 3.23). A depressed level of NE indicates higher NE use, indicating higher SNS activity and is a predictor of increased mortality.

3.3.4 Plasma NE

Plasma NE is an indicator of cardiovascular health, higher plasma NE is associated with higher mortality. No difference was found between baseline Sham and baseline IR rat plasma NE levels. At 3 weeks, a significant 37% increase in plasma NE was detected ($p<0.05$) compared to Sham (Figure 3.24).

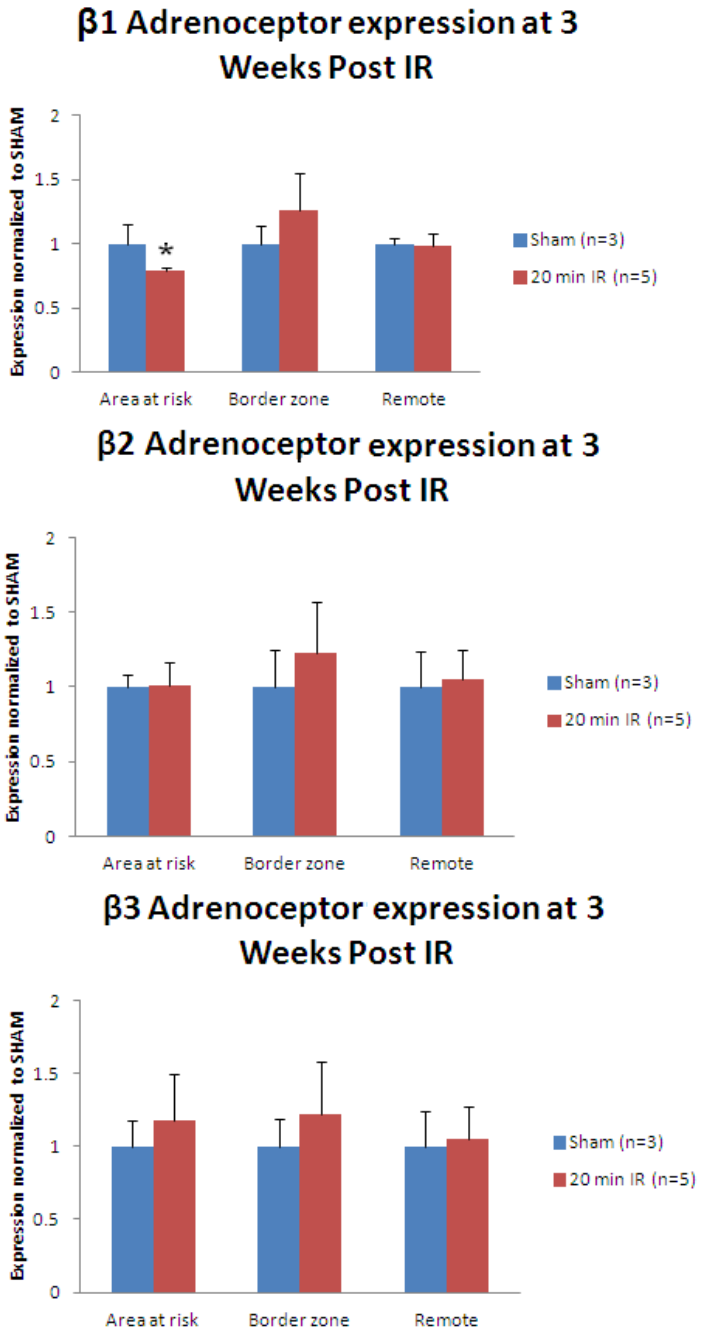

Figure 3.20: Western Blot quantification of β_1, β_2 , β_3 expression in infarcted, peri-infarcted and non-infarcted left ventricle homogenates at 3 weeks post-20 min IR surgery. Data is normalized to GAPDH, then expressed as a ratio to sham-treated controls. Student's t-test was performed with $p < 0.05$ considered significant (*). Abbreviations; GAPDH, glyceraldehyde 3 phosphate dehydrogenase, IR, ischemia reperfusion, LAD, left anterior descending.

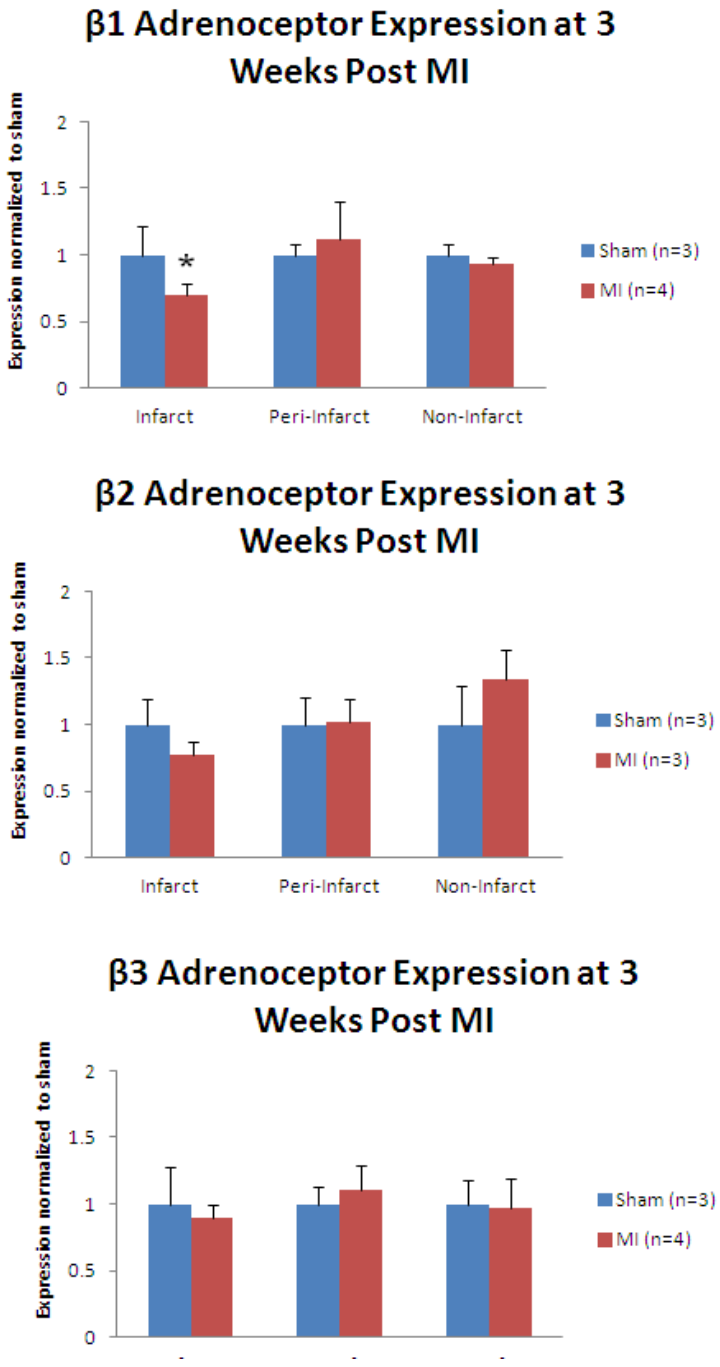

Figure 3.21: Western Blot quantification of β_1, β_2, and β_3 expression in infarcted, peri-infarcted and non-infarcted left ventricle homogenates at 3 weeks post left LAD coronary artery ligation producing MI surgery. Data is normalized to GAPDH, then expressed as a ratio to sham-treated controls. Student's t-test was performed with $p < 0.05$ considered significant (*). Abbreviations; GAPDH, glyceraldehyde 3 phosphate dehydrogenase, LAD, left anterior descending, MI, myocardial infarction.

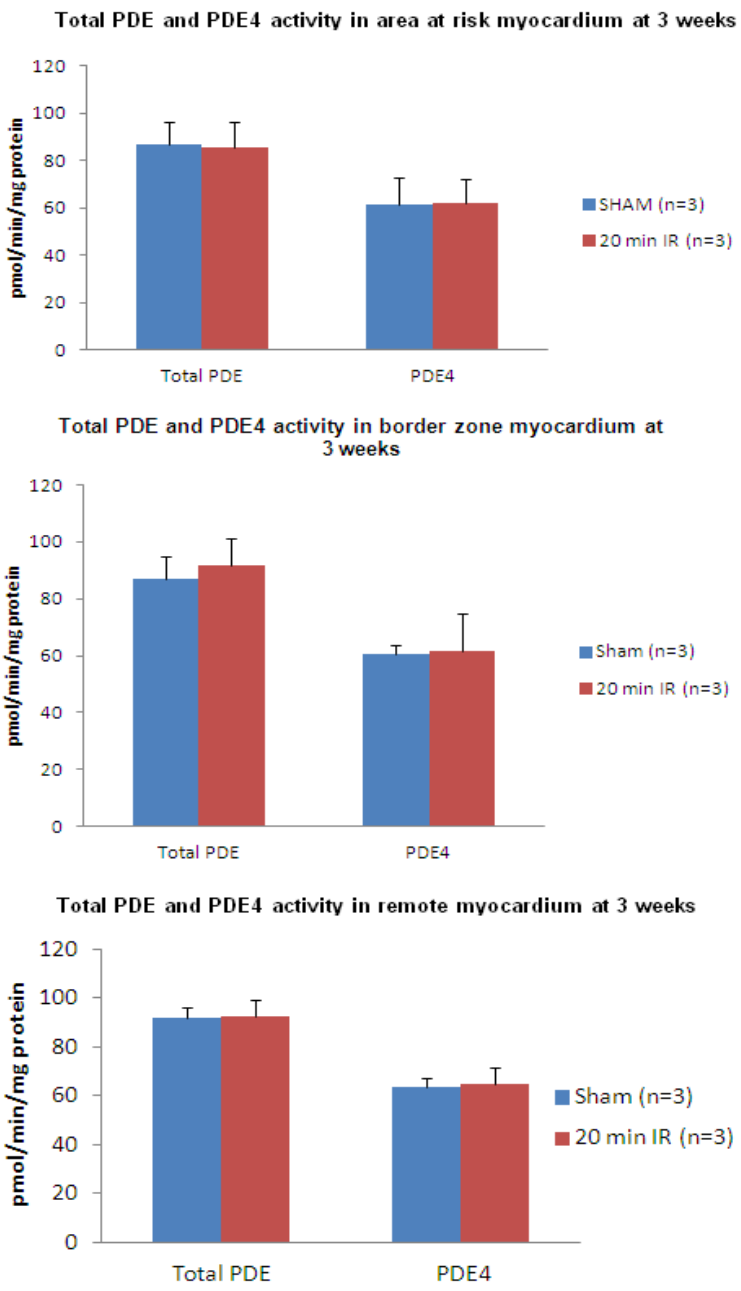

Figure 3.22: PDE4 enzyme activity in the homogenates of non-infarcted and infarcted portions of LV of 20 min IR and sham-treated rats, expressed as pmol of cAMP hydrolyzed per min per mg of protein. PDE4 activity was determined by incubating the first (cAMP-hydrolyzing) step in the presence of (R/S)-Rolipram inhibitor. Student's t-test was performed with $p < 0.05$ considered significant (*). Abbreviations: cAMP, cyclic adenosine monophosphate, IR, ischemia reperfusion, LV, left ventricle, PDE, phosphosidesterase, PDE4, phosphodiesterase 4.

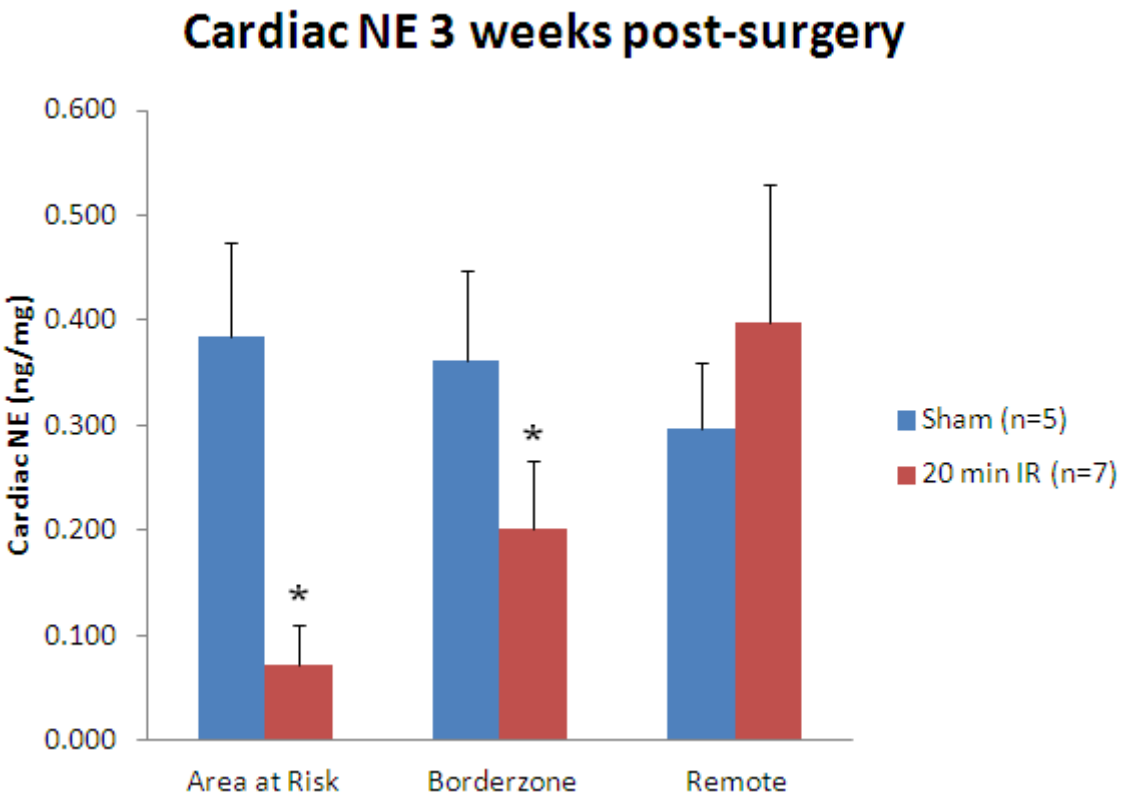

Figure 3.23: NE measrements from 3 week post-20 minute IR rat's area at risk, borderzone and remote myocardium left ventricle using high performance liquid chromatography and electrochemical detection. Student's t-test was performed with $p < 0.05$ considered significant (*). Abbreviations: IR, ischemia reperfusion, NE, norepinephrine.

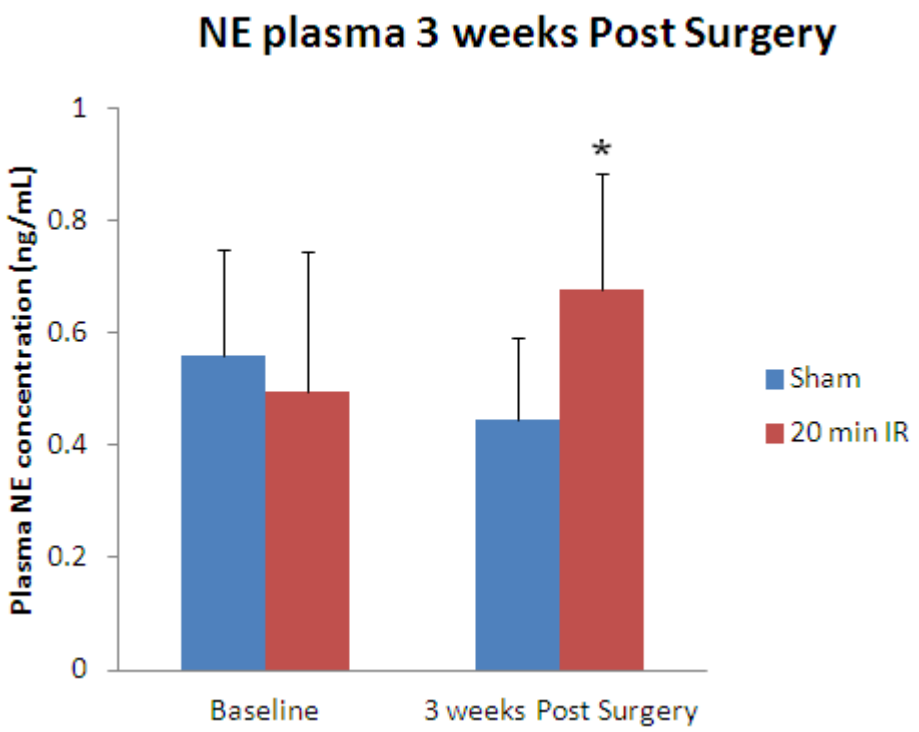

Figure 3.24: Plasma NE measrements using ELISA at baseline (before surgery) and 3 week post-20 minute IR surgery. Baseline sham (n=7), Baseline 20 min IR (8), 3 week sham (n=7) and 3 week post-20 min IR surgery (n=6). Student's t-test was performed with $p < 0.05$ considered significant (*). Abbreviations; ELISA, enzyme-linked immunsorbant assay, IR, ischemia reperfusion, NE, norepinephrine.

CHAPTER 4

Discussion

4.0 Significant Findings & Potential Importance

This thesis explores the SNS and its role in two models of IR, 45 min and 20 min, as well as MI at early time points (2-5 weeks), deemed an important remodelling phase post myocardial injury. Special attention was paid to the intracellular cAMP-hydrolyzing enzyme PDE4. This thesis sought to test PDE4's importance and responsiveness post ischemic injury, as an intracellular biomarker. A timeline of PDE4 expression was tested in 20 min IR and MI from 2-5 weeks. A clear pattern of increased PDE4 expression occurred at 3 weeks in both 20 min IR and MI. This time point was further explored with echocardiography, Doppler, PDE4 activity, cardiac and plasma NE levels. Echo and analysis of NE revealed restrictive cardiac filling and increased NE turnover, respectively, supporting PDE4 as a potential biomarker of SNS activity. This thesis also supports the use of (*R*)-[^{11}C]Rolipram PET to measure non-invasively PDE4 at early timepoints post ischemic injury for potential prognosis and therapy guidance.

4.1 Animal Model Characteristics of 45 min IR surgery

In dogs, 30-60 min of IR injury produces similar myocardial necrosis as total ligation (Jennings et al. 1960), though it is unclear how long of an IR injury in rats would produce similar necrosis to MI. 45 min IR rat model was described by Gao et al. (2012) producing a small anterolateral infarct. The 45 min IR model was reproduced and showed myocardial glucose uptake defect at 2-4 days and low EF at 2 weeks through 7 weeks, and fibrosis confirmed by histology. The

model also displayed myocardial blood flow defect in the anterolateral wall using [^{13}N]NH_3 PET at 2 weeks, matching FDG uptake defect. The goal to produce an ischemic model without flow impairment at rest was not accomplished by this model and it was deemed unsuitable for the study of PET tracers in the area at risk/infarct zone. Though this model may have ischemia reperfusion injury and areas of damage with flow, the differences between 45 min IR model and MI model were predicted to be too subtle for the scope of a Master's thesis. No further experiments were done with the 45 min IR model, however, this may develop into a suitable model for future investigation of small scale infarction.

4.2 Animal Model Characteristics of 20 min IR surgery

20 min IR rat model was produced as described previously by our group (Thorn et al. *unpublished*; McKasey 2012). This model produces neither myocardial uptake defect with FDG at 2-4 days, nor any blood flow defect at 2 weeks, confirmed by histology. Dobutamine rest/stress [^{13}N]NH_3 study through 2.5-5 weeks post-surgery revealed only trends ($p>0.05$) in reduced myocardial flow reserve compared to sham. Despite this, it appears that with increased sample size, there may be a significant reduction in both myocardial ratio (stress flow/ rest flow) and delta (stress flow – rest flow), indicating impaired myocardial response to pharmacological stress that improves over time. Rats that underwent MI instead of IR appear to have more myocardial reserve impairment than age matched 20 min IR rats, though again this is not significant ($p>0.05$). This is the first time, to our group's knowledge, that rest/stress [^{13}N]NH_3 PET has been explored post IR or MI in rats. The 20 min IR rat model presents no resting flow

defect and an adequate model to study the area at risk post IR injury with PET tracers. The model was further explored for signs of diastolic dysfunction, activation of SNS and changes in β-AR and PDE4 expression as well as PDE4 activity.

Preserved EF is also observed in this model as late as 3 weeks post-surgery, although this did not occur with Dr. Stephanie Thorn as surgeon. These rats (n=3) showed depressed LVEF at 2 weeks persisting to 7 weeks. This is attributed to the difficulty and variability in surgery, the low n number (n=3), and complications due to surgery and perhaps unexplained differences in surgical technique. Mr. Rick Seymour performed more rat surgeries (n=12), also with variability but the large n number accounted for this to give a preserved EF in this model. As stated in methods, only 2 week IR rats in the imaging studies were performed by Dr. Stephanie Thorn. All in vitro work with was produced from IR and MI rats that underwent surgery by Mr. Rick Seymour.

4.3 Assessment of Systolic and Diastolic Function Using Echocardiography in 20 min IR Rat Model

Echocardiography of systolic and diastolic dysfunction produced similar results to previous work by our group (Thorn et al *unpublished* ; McKasey 2012; Kenk et al. *unpublished*). Systolic dysfunction was not observed in this model as evidence from EF at baseline and 3 weeks while E/A ratio was elevated at 3 weeks. Diastolic dysfunction has been linked to alterations in mitral filling patterns, slightly enlarged or normal LV and measured with the E/A ratio

(Federmann & Hess 1994). A low E/A ratio is associated with impaired relaxation with enhanced isovolumetric relaxation time and a high E/A ratio represents restrictive filling by means of shortened isovolumetric relaxation (Thomas 1993). Female Wistar rats also showed increased E/A ratio 1 week after MI (Saraiva et al. 2007) though there appears to be a large difference between female Wistar and male Sprague Dawley rat's E and A waves. Variations undoubtedly occur between species and so to correct for this, baseline and 3 week E/A ratios were measured in rat mitral valves in both sham and 20 min IR rats. This established a baseline/normal value in Sprague-Dawley rats. 20 min IR rats also showed a significant increase in Doppler analysis E/A ratio compared to 3 week controls, while the baseline values or sham and IR rats were not different. This finding supports diastolic dysfunction by means of IR injury and creating restricted diastolic filling and increased LA pressure.

4.4 Evidence of Increased SNS Activity in 20 min IR Model

Elevated Plasma NE has long been associated with poor cardiac health outcomes (Cohn et al. 1995; Brunner-La Rocca 2001). NE spillover increased 500% and 200% from the heart and kidney, respectively, in HF patients (Hasking et al. 1986). Interestingly, at 3 weeks post IR, rats show elevated levels of plasma NE indicating heightened SNS activity in response to ischemic injury.

The appropriate way to collect plasma from rats for NE analysis can be a source of debate. Factors such as stress, anaesthesia and blood loss can affect circulating NE levels. As described by Popper et al. (1977), after sleeping for 3 minutes rat plasma had NE levels approximately 30% lower ($p < 0.01$) than

awake rats, but when immobilized or decapitated for blood collection the NE levels rise dramatically over the same timeframe (300% and 900% respectively). Indeed, the presented data on NE plasma is likely underestimated but collected in a reproducible and humane way.

Literature points to HF reducing tissue NE levels and elevating plasma NE. High NE spillover is correlated with β_1-AR receptor downregulation (Bristow et al. 1982) but how then are low tissue NE levels also present? The proposed mechanism is tissue NE is used up and not replaced as SNS activity remains high. NE spills over into the blood, and is eventually excreted in the urine. Tissue NE levels, within the atrium appendage, are depressed by approximately 50% in chronic HF patients, and low atrial NE levels correlated with low ventricular papillary muscle NE levels in humans (Chidsey et al. 1965). Increased plasma NE and decreased tissue NE are found in humans and increase the cumulative incidence of death (Brunner-La Rocca et al. 2001). In rats, Mathes et al. (1971) observed a rapid elimination of NE levels in the infarct zone of a MI rat model. In the non-infarct, a slow decrease of NE levels was observed at 3 weeks followed by full tissue NE level recovery at 5 weeks. Rats with HF have increased plasma NE and decreased tissue NE (Delehanty 1994). NE nerve terminals, measured by tyrosine hydroxylase histofluorescence, were reduced in HF and NE-infused rats (Qin et al. 2002). Indeed, low tissue NE stores are commonly found shortly after a variety of different ischemic episodes.

Instead of being recycled, NE spillover eventually is excreted into the urine, thus tissue NE stores are depressed post IR injury. Increased NE excretion via urine is

correlated with worsening NYHA class (Chidsey et al. 1965). Smaller atrial NE concentrations are correlated with larger NE excretion (Chidsey et al., 1965). At 3 weeks post IR there is a significant ($p = 0.025$) 80% reduction in NE levels displayed in area at risk tissue from 3 week post IR rats. This reduction is similar in MI rats at 8 weeks post-surgery also done by our group (Tayyabi 2014). Interestingly this is the first exploration of tissue levels in a 20 min IR model.

4.5 Western Blotting β-AR in 20 min IR Model and MI

β_1-AR downregulation and maintenance of β_2-AR density post MI demonstrated in this thesis is well supported by literature. β_1-AR downregulation is commonly observed post MI in the heart in both humans and rat models (Bristow et al. 1982; Lohse et al. 2003; Ohte et al. 2012; Leosco et al. 2008; for review see Gilbert et al. 1993) while β_2-AR are not downregulated but uncoupled (Bristow et al. 1989; Bristow et al. 1986). Thus current guidelines for treating post-MI patients endeavour to reduce catecholamine activation in the heart (Cesario & Fonarow 2002; Sauls & Rone 2005; Thygesen et al. 2007). β_1-AR, not β_2-AR, stimulation is thought to be responsible for cardiac hypertrophy (Morisco et al. 2001), supported by the efficacy of a meta-analysis of primarily β_1-AR blocker therapy (Doughty et al. 1997) that are able to reduce mortality by 30-60% (Packer 1996). Interestingly, both 3 week MI and 3 week IR rats show similar β1-AR downregulation.

The complex timeline of SNS overactivity and β_1-AR density post IR/MI is poorly understood. Many groups focus on HF and MI, later time points and a variety of models. With one week of constant infusion of NE, β_1-AR ventricular

myocytes have actually been shown to be upregulated while β_2-AR are downregulated (Zhao et al. 1996). In contrast, rats exposed to 3 weeks of constant hypoxia showed a ~25% downregulation in β_1-ARs (Kacimi 1992), indirectly supporting ischemia as cause for SNS activity. This work demonstrates that MI and IR have similar β_1-AR downregulation at 3 weeks and both restricted to the infarct and area at risk, respectively. Few studies have compared MI and IR damage during the healing phase, and this may be the first such comparison. This finding is additive to and supported by the theory that all etiologies of cardiomyopathy involve β_1-AR downregulation, β_2-AR uncoupling and tissue NE depletion, as observed in idiopathic dilated cardiomyopathy, post MI, remodelling pressure overload HF (Bristow et al. 1991) and now, IR injury.

4.6 Western Blot of PDE4 and Measurement of PDE4 Activity in 20 min IR Rat Model

The rationale for exploring the early time-point of 3 weeks is that literature has established a decrease in PDE4 expression, activity, or sensitivity to inhibitors at late (5 or more weeks) time-points post MI. Indeed, in the review by Osadchii (2007), PDE cAMP-hydrolyzing capabilities are impaired in many animal models of HF. PDE4 activity was depressed 6 weeks post LAD coronary artery ligation in rats and the heart muscle was non-responsive to cAMP increases by Rolipram (Afzal et al. 2010). 5 weeks post-aortic banding, rats had severe cardiac reserve impairment and approximate 60% reduction in PDE4A and B protein expression (Abi-gerges et al. 2009). In human ventricles, PDE4 activity

was decreased in idiopathic cardiomyopathy compared to normals (Richter et al. 2011).

2-3 weeks after an ischemic episode has been deemed an important time point in early ventricular remodelling in humans and animal models yet there is little data on β_1-AR, PDE4 and NE levels, likely because recovery of contractile function is common. Theroux et al. (1977) demonstrated that 3 weeks post MI was an important "healing" phase post MI in dogs, observing that the infarct zone suffered initially from dyskinesia (erratic contraction) and later to akinesia (non-contraction). This group also showed compensation in the contractile pattern of the non-infarcted zone. Human patients 2 weeks after admission that were assessed with cardiac catheterization, following Q wave (from ECG) myocardial infarcts caused expansion of the ventricle and this correlated with the progression from dyskinesis to akinesis in the infarcted zone (McKay et al. 1986). At 3 weeks post MI in rats, the ventricular infarct is apparent with greater ventricular volume (Fletcher et al. 1981) but continues to expand through time in moderate sized infarcts (Pfeffer et al. 1985). This finding demonstrates that mechanisms in the infarct and non-infarct are both working during remodelling (Pfeffer & Braunwald 1990).

Through 2-5 weeks post MI and IR, a clear and novel pattern emerged at 3 weeks post-surgery. Three isoforms of PDE4D and 2 isoforms of PDE4B were upregulated in the area at risk while PDE4A was upregulated in the borderzone and remote myocardium 3 weeks post IR. MI rat infarct also showed a similar trend. 1 PDE4D isoform and 2 PDE4B isoforms were upregulated in the infarct,

while PDE4D4 levels were depressed in the peri-infarct and PDE4B4 levels were elevated in the non-infarct. Other changes in PDE4 expression were decreased PDE4A expression at 2 weeks post IR surgery and increased PDE4A expression in the remote myocardium at 4 weeks post IR.

PDE4 expression increases with treatments that increase NE, serotonin, and histamine, but not dopamine (Lourenco et al. 2006), and ischemic injury produces SNS activation (Triposkiadis et al. 2009) supporting the results presented here. Most research on activation of SNS occurs with respect to MI, not IR. One study by Graham et al. (2002) investigated post MI patients with preserved ejection fraction (mean 52%) and observed that they had higher sympathetic nerve activity than healthy controls and patients with stable coronary artery disease. Non-ischemic cardiomyopathy patients with low EF had lower sympathetic nerve activity than patients with ischemic cardiomyopathy (Notarius et al. 2007). Floras (2009) state that myocardial ischemia/infarction increases sympathetic outflow but does not necessarily correlate with increased EF. The findings presented displaying upregulated PDE4 in IR and MI area at risk/infarct support the hypothesis. In addition, changes in NE tissue and plasma levels also support PDE4 involvement in SNS. Preserved EF in this model is in contrast to the established relationship between low EF and large infarct size (Pfeffer & Braunwald 1990). In summary, it appears that the heart at 3 weeks post IR is compensating and remodelling, PDE4 is more upregulated in IR than MI, indicating PDE4 expression is impaired in MI due to neuronal damage and unable to compensate.

PDE3 and PDE4 contribute approximately 90% of cAMP-hydrolyzing activity in the rat heart (Afzal et al. 2010, Richter et al. 2011; Mongillo et al. 2004), murine heart (Richter et al. 2011, Xiang et al. 2005; Georget et al. 2003) and the sheep heart (Lugnier et al 1999). To investigate the effect of HF on the activity of PDE, one group investigated rats with LAD coronary artery ligation at 6 weeks post-surgery (Afzal et al. 2010). Total PDE activity was significantly ($p<0.05$) reduced by 22% and PDE4 activity was decreased by 18%. In human idiopathic dilated cardiomyopathy, Richter et al. (2011) found an approximate 33% and 20% decrease in PDE4A and D activity, respectively. 5 weeks post-aortic banding in rats, Abi-Gerges et al. (2009) observed decreased activity of total PDE, PDE4A and B, but not D. Total PDE and PDE4 activity was unchanged in 20 min IR rats 3 weeks post-surgery. Previous work by our group (Kenk et al. unpublished) investigated β_1-AR and PDE4 at 8-12 weeks post MI. No changes were found in PDE4 isoform expression or activity, while β_1-AR receptors were downregulated by 21%, similar to IR and MI rats at 3 weeks post-surgery. MI rats at 8-12 weeks post-surgery only had mortality in the first 48 hours, indicating that they are compensating despite the low EF and also supported by unchanged (*R*)-[^{11}C] Rolipram uptake in the heart. Furthermore, when treated with DMI, MI rats displayed a ~30% increase in (*R*)-[^{11}C]Rolipram uptake, similar to shams, indicating preserved PDE4 reserve response to increased NE. These finding are in agreement with current literature above and summarized well by Osadchii (2007) that PDE4 activity is significantly reduced in animal models of HF but preserved in compensated cardiac dysfunction.

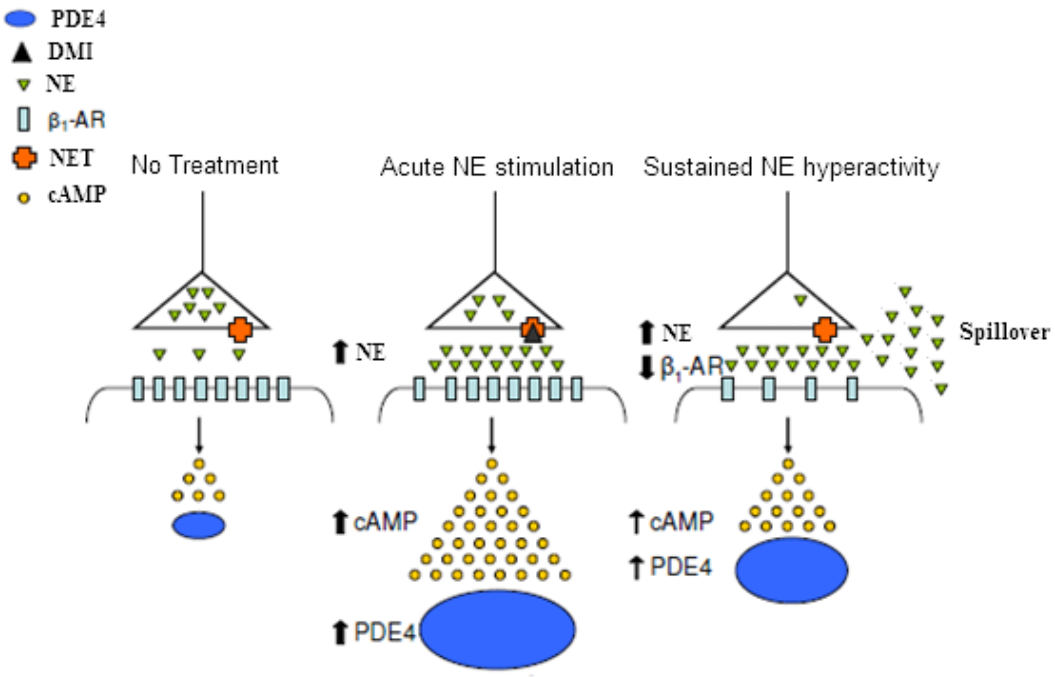

Figure 4.0: Representation of alterations in cAMP/PDE4 signaling. Acute increases in NE result in increases in PDE4 expression in the rodent heart, while sustained increases in NE, like after a myocardial IR, downregulate β-AR but also continue to increase cAMP/PDE4. Sustained NE depletes storage within the neuron and causes spillover to the interstitial space and plasma. Adapted from Duman et al. (1997) and Kenk (2010). Abbreviations: β_1-AR, beta-1 adrenoceptor, cAMP, cyclic adenosine monophosphate, DMI, desipramine, NE, norepinephrine, NET, norepinephrine transporter, PDE4, phosphodiesterase 4.

4.7 Clinical Relevance

Cardiovascular disease is characterized by activation of the SNS (Triposkiadis et al. 2009). Evidence of SNS upregulation includes increased urinary catecholamines, increase plasma NE, abnormal cardiovascular reflexes and increased sympathetic activation (Zhang et al. 2014). The degree of plasma NE (Cohn et al. 2003) and urinary (Chidsey et al., 1965) correlated with NYHA functional capacity and prognosis. More recently, CVD patients with low tissue NE and higher plasma NE were at greater risk of all-cause mortality than patients

with normal levels (Brunner-La Rocca 2001). The 20 min IR rat model, studied at 3 weeks post-surgery, provides evidence of SNS upregulation with low tissue NE and high plasma NE but also PDE4 upregulation. This work provides support that PDE4 is an important member of the SNS signal transduction pathway in the heart, and unique as it is an intracellular protein.

This rat model does not appear to develop the characteristics observed in "human HF", but instead displayed signs of diastolic impairment and LV remodeling. Rats did not overtly exhibit (as monitored by Animal Care) the symptoms of human HF (breathlessness, peripheral and pulmonary edema) but do have significant changes in a variety of physiological measurements indicative of remodelling and neurohormonal activation present in human HF.

This model provides support for a novel measurement of SNS activity, a PDE4:β1-AR ratio (Figure 4.0). β-AR density can be measured non-invasively with β_1-AR inhibitor [^{11}C]CGP12177 PET and has been tested as safe and effective in humans (Merlet et al. 1993). PDE4 measurements can be achieved in a similar fashion with (*R*)-[^{11}C]Rolipram PET, as Rolipram is a potent PDE4 inhibitor (Wachtel, 1983; Zeller et al. 1984; Bertolino et al. 1988). (*R*)-[^{11}C]Rolipram has been deemed safe and produces relevant uptake in the human brain (DaSilva et al. 2002) and effective in the detection of major depression (Fujita et al. 2005) but not yet explored in human CVD.

Theoretically, SNS activation produces high levels of PDE4 and depressed levels of β-AR in the post ischemic/infarcted myocardium. This scenario would produce a large PDE4:β-AR ratio compared to normal patients. End stage HF is

predicted to produce decreased PDE4 and β-AR, eventually lowering this ratio. A combination of symptoms (NYHA class) and PDE4:β-AR ratio could provide superior prognosis. [^{11}C]CGP12177 and (*R*)-[^{11}C]Rolipram may non-invasively provide an index of SNS signalling that can be used for patient therapy guidance and prognosis.

4.8 Limitations

While PDE4 comprises up to 50% of total PDE activity in the rodent heart, it comprises approximately 10% in human ventricles (Richter et al. 2011). PDE3 is the major PDE in the human heart whereas PDE4 is within the rodent heart (Eschenhagen 2013). PDE3 is expressed in higher levels in the heart and localized on the sarcoplasmic reticulum (Movsesian et al., 1991). Though PDE4 may not be the major PDE in the human heart, this does not mean for certain that its measurement would not be useful, however, for translational studies, PDE1, 2 and 3 also require rigorous investigation.

It is unclear how the timeline post-surgery in a rodent model correlates with the timeline post MI/IR in humans. For example, it is unknown whether 3 weeks post-surgery in rats would correlate in humans. A meta-analysis of cardiac dysfunction markers at various timepoints in both humans and rodent models could be conducted to further analyze this. A timeline like this could translate animal research to clinical trials faster by accounting for differences in the speed of injury and LV remodelling.

Only 8 of the 25 or more PDE4 isoforms in the rat heart were measured with western blotting, as mentioned above, investigation of PDE3 in the rodent

heart may be important for pathophysiology. All surgical models come with variability within the same treatment group. This is present in this thesis, as demonstrated by the depressed LVEF (Table 1) by one animal surgeon, but not another (Table 2). Indeed the variability is higher in IR surgery versus MI, which also suffers from variability limitations as well as small infarct size (Tucci 2009). A variety of other methods to induce MI are available such as cryo-injury (Huwer et al. 2000) and radio frequency ablation (Antonio et al. 2009), the latter showing low mortality and low MI size variance.

4.9 Conclusions and Future Directions

After a 45 min IR injury, rats show a small sized infarct both with FDG PET imagining, [^{13}N]NH_3 imaging, and confirmation by histology. 45 min IR rats also have systolic dysfunction confirmed by low EF and anterolateral blood flow impairment making it perhaps a suitable model of small scale infarction but lack of blood flow to 18% of the LV prevents the uptake of PET tracers and its similarities to MI may be difficult to distinguish within the scope of a master's thesis. This model could be further explored for investigation of small infarct physiology, but this work focused more on the 20 min IR rat model.

After 20 min IR injury, rats have received an insult but are compensating with impaired pump function by effectively increasing SNS output to maintain normal EF. At 3 weeks post-surgery the increased SNS output preserves EF even with downregulated β_1-AR and depleted tissue NE, causing spillover and elevated plasma NE. IR rats 2.5 to 5 weeks post-surgery show trends in impairment of myocardial reserve in the anterolateral wall but no resting flow defect.

Interestingly, PDE4 levels are increased at 3 weeks post-surgery as well, suggesting their connection to SNS activity and importance in compensation of cardiac output. These findings support the utility of the PDE4 inhibitor (*R*)-[^{11}C]Rolipram to study the area at risk with PET to assess cAMP-specific PDE4 and thus infer SNS activity non-invasively post IR while the LV is remodelling.

This project provides support for the pursuit of long term goals involving the assessment of PDE4 as a marker of SNS activity in animal models of ischemia and infarction. This work provides evidence that in a model of IR, classical measurements of SNS activity correspond to increased levels of PDE4. Establishing a more detailed timeline (1-10 weeks) of 20 min IR, 45 min IR, and MI SNS activity and PDE4 levels would provide a greater understanding of IR and MI compensation over time. The 20 min IR model provides unimpaired blood flow at rest to the area at risk for the study of this region with various PET tracers such as [^{11}C]CGP12177 and (*R*)-[^{11}C]Rolipram. PDE3 is also an important cAMP-hydrolyzing agent in the rat heart and requires similar exploration that PDE4 has undergone in rodents. For translational studies, animal models that have meaningful PDE1 and PDE2 activity may need exploration, as these isoforms are also prominent in the human heart.

CHAPTER 5

References

Abbara, S. & S.P. Kalva, Ed. Problem Solving in Cardiovascular Imaging. Philadelphia, PA: Elsevier Saunders 2013. Print.

Abi-Gerges, A., Richter, W., Lefebvre, F., Mateo, P., Varin, A., Heymes, C., ... & Vandecasteele, G. 2009. Decreased expression and activity of cAMP phosphodiesterases in cardiac hypertrophy and its impact on β-adrenergic cAMP signals. Circulation research, 105(8), 784-792.

Abramson, S. et al. 1988. Interaction of b-adrenergic receptors with the inhibitory guanine nucleotide binding protein of adenylate cyclase in membranes prepared from cyc- S49 lymphoma cells. Biochem. Pharmacol. 37, 4289–4297.

Ackerman MJ, Priori SG, Willems S, Berul C, Brugada R, Calkins H, Camm AJ, Ellinor PT, Gollob M, Hamilton R, Hershberger RE, Judge DP, Le Marec H, McKenna WJ, Schulze-Bahr E, Semsarian C, Towbin JA, Watkins H, Wilde A, Wolpert C, Zipes DP. HRS/EHRA expert consensus statement on the state of genetic testing for the channelopathies and cardiomyopathies: this document was developed as a partnership between the Heart Rhythm Society (HRS) and the European Heart Rhythm Association (EHRA). Heart Rhythm 2011;8: 1308–1339.

Afzal, F., Aronsen, J.M., Moltzau, L.R., Sjaastad, I., Levy, F.O., Skomedal, T., Osnes, J.B. & E. Qvigstad. 2010. Differential regulation of B2-adrencoceptor-mediated inotropic and lusitropic response by PDE3 and PDE4 in failing and non-failing rat cardiac ventricle.

Aggarwal, A., Esler, M.D., Lambert, G.W., Hastings, J., Johnston, L., & Kaye, D.M. 2002. Norepinephrine turnover is increased in suprabulbar subcortical brain regions and is realted to whole-body sympathetic activity in human heart failure. Circulation 105: 1031-1033.

Ahmed, A. 2003. Myocardial beta-1 adrenoceptor down-regulation in aging and heart failure: implications for beta-blocker use in older adults with heart failure.European journal of heart failure, 5(6), 709-715.

Amann, K., I. Rychlik, et al. 1998. Left ventricular hypertrophy in renal failure. Kidney Int Suppl 68: S78-85.

Ambrosio, G., Zweier, J.L.... & J.T. Flaherty. 1991. The relationship between oxygen radical generation and impairment of myocardial energy metabolism following post-ischemic reperfusion. Journal of Molecular and Cellular Cardiology 23: 1359-1374.

Antonio EL, Santos AA, Araujo SRR, Bocalini D, dos Santos L, Fenelon G, et al. Left ventricle radio-frequency ablation in the rat: a new model of heart failure due to myocardial infarction homogeneous in size and low in mortality.

J Card Fail. 2009; 15 (6): 540-8.

Baillie G.S., MacKenzie S.J., McPhee I., Houslay M.D. 2000. Sub-family selective actions in the ability of Erk2 MAP kinase to phosphorylate and regulate the activity of PDE4 cyclic AMP-specific phosphodiesterases. Br J Pharmacol 131:811–819.

Baillie G.S., Huston E., Scotland G., Hodgkin M., Gall I., Peden A.H., MacKenzie C., Houslay E.S., Currie R., Pettitt T.R., Walmsley A.R., Wakelam M.J., Warwicker J., Houslay M.D. 2002. TAPAS-1, a novel microdomain within the unique N-terminal region of the PDE4A1 cAMPspecific phosphodiesterase that allows rapid, Ca2_-triggered membrane association with selectivity for interaction with phosphatidic acid. J Biol Chem 277: 28298–28309.

Baillie G.S., Adams D.R., Bhari N., Houslay T.M., Vadrevu S., Meng D., Li X., Dunlop A., Milligan G., Bolger G.B., Klussmann E., Houslay M.D. 2007. Mapping binding sites for the PDE4D5 cAMP-specific phosphodiesterase to the N- and C-domains of beta-arrestin using spot-immobilized peptide arrays. Biochem J 404: 71–80.

Baltas, L.G., Karczewski, P., Bartel, S. & E.G. Krause. 1997. The endogenous cardiac sarcoplasmic reticulum Ca2+/calmodulin dependent kinase is activated in response to beta-adrenergic stimulation and becomes Ca2+-independent in intact beating hearts. FEBS Lett Jun 9;409(2):131–136.

Barbuti, A., & DiFrancesco, D. 2008. Control of cardiac rate by "funny" channels in health and disease. Annals of the New York Academy of Sciences 1123(1): 213-223.

Barry, S.P., Davidson, S.M., Townsend, P.A. 2008. Molecular regulation of cardiac hypertrophy. Int J Biochem Cell Biol. 40: 2023-2039.

Bauman, A.L., & J.D. Scott. 2002. Kinase and phosphatise-anchoring proteins: harnessing the dynamic duo. Nat. Cell. Biol. 4(8): E203-E206.

Baxendale R.W., Fraser L.R. 2005. Mammalian sperm phosphodiesterases and their involvement in receptor-mediated cell signaling important for capacitation. Mol Reprod Dev, 71, 4.

Beard M.B., Huston E., Campbell L., Gall I., McPhee I., Yarwood S., Scotland G., Houslay M.D. 2002. In addition to the SH3 binding region, multiple regions within the N-terminal noncatalytic portion of the cAMP-specific phosphodiesterase, PDE4A5, contribute to its intracellular targeting. Cell Signal 14: 453–465.

Beavo, J.A. 1995. Cyclic nucleotide phosphodiesterases: functionl implications of multiple isoforms. Physiol. Rev. 75: 725-748.

Beavo, J. A. and Brunton, L. L. 2002. Cyclic nucleotide research ; still expanding after half a century. Nat. Rev. Mol. Cell Biol. 3, 710-718.

Beavo, J. A., and Reifsnyder, D. H. 1990. Primary sequence of cyclic nucleotide phosphodiesterase isozymes and the design of selective inhibitors Trends Pharmacol. 11, 150–155

Bender A.T., Beavo J.A. 2006. Cyclic nucleotide phosphodiesterases: molecular regulation to clinical use. Pharmacol Rev 58: 488–520.

Berlan, M., Galitzky, J., Bousquet-Melou, A., et al. 1994. Beta-3 adrenoceptor-mediated increase in cutaneous blood flow in the dog. The Journal of Pharmacology and Experimental Therapeutics, 268, 1444–1451.

Bertolino, A.D. Crippa, S. Di Dio, K. Fichte, G. Musmeci, V. Porro, V. Rapisarda, M. Sastre-y-Hernandez and M. Schratzer. 1988. Rolipram versus imipramine in inpatinets with major, “minor” or atypical depressive disorder: a double-blind double-dummy study aimed at testing a novel. Int. Clin. Psychopharmacol 3(3):245-253.

Black, S. C. 2000. In vivo models of myocardial ischemia and reperfusion injury: application to drug discovery and evaluation. Journal of pharmacological and toxicological methods, 43(2), 153-167.

Blair, J. E., Huffman, M., & Shah, S. J. 2013. Heart failure in north america.Current cardiology reviews, 9(2), 128-146.

Bloom T.J., Beavo J.A. 1996. Identification and tissue-specific expression of PDE7 phosphodiesterase splice variants. Proc Natl Acad Sci USA 93: 14188–14192.

Bodi I., Mikala G., Koch S.E., Akhter S.A., Schwartz A. 2005. The L-type calcium channel in the heart: the beat goes on. J Clin Invest 115:3306–17.

Bolger G.B. 1994. Molecular biology of the cyclic AMP-specific cyclic nucleotide phosphodiesterases: a diverse family of regulatory enzymes. Cell. Signal. 6: 851-859.

Bolger, G. B., S. Erdogan, R. E. Jones, K. Loughney, G. Scotland, R. Hoffmann, I.Wilkinson, C. Farrell & M. D. Houslay. 1997. Characterization of five different proteins produced by alternatively spliced mRNAs from the human cAMP-specific phosphodiesterase PDE4D gene. Biochem J 328(Pt 2): 539-48.

Bolger G.B., McCahill A., Yarwood S.J., Steele M.R., Warwicker J., Houslay M.D. 2002. Delineation of RAID1, the RACK1 interaction domain located within the unique N-terminal region of the cAMP-specific phosphodiesterase, PDE4D5. BMC Biochem 3: 24.

Braunwald, E. & Kloner, R.A. 1982. The stunned myocardium: Prolonged, postischemic ventricular dysfunction. Circulation 66(6): 1146-1149.

Bristow, M.R., Ginsburg, R., Minobe, W., Cubicciotti, R., Sageman, W.S., Lurie, K., et al. 1982. Decreased catecholamine sensitivity and β-adrenergic receptor density in failing human hearts. N Engl J Med. 307: 205-211.

Bristow, M.R., Ginsburg, R., Umans, V., Fowler, M., Minobe, W., Rasmussen, R., et al. 1986. β1- and β2-adrenergic receptor subpopulations in nonfailing and failing human centricular myocardium: coupling of both receptor subtypes to muscle contraction and selective β1-receptor downregulation in heart failure. Circ Res 59:297-309.

Bristow, M.R., Hershberger, R.E., Port, J.D. & R. Rasmussen. 1989. B1 and B2 adrenergic receptor mediated adenylate cyclase stimulation in nonfailing and failing human ventricular myocardium. Mol Pharmacol 35: 293-303.

Brixius, K., Bloch, W., Ziskoven, C., et al. 2006. Beta3-adrenergic eNOS stimulation in left ventricular murine myocardium. Canadian Journal of Physiology Pharmacology, 84: 1051–1060.

Brodde O.E. 1991. b1- and b2-adrenoceptors in the human heart: Properties, function, and alterations in chronic heart failure. Pharmacol Rev 43:203–242.

Brodde, O.E. 1993. Beta-adrenoceptors in cardiac disease. Pharmacol Ther 60:405-430.

Brodde, O.E., & M.C. Michel. 1999. Adrenergic and muscarinic receptors in the human heart. Pharmacol. Rev. 51:651-690.

Brodde, O.E., H. Bruck, K., Leineweber, & T. Seyfarth. 2001. Prescence, distribution and physiological function of adrenergic an muscarinic receptor subtypes in the human heart. Basic Res. Cardiol. 96(6):528-538.

Bristow MR, Ginsburg R, Minobe WA et al. 1982. Decreased catecholamine sensitivity and adrenergic-receptor density in failing human hearts. N Engl J Med 307: 205–11.

Bristow, M. R., Ginsburg, R., Umans, V., Fowler, M., Minobe, W., Rasmussen, R. & Jamieson, S. 1986. Beta 1-and beta 2-adrenergic-receptor subpopulations in non-failing and failing human ventricular myocardium: coupling of both receptor

subtypes to muscle contraction and selective beta 1-receptor down-regulation in heart failure. Circulation Research, 59(3), 297-309.

Bristow, M. R., Port, J. D., Hershberger, R. E., Gilbert, E. M., & Feldman, A. M. 1989. The β-adrenergic receptor-adenylate cyclase complex as a target for therapeutic intervention in heart failure. European heart journal, 10(suppl B), 45-54.

Bristow, M.R., Anderson, F.L., Port, J.D., Skerl, L., Hershberger, R.E., Larracbee, P., O'Connell, J.B., Renlund, D.G., Wolkman, K., Murray, J. & A.M. Feldman. 1991. Differences in β-adrenergic neuroeffector mechanisms in ischemic versus idiopathic dilated cardiomyopathy. Circulation 84:1024-1039.

Bristow, M.R. 1993. Changes in myocardial and vascular receptors in heart failure. J. Am. Coll. Cardiol. 22(4 Suppl A): 61A-71A.

Brunner-La Rocca, H.P., Esler, M.D., Jennings, G.L. & D.M. Kaye. 2001. European Heart Journal 22: 1136-1143.

Burns M.E., Arshavsky V.Y. 2005. Beyond counting photons: trials and trends in vertebrate visual transduction. Neuron 48: 387–401.

Bylund, D.B., Eikenberg, D.C., Hieble, J.P., Langer, S.Z., Lefkowitz, R.J., Minneman, K.P., et al. 1994. International union of pharmacology nomenclature of adrenoceptors. Pharmacol. Rev. 46: 121-136.

Cameron, R.T., & G.S. Baillie. 2012. cAMP-specific phosphodiesterases: modulation, inhibition, and activation in "Therapeutic targets: modulation, inhibition, and activation, 1e. Ed. Luis M. & M. Loza. John Wiley & sons, Inc.

Cesario, D.A. & G.C. Fonarow. 2002. Beta-blocker therapy for heart failure: the standard of care. Rev Cardiovasc Med 3: 14-21.

Chan, S., & C. Yan. 2011. PDE1 isozymes, key regulators of pathological vascular remodeling. Current opinion in pharmacology, 11(6): 720-724.

Chérin, Emmanuel, Ross Williams, Andrew Needles, Godwin Liu, Christopher White, Allison S. Brown, Yu-Qing Zhou, and F. Stuart Foster. 2006. "Ultrahigh frame rate retrospective ultrasound microimaging and blood flow visualization in mice in vivo." Ultrasound in Medicine & Biology 32.5: 683-691.

Chidsey, A.C., Braunwald, E., Morrow, A.G. & J.T. Mason. 1963. Myocardial norepinephrine concentration in man. N Engl J Med 269: 653-658.

Chidsey, C., Kaiser, G.A., Sonneblick, E.G., Spann J.F. & E. Braunwald. 1964. Cardiac norepinephrine stores in experimental heart failure in the dog. J Clin Invest 43: 2386-2393.

Chidsey, C.A., Braunwald, E., & A.G. Morrow. 1965. Catecholamine excretion and cardiac stress of norepinephrine in congestive heart failure. Am J Med 39: 442-451.

Christ, T., Engel, A., Ravens, U., & Kaumann, A. J. 2006. Cilostamide potentiates more the positive inotropic effects of (−)-adrenaline through β2-adrenoceptors than the effects of (−)-noradrenaline through β1-adrenoceptors in human atrial myocardium. Naunyn-Schmiedeberg's archives of pharmacology,374(3), 249-253.

Choi Y, Huang SC, Hawkins RA, Kuhle WG, Dalbom M, Hoh CK, et al. 1993. A simplified method for quantification of myocardial blood flow using nitrogen-13-ammonia and dynamic PET. J Nucl Med 34:488-97.

Choi, H., Yoo, B. S., Doh, J. H., Yoon, H. J., Ahn, M. S., Kim, J. Y., ... & Yoon, J. 2013. The optimal time of B-type natriuretic peptide sampling associated with post-myocardial infarction remodelling after primary percutaneous coronary intervention: cardiovascular topics. Cardiovascular journal of Africa, 24(5), 165-170.

Cohn, J.N., Johnson, G.J., Veterans Administration Cooperative Study Group. 1990. Heart failure with normal ejection fraction: The V-Heft study. Circulation 81 (Suppl III): III-48-III-53.

Cohn, J.N. 1995. Plasma norepinephrine and mortality. Clin Cardiol 18(suppl. I), I-9-I-12.

Cohn, J. N., Pfeffer, M. A., Rouleau, J., Sharpe, N., Swedberg, K., Straub, M., ... & Wright, T. J. 2003. Adverse mortality effect of central sympathetic inhibition with sustained-release moxonidine in patients with heart failure (MOXCON). European journal of heart failure, 5(5), 659-667.

Cohen, M. L., Bloomquist, W., Kriauciunas, A., et al. 1999. Aryl propanolamines: Comparison of activity at human beta3 receptors, rat beta3 receptors and rat atrial receptors mediating tachycardia. British Journal of Pharmacology, 126, 1018–1024.

Colledge, M. and Scott, J. D. 1999. AKAPs: from structure to function. Trends Cell Biol. 9, 216-221.

Conti M., Nemoz G., Sette C., Vicini E. 1995. Recent progress in understanding the hormonal regulation of phosphodiesterases. Endocr Rev 16:370–389.

Conti, M. and Jin, S. L. C. 1999. The molecular biology of cyclic nucleotide phosphodiesterases. Progr. Nucleic Acid Res. 63, 1-38.

Conti M., Beavo J. 2007. Biochemistry and physiology of cyclic nucleotide phosphodiesterases: essential components in cyclic nucleotide signaling. Annu Rev Biochem 76: 481–511.

Conti, A.C. et al. 2007. Distinct regional and subcellular localization of adenylyl cyclases type 1 and 8 in mouse brain. Neuroscience 146: 713-729.

Cooke, G.A., Marshall, P., al-Timman, J.K., Wright, D.J., Riley, R., Hainsworth, R., Tan, L.B. 1998. Physiological cardiac reserve: development of a non-invasive method and first estimates in man. Heart 79(3): 289-294.

Corbin J.D. & Francis, S.H. 1999. Cyclic GMP phosphodiesterase-5: target of sildenafil. J. Biol. Chem. 274:13729-13732.

Cote R.H. 2006. Photoreceptor phosphodiesterase (PDE6): a G-proteinactivated PDE regulating visual excitation in rod and cone photoreceptor cells. In: Cyclic Nucleotide Phosphodiesterases in Health and Disease, edited by Beavo JA, Francis SH, Houslay MD. Boca Raton, FL: CRC, p. 165–193.

Covell, J.W., Chidsey, C.A. & E. Braunwald. 1966. Reduction of the Cardiac Response to
Postganglionic Sympathetic Nerve Stimulation in Experimental Heart Failure. Circ Res 19:51-56.

D'Sa, C., L.M. Tolbert, M. Conti, & R.S. Duman. 2002. Regulation of cAMP-specific phosphodiesterases type 4B and 4D (PDE4) splice variants by cAMP signaling in primary cortical neurons. J. Neurochem. 81 (4) 745-757.

DaSilva, J.N., C.M. Valente, A.A. Wilson, J.J. Warsh and S. Houle. 1997. Carbon-11 labeling of the selective inhibitors of phosphodiesterase-IV Ro 20-1724 and Rolipram. J. Lable. Compd. Radiopharm. 40:678-680.

DaSilva, J. N., Lourenco, C. M., Meyer, J. H., Hussey, D., Potter, W. Z., & Houle, S. 2002. Imaging cAMP-specific phosphodiesterase-4 in human brain with R-[11C] Rolipram and positron emission tomography. European journal of nuclear medicine and molecular imaging, 29(12), 1680-1683.

DaSilva, J. N., Lourenco, C. M., Wilson, A. A., & Houle, S. (2001). Syntheses of the phosphodiesterase-4 inhibitors [^{11}C] Ro 20-1724, R-, R/S-and S-[^{11}C] Rolipram. Journal of Labelled Compounds and Radiopharmaceuticals, 44(5), 373-384.

de Tombe P.P., Stienen G.J.M. 1995. Protein kinase A does not alter economy of force maintenance in skinned rat cardiac trabeculae. Circ Res. 76:734–741.

Delehanty, J.M., Himura, Y., Elam, H., Hood., W.B. & C.S. Liang. 1994. B-Adrenoceptor downregulation in pacing-induced heart failure is associated with increased interstitial NE content. American Journal of Physiology-Heart and Circulatory Physiology, 266(3), H930-H935.

Dent, G., S.R., White, H., Tenor, K., Bodtke, C. Schudt, A.R., Leff, H., Magnussen, & K.F. Rabe. 1998. Cyclic nucleotide phosphodiesterase in human bronchial epitheial cells: characterization of isoenzymes and functional effects of PDE inhibitors. Pulm. Pharmacol. Ther. 11(1): 47-56.

Dessy, C., & Balligand, J. L. 2010. Beta-3-adrenergic receptors in cardiac and vascular tissues: emerging concepts and therapeutic perspectives. Advances in pharmacology, 59, 135-163.

Dickhout, J. G., R. E. Carlisle, et al. 2011. Interrelationship between cardiac hypertrophy heart failure, and chronic kidney disease: endoplasmic reticulum stress as a mediator of pathogenesis. Circ Res 108(5): 629-642.

Dickstein K, Cohen-Solal A, Filippatos G, McMurray JJ, Ponikowski P, Poole-Wilson PA, Stromberg A, van Veldhuisen DJ, Atar D, Hoes AW, Keren A, Mebazaa A, Nieminen M, Priori SG, Swedberg K. ESC guidelines for the diagnosis and treatment of acute and chronic heart failure 2008: the Task Force for the diagnosis and treatment of acute and chronic heart failure 2008 of the European Society of Cardiology. Developed in collaboration with the Heart Failure Association of the ESC (HFA) and endorsed by then European Society of Intensive Care Medicine (ESICM). Eur J Heart Fail 2008; 10:933–989.

Dodge-Kafka K.L., Soughayer J., Pare G.C., Carlisle Michel J.J., Langeberg L.K., Kapiloff M.S., Scott J.D. 2005. The protein kinase A anchoring protein mAKAP coordinates two integrated cAMP effector pathways. Nature 437: 574–578.

Donckier, J. E., Massart, P. E., Van, M. H., et al. 2001. Cardiovascular effects of beta 3-adrenoceptor stimulation in perinephritic hypertension. European Journal of Clinical Investigation, 31, 681–689.

Dorn, G.W. II., Tepe, N.M., Lorenz, J.N., Koch, W.J., & Liggett, S.B. 1999. Low- and high-level transgenic expression of β2-adrenergic receptors differentially affect cardiac hypertrophy and function in Gαq-overexpressing mice. Proc Natl Acad Sci U.S.A. 96: 6400-6405.

Dougherty, A.H., Naccarelli, G.V., Gray, E.L., Hicks, C.H., & R.A. Goldstein. 1984. Congestive heart failure with normal systolic function. Am J Cardiol 54:778-782.

Doughty, R. E. A., Rodgers, A., Sharpe, N., & MacMahon, S. 1997. Effects of beta-blocker therapy on mortality in patients with heart failure A systematic overview of randomized controlled trials. European heart journal, 18(4), 560-565.

Dunman, R.S., Heninger, G.R. & E.J. Nestler. 1997. A molecular and cellular theory of depression. Arch Gen Psychiatry 54: 597-606.

Dupre, D.J., A., Baragli, R.V., Rebois, N., Ethier & T.E. Hebert. 2007. Signalling complexes associated with adenylyl cuclase II are assembled during their biosynthesis. Cell Signal 19(3):481-489.

Dzimiri N. 1999. Regulation of beta-adrenoceptor signaling in cardiac function and disease. Pharmacol Rev. 51(3):465-501.

Eichinger L., Pachebat J.A., Glockner G., Rajandream M.A., Sucgang R., Berriman M., Song J., Olsen R., Szafranski K., Xu Q., Tunggal B., Kummerfeld S., Madera M., Konfortov B.A., Rivero F., Bankier A.T., Lehmann R., Hamlin N., Davies R., Gaudet P., Fey P., Pilcher K., Chen G., Saunders D., Sodergren E., Davis P., Kerhornou A., Nie X., Hall N., Anjard C., Hemphill L., Bason N., Farbrother P., Desany B., Just E., Morio T., Rost R., Churcher C., Cooper J., Haydock S., van Driessche N., Cronin A., Goodhead I., Muzny D., Mourier T., Pain A., Lu M., Harper D., Lindsay R., Hauser H., James K., Quiles M., Madan Babu M., Saito T., Buchrieser C., Wardroper A., Felder M., Thangavelu M., Johnson D., Knights A., Loulseged H., Mungall K., Oliver K., Price C., Quail M.A., Urushihara H., Hernandez J., Rabbinowitsch E., Steffen D., Sanders M., Ma J., Kohara Y., Sharp S., Simmonds M., Spiegler S., Tivey A., Sugano S., White B., Walker D., Woodward J., Winckler T., Tanaka Y., Shaulsky G., Schleicher M., Weinstock G., Rosenthal A., Cox E.C., Chisholm R.L., Gibbs R., Loomis W.F., Platzer M., Kay R.R., Williams J., Dear P.H., Noegel A.A., Barrell B., Kuspa A. 2005. The genome of the social amoeba Dictyostelium discoideum. Nature 435(7038): 43-57.

Eisenhofer, G., Kopin, I. J., & Goldstein, D. S. (2004). Catecholamine metabolism: a contemporary view with implications for physiology and medicine. Pharmacological reviews, 56(3), 331-349.

El Bawab S., Macovschi O., Sette C., Conti M., Lagarde M., Nemoz G., Prigent A.F. 1997. Selective stimulation of a cAMP-specific phosphodiesterase (PDE4A5) isoform by phosphatidic acid molecular species endogenously formed in rat thymocytes. Eur J Biochem 247: 1151–1157.

Emorine, L. J., Marullo, S., Briend-Sutren, M. M., et al. 1989. Molecular characterization of the human beta3-adrenergic receptor. Science, 245, 1118–1121.

Eschenhagen, T. 2013. PDE4 in the human heart–major player or little helper?. British journal of pharmacology, 169(3), 524-527.

Federmann, M., & O.M. Hess. 1994. Differentiation between systolic and diastolic dysfunction. European Heart Journal 15 (supplement D):2-6.

Fernstrom, J.D. & M.H. Fernstrom. 2007. Tyrosine, Phenylalaine, and Catecholamine Sythesis and Function in the Brain. The Journal of Nutrition 137(6 Suppl 1):1539S-1547S; discussion 1548S.

Ferrero P., Said M., Sanchez G., Vittone L., Valverde C., Donoso P., et al. 2007. Ca2+- kinase II increases ryanodine binding and Ca^{2+}-induced sarcoplasmic reticulum Ca2 release kinetics during betaadrenergic stimulation. J Mol Cell Cardiol Sep;43(3):281–291.

Fiechter, M., Ghadri, J. R., Gebhard, C., Fuchs, T. A., Pazhenkottil, A. P., Nkoulou, R. N., ... & Kaufmann, P. A. 2012. Diagnostic value of 13N-ammonia myocardial perfusion PET: added value of myocardial flow reserve. Journal of Nuclear Medicine, 53(8): 1230-1234.

Fiechter, M., Gebhard, C., Ghadri, J. R., Fuchs, T. A., Pazhenkottil, A. P., Nkoulou, R. N., ... & Kaufmann, P. A. 2013. Myocardial perfusion imaging with< sup> 13</sup> N-Ammonia PET is a strong predictor for outcome. International journal of cardiology, 167(3): 1023-1026.

Fletcher, P.J., Pfeffer, J.M., Pfeffer, M.A. & E. Braunwald. 1981. Left ventricular diastolic pressure-volume relations in rats with healed myocardial infarction. Circ Res 49: 618-626.

Floras, J.S. 2009. Sympathetic nervous system activation in human heart failure: clinical implications of an updated model. J Am Coll Cardiol 54(5): 375-385.

Follath, F., Cleland, J.G.F., Klein, W., & R. Murphy. 1998. Etiology and response to drug treatment in heart failure. JACC 32(5): 1167-1172.

Forster, C. 1998. Autonomic nervous system neurotransmitters. In Principles of Medical pharmacology. H. Kalant, Roschlau, W., editor. Oxford University Press, New York. 135-148.

Francis J, Weiss RM, Wei SG, Johnson AK, Felder RB. Progression of heart failure after myocardial infarction in the rat. Am J Physiol Regul Integrat Comp Physiol. 2001; 281 (4): R1734-R1745.

Francis S.H., Zoraghi R., Kotera J., Ke H., Bessay E.P., Blount M.A., Corbin J.D. 2006. Phosphodiesterase-5: molecular characteristics relating to structure, function, and regulation. In: Cyclic Nucleotide Phosphodiesterases in Health and Disease, edited by Beavo JA, Houslay MD, Francis SH. Boca Raton, FL: CRC, p. 131–164.

Francis, S.H., Blount, M.A. & J.D. Corbin. 2011. Mammalian cyclic nucleotide phosphodiesterases: molecular mechanisms and physiological functions. Physiol. Rev. 91: 651-690.

Frank, A., Bonney, M., Bonney, S., Weitzel, L., Koeppen, M., & Eckle, T. (2012, September). Myocardial Ischemia Reperfusion Injury From Basic Science to Clinical Bedside. In Seminars in cardiothoracic and vascular anesthesia (Vol. 16, No. (3): 123-132.

Freedman, N.J. & R.J. Lefkowitz. 1996. Desensitization of G protein-couple receptors. Recent Prog Horm Res (51): 319-351.

Fujita, M., Zoghbi, S. S., Crescenzo, M. S., Hong, J., Musachio, J. L., Lu, J. Q., ... & Innis, R. B. 2005. Quantification of brain phosphodiesterase 4 in rat with (*R*)-[^{11}C] Rolipram-PET. Neuroimage, 26(4), 1201-1210.

Gajarsa, J.J., Kloner, R.A. 2011. Left ventricular remodelling in the post-infarction heart: a review of cellular, molecular mechanisms, and therapeutic modalities. Heart Failure Rev. 16:13-21.

Gaudron, P., Eilles, C., Ertl, G., & Kochsiek, K. 1990. Early remodelling of the left ventricle in patients with myocardial infarction. European heart journal,11(suppl B), 139-146.

Graham, L.N., Smith, P.A., Stoker, J.B., et al. 2002. Time course of sympathetic neural hyperactivity after uncomplicated acute myocardial infarction. Circulation 106(7): 793-797.

Grange M., Sette C., Cuomo M., Conti M., Lagarde M., Prigent A.F., Nemoz G. 2000. The cAMP-specific phosphodiesterase PDE4D3 is regulated by phosphatidic acid binding.Consequences for cAMP signaling pathway and characterization of a phosphatidic acid binding site. J Biol Chem 275:33379–33387.

Greene, M., Thackeray, J.T., Kenk, M., Thorn, S.L., Bevilacqua, L., Harper, M.E., Beanlands, R.S. & Dasilva J.N. 2009. Reduced in vivo phosphodiesterase-4 response to acute noradrenaline challenge in diet-induced obese rats. Can J Physiol Pharmacol 87(3): 196-202.

Gao T., Yatani A., Dell'Acqua M.L., Sako H., Green S.A., Dascal N., et al. 1997. cAMP-dependent regulation of cardiac L-type Ca^{2+} channels require membrane targeting of PKA and phosphorylation of channel subunits. Neuron 19:185–96.

Gao, H., Kiesewetter, D.O., Zhang, X., Huang, X., Guo, N., Lang, L., Hida, N., Wang, W., Wang, H., Cao, F., Niu, G. & X. Chen. 2012. Pet of glucagonlike peptide receptor upregulation after myocardial ischemia or reperfusion injury. J Nucl Med. 53: 1960-1968.

Gauthier, C., Tavernier, G., Charpentier, F., et al. 1996. Functional beta3-adrenoceptor in the human heart. The Journal of Clinical Investigation, 98, 556–562.

Gauthier, C., Leblais, V., Kobzik, L., et al. 1998. The negative ionotropic effect of beta3-adrenoceptor stimulation is mediated by activation of a nitric oxide synthase pathway in human ventricle. The Journal of Clinical Investigation, 102, 1377–1384.

Georget, M., Mateo, P., Vandescasteele, G., Lipskaia, L., Defer, N., Hanoune, J., ... & Fischmeister, R. 2003. Cyclic AMP compartmentation due to increased cAMP-phosphodiesterase activity in transgenic mice with a cardiac-directed expression of the human adenylyl cyclase type 8 (AC8). The FASEB journal, 17(11), 1380-1391.

Ghosh, N., Rimoldi, O.E., Beandlands, R.S., & Camici, P.G. 2010. Assessment of myocardial ischemia and viability: role of positron emission tomography. Eur. Heart J. 31(24):2984-2995.

Gilman, A.G. 1987. G proteins: Transducers of receptor-generated signals. Ann. Rev. Biochem. 56: 615-649.

Gilbert, E. M., Olsen, S. L., Renlund, D. G., & Bristow, M. R. 1993. Beta-adrenergic receptor regulation and left ventricular function in idiopathic dilated cardiomyopathy. The American journal of cardiology, 71(9), C23-C29.

Go et al. 2012. Heart Disease and Stroke Statistics-2013 Update A report from the American heart association. Circulation 127:6-245.

Goldsmith S.R., Francis G.S., Cohn J.N. 1985. Norepinephrine infusions in congestive heart failure. Am J Cardiol 56(12): 802–804.

Gordon A.M., Homsher E., Regnier M. 2000. Regulation of contraction in striated muscle. Physiol Rev. 80:853–924.

Griffiths, E.J., & Halestrap, A.P. 1995. Mitochondrial non-specific pores remain closed during cardiac ischaemia, but open ipon reperfusion. Biochem. J. 307: 93-98.

Hadcock, J. R., & Malbon, C. C. 1988. Down-regulation of beta-adrenergic receptors: agonist-induced reduction in receptor mRNA levels. Proceedings of the National Academy of Sciences, 85(14), 5021-5025.

Hardman, J.G. et al. 1971. The formation and metabolism of cyclic GMP. Ann NY Acad Sci 185:27-35.

Hasking, G.J., Esler, M.D., Jennings, G.L., Burton, D., Johns, J.A., & P.I. Korner. 1986. Norepinephrine spillover to plasma in patients with congestive heart failure: evidence of increased overall and cardiorenal sympathetic nervous activity. Circulation 73: 615-621.

Hausdorff, W. P. et al. 1989. Phosphorylation sites on two domains of the β2-adrenergic receptor are involved in distinct pathways of receptor desensitization. J. Biol. Chem. 264, 12657–12665.

Hausenloy, D. J., & Yellon, D. M. 2003. The mitochondrial permeability transition pore: its fundamental role in mediating cell death during ischaemia and reperfusion. Journal of molecular and cellular cardiology, 35(4), 339-341.

Heller, G.V., Calnon, D., & Dorbala, S. 2009. Recent advances in cardiac PET and PET/CT myocardial perfusion imaging. J. Nucl. Cardiol. 16(6):962-969.

Hendel R.C., Berman D.S., Di Carli M.F., et al. 2009. ACCF/ASNC/ACR/AHA/ASE/SCCT/SCMR/SNM 2009 Appropriate Use Criteria for Cardiac Radionuclide Imaging: A Report of the American College of Cardiology Foundation Appropriate Use Criteria Task Force, the American Society of Nuclear Cardiology, the American College of Radiology, the American Heart Association, the American Society of Echocardiography, the Society of Cardiovascular Computed Tomography, the Society for Cardiovascular Magnetic Resonance, and the Society of Nuclear Medicine. J Am Coll Cardiol. 53(23):2201-29.

Hess, O.M. 1993. Hemodynamic in cardiac failure: systolic and diastolic dysfunction. Ther Umsch 50:414-418.

Heyndrickx, G. R., Baig, H. A. N. K., Nellens, P. A. U. L., Leusen, I. S. I. D. O. O. R., Fishbein, M. C., & Vatner, S. F. 1978. Depression of regional blood flow

and wall thickening after brief coronary occlusions. American Journal of Physiology-Heart and Circulatory Physiology, 234(6), H653-H659.

Hildreth, V., Anderson, R., Henderson, D. 2009. Clinical Anatomy 22: 36-46.

Higuchi, T., & Bengel, F.M. 2008. Cardiovascular nuclear imaging: from perfusion to molecular function: non-invasive imaging. Heart 94(6): 809-816.

Hill JH, Ward PA. C3 leukotactic factors produced by a tissue protease. J Exp Med 1969;130:505–18.

Hoffman, R., I.R. Wilkinson, J.F. McCallum, P. Engels & M.D. Houslay. 1998. cAmp-specific phosphodiesterase Hspde4d3 mutants which mimic activation and changes in Rolipram inhibition triggered by protein kinase A phosphorylation of Ser-54: generation of a molecular model. Biochem. J. 333(1): 139-149.

Hoffmann R., Baillie G.S., MacKenzie S.J., Yarwood S.J., Houslay M.D. 1999. The MAP kinase ERK2 inhibits the cyclic AMP-specific phosphodiesterase HSPDE4D3 by phosphorylating it at Ser579. EMBO J 18:893–903.

Horvath A., Faucz F., Finkielstain G.P., Nikita M.E., Rothenbuhler A., Almeida M., Mericq V., Stratakis C.A. 2010. Haplotype analysis of the promoter region of phosphodiesterase type 8B (PDE8B) in correlation with inactivating PDE8B mutation and the serum thyroid-stimulating hormone levels. Thyroid 20: 363–367.

Houslay, M. D. and Milligan, G. 1997. Tailoring cAMP signalling responses through isoform multiplicity. Trends Biochem. Sci. 22, 217-224.

Houslay, M.D. & Adams, D.R. 2003. PDE4 cAMP phosphodiesterases: modular enzymes that orchestrate signalling cross=talk, desensitization and compartmentalization. Biochem J. 370: 1-18.

Houslay M.D., Baillie G.S. 2003. The role of ERK2 docking and phosphorylation of PDE4 cAMP phosphodiesterase isoforms in mediating cross-talk between the cAMP and ERK signalling pathways. Biochem Soc Trans 31, 1186–1190.

Huai, Q., Colicelli, J., Ke H. 2003. The crystal structure of AMP-bound PDE4 suggests a mechanism for phosphodiesterase catalysis. Biochemistry 42: 13220-13226.

Hulme J.T., Lin T.W., Westenbroek R.E., Scheuer T., Catterall W.A. 2003. Beta-adrenergic regulation requires direct anchoring of PKA to cardiac Cav1.2 channels via a leucine zipper interaction with A kinaseanchoring protein 15. Proc Natl Acad Sci U S A 100:13093–8.

Huston E., Beard M., McCallum F., Pyne N.J., Vandenabeele P., Scotland G., Houslay M.D. 2000. The cAMP-specific phosphodiesterase PDE4A5 is cleaved downstream of its SH3 28 cAMP-SPECIFIC PHOSPHODIESTERASES: MODULATION, INHIBITION, AND ACTIVATION interaction domain by caspase-3. Consequences for altered intracellular distribution. J Biol Chem 275:28063–28074.

Hutchinson, D. S., Bengtsson, T., Evans, B. A., et al. 2002. Mouse beta3a-and beta 3b-adrenoceptors expressed in Chinese hamster ovary cells display identical pharmacology but utilize distinct signalling pathways. British Journal of Pharmacology, 135, 1903–1914.

Huwer H, Winning J, Vollmar B, Welter C, Menger MD, Schafers HJ. 2000. Model of chronic systolic and diastolic dysfunction after cryothermia-induced myocardial necrosis in rats. Comp Med. 50 (4): 385-90.

Ito, M., M., Nishikawa, M., Fujioka, M., Miyahara, N., Isaka, H., Shiku, & T. Nakano. 1996. Characterization of the isoenzymes of cyclic nucleotide phosphodiesterase in human platelets and the effects of E4021. Cell Signal. 8: 575-581.

Janssen P.M.L., de Tombe P.P. 1997. Protein kinase A does not alter unloaded velocity of sarcomere shortening in skinned rat cardiac trabeculae. Am J Physiol. 273:H2415–H2422.

Jennings RB, Sommers HM, Smyth GA, Flack HA, Linn H. 1960 Myocardial necrosis induced by temporary occlusion of a coronary artery in the dog. Arch Pathol 70:68–78.

Jin S.L., Latour A.M., Conti M. 2005. Generation of PDE4 knockout mice by gene targeting. Methods Mol Biol. 307: 191–210.

Johns E.C., Simnett S.J., Mulligan I.P., Ashley C.C. 1997. Troponin I phosphorylation does not increase the rate of relaxation following laser flash photolysis of diazo-2 in guinea pig skinned trabeculae. Pflug Arch.;433:842– 844.

Kaasik, A., Ohisalo, J.J. 1996. Membrane-bound phosphodiesterases in rat myocardium. J. Pharm. Pharmacol. 48: 962-964.

Kacimi, R., Richalet, J. P., Corsin, A., Abousahl, I., & Crozatier, B. 1992. Hypoxia-induced downregulation of beta-adrenergic receptors in rat heart. Journal of Applied Physiology, 73(4), 1377-1382.

Katz, A.M. 1989. Changing strategies in the management of heart failure. J. Am. Coll. Cardiol. 13(3): 513-523.

Karmazyn, M. 1988. Amiloride enhances postischemic ventricular recovery: possible role of Na+-H+ exchange. Am J Physiol, 255(3 Pt 2), H608-615.

Kaufman, S. & E.E. Kaufman. 1985. Tyrosine hydroxylase. In: Blakley R.L, Benkovic, S.J. Editors. Folates and pterins. 2nd vol. Chemistry and biochemistry of the pterins. New York: John Wiley and Sons P. 251-352.

Kaumann A.J., Hall J.A., Murray K.J., Wells F.C. and Brown M.J. 1989. A comparison of the effects of adrenaline and noradrenaline on human heart: the role of b1- and b2 adrenoceptors in the stimulation of adenylate cyclase and contractile force. Eur Heart J 10 (Suppl B):29–37.

Kaumann, A. J., & Molenaar, P. 1996. Differences between the third cardiac beta-adrenoceptor and the colonic beta3-adrenoceptor in the rat. British Journal of Pharmacology, 118, 2085–2098.

Kaumann A.J. & P. Molenaar. 1997. Modulation of human cardiac function through 4 b-adrenoceptor populations. Naunyn-Schmiedeberg's Arch Pharmacol 355:667–681.

Ke, H. 2004. Implications of PDE4 structure on inhibitor selectivity across PDE families. International Journal of Impotence Research 16: S24-S27.

Kearfott K.J., Elmaleh D.R., Goodman M., Correia J.A., Alpert N.M., Ackerman R.H., Brownell G.L., and Strauss W.H. Comparison of 2- and 3-18F-fluoro-deoxy-D-glucose for studies of tissue metabolism. Int J Nucl Med Biol 11: 15–22, 1984.

Keef K.D., Hume J.R., Zhong J. 2001. Regulation of cardiac and smooth muscle Ca2+ channels (Ca(V)1.2a,b) by protein kinases. Am J Physiol Cell Physiol 28:C1743–56.

Kelly M.P., Logue S.F., Brennan J., Day J.P., Lakkaraju S., Jiang L., Zhong X., Tam M., Sukoff Rizzo S.J., Platt B.J., Dwyer J.M., Neal S., Pulito V.L., Agostino M.J., Grauer S.M., Navarra R.L., Kelley C., Comery T.A., Murrills R.J., Houslay M.D., Brandon N.J. 2010. Phosphodiesterase 11A in brain is enriched in ventral hippocampus and deletion causes psychiatric disease-related phenotypes. Proc Natl Acad Sci USA 107: 8457–8462.

Kenk, M., Greene, M., Thackeray, J., deKemp, R.A., Lortie, M., Thorn, S., Beanlands, R.S., DaSilva, J.N. 2007. In vivo selective binding of (R)-[11C]Rolipram to phosphodiesterase-4 provides the basis for studying intracellular cAMP signaling in the myocardium and other peripheral tissues. Nucl Med Biol 34(1):71-77.

Kenk, M., Greene, M., Lortie, M., deKemp, R.A., Beanlands, R.S., DaSilva, J.N. 2008. Use of a column-switching high-performance liquid chromatography method to assess the presence of specific binding (R)- and (S)-[(11)C]Rolipram and their labeled metabolites to the phosphodiesterase-4 enzyme in rat plasma and tissues.

Kenk, M. 2010. In vivo evaluation of (*R*) and (*S*)-[^{11}C] Rolipram for imaging cardiac phosphodiesterase-4 enzymes: characterization and applications in rat models of heart failure. Ph.D. thesis. University of Ottawa. Canada.

Kenk, M., Thackeray, J.T., Thorn, S.L., Dhami, K., Chow, B.J., Ascah, K.J., DaSilva, J.N., Beanlands, R.S. 2010. Alterations of pre- and postsynaptic noradrenergic signaling in a rat model of adriamycin-induced cardiotoxicity. J Nucl Cardiol 17(2):254-263.

Kenk, M., Thorn, S., Vaskas, J., Renaud, J., Kolajova, M., Klein, R., Lortie, M., de Kemp, R., Beanlands, R.S. & J.N. Dasilva. cAMP-Mediated PDE4 Signaling is Maintained Despite Down Regulated β1-AR at 8-12 Weeks Post-MI in Non-Infarcted Rat Myocardium Measured by (R)-[11C]Rolipram PET. *Unpublished* .

Kim, J.S., Jin, Y., & Lemasters, J.J. 2006. Reactive oxygen species, but not Ca2+ overloading, trigger pH- and mitochondrial permeability transition-dependent death of adult rat myocytes after ischemia-reperfusion. Am. J. Heart. Circ. Physiol. 290:H2024-H2034.

Kirstein, M., Rivet-Bastide, M., Hatem, S., et al. 1995. Nitric oxide regulates the calcium current in isolated human atrial myocytes. The Journal of Clinical Investigation, 95, 794–802.

Klocke, R, W Tian, M Kuhlmann, and S Nikol. "Surgical animal models of heart failure related to coronary heart disease."Cardiovascular Research 74.1 (2007): 29-38.

Komas, N., Movsesian, M., Kedev, S., Degerman, E., Belfrage, P., and Manganiello, V. C. 1996. in Handbook of Pharmacology: Phosphodiesterase Inhibitors (Schudt, C., Dent, G., and Rabe, K. F., eds. pp. 89–109, Academic Press, London.

Kostic, M.M., Erdogan, S., Rena, G., Borchert, G., Hoch, B., Bartel, S., Scotland, G., Huston, E., Houslay, M.D. & E.G. Kraus. 1997. Altered expression of PDE1 and PDE4 cyclic nucleotide phosphodiesterase isoforms in 7-oxo-prostacyclin-preconditioned rat heart. J Mol Cell Cardiol 29(11): 3135-3146.

Krupnick J.G., Gurevich V.V., Benovic J.L. 1997. Mechanism of Quenching of Phototransduction: Binding competition between arrestin and transducin for phosphorhodopsin. J Biol Chem 272:18125–18131.

Kuschel M., Karczewski P., Hempel P., Schlegel W.P., Krause E.G., Bartel S. 1999. Ser16 prevails over Thr17 phospholamban phosphorylation in the beta-adrenergic regulation of cardiac relaxation. Am J Physiol May 276(5 Pt 2):H1625–H1633.

Kuwahara, K., Nishikimi, T. & Nakao, K. 2012. Transcriptional regulation of the fetal cardiac gene program. J. Pharmacol Sci 119: 198-203.

Kvetnansky, R., Sabban, E. L., & Palkovits, M. (2009). Catecholaminergic systems in stress: structural and molecular genetic approaches. Physiological reviews, 89(2), 535-606.

Lefkowitz, R.J. & Shenoy, S.K. 2005. Transduction of receptor signals by beta-arrestins. Science 308: 512-517.

Leineweber, K., Wangemann, T., Giessler, C., Bruck, H., Dhein, S., Kostelka, M., et al. 2002. Age-dependent changes of cardiac neuronal noradrenaline reuptake transporter (uptake1) in the human heart. JACC 40: 1459.

Le Jeune, I.R., M. Shepherd, G. Van Heeke, M.D. Houslay & I.P. Hall. 2002. Cyclic AMP-dependent Transcriptional Up-regulation of Phosphodiesterase 4D5 in Human Airway Smooth Muscle Cells J. Biol. Chem. 277 (39) 35980-35989.

Lehnart, S.E., Wehrens, X.H.T., Reiken, S., Warrier, S., Belevych, A.E., Harvey R.D. et al. 2005. Phosphodiesterase 4D deficiency in the Ryanodine-receptor complex promotes heart failure and arrhythmias. Cell 23:25-35.

Lemasters, J.J., Bond, J.M., Chacon, E., et al. 1996. The pH paradox in ischemia-reperfusion injury to cardiac myocytes. EXS 76:99-114.

Leosco, D., Rengo, G., Iaccarino, G., Golino, L., Marchese, M., Fortunato, F., ... & Rengo, F. 2008. Exercise promotes angiogenesis and improves β-adrenergic receptor signalling in the post-ischaemic failing rat heart.Cardiovascular research, 78(2), 385-394.

Leroy, J., Richter, W., Mika, D., Castro, L.R., Abi-Gerges, A., Xie, M., Scheitrum, C., Lefebvre, F., Schittl, J., Mateo, P., Westenbroek, R., Catterall, W.A., Charpentier, F., Conti, M., Fischmeister, R. & G. Vandecasteele. 2011. Phosphodiesterase 4B in the cardiac L-type Ca2+ channel complex regulates Ca2+ current and protects against ventricular arrhythmias in mice. J Clin Invest 121: 2651-2661.

Levy, D., Kenchaiah, S., Larson, M.G., et al. 2002. Long-term trends in the incidence of and survival with heart failure. N. Engl. J. Med. 347(18):1397-1402.

Levy, W.C. & D.T. Linker. 2008. Prediction of mortality in patients with heart failure and systolic dysfunction. Current cardiology reports 10:198-205.

Li X, Baillie G.S., Houslay M.D. 2009. Mdm2 directs the ubiquitination of betaarrestin-sequestered cAMP phosphodiesterase-4D5. J Biol Chem 284:16170–16182.

Li, L., Miano, J.M., Cserjesi, P., & Olson E.N. 1996. SM22 alpha, a marker of adult smooth muscle, is expressed in multiple myogenic lineages during embryogenesis. Circ Res. 78: 199-195.

Liang, W. & S.E. Mills. 2002. Quantitative anaylsus of beta-adrenergic receptor subtypes in pig tissues. J. Anim. Sci. 80(4): 963-970.

Ligget, S.B., Tepe, N.M., Lorenz, J.N., Canning, A.M., Jantz, T.D., Mitarai, S., et al. 2000. Early and delayed consequences of beta(2)-adrenergic receptor overexpression in mous hearts: critical role for expression level. Circulation 101: 1707-1714.

Liu YH, Yang XP, Nass O, Sabbah HN, Peterson E, Carretero OA. Chronic heart failure induced by coronary artery ligation in Lewis inbred rats. Am J Physiol 1997;272:H722–7.

Liu, H. & D.H. Maurice. 1999. Phosphorylation-mediated activation and translocation of the cyclic AMP-specific phosphodiesterase PDE4D3 by cyclic AMP-dependent protein kinase and mitogen-activated protein kinases. A potential mechanism allowing for the coordinated regulation of PDE4D activity and targeting. J. Biol. Chem. 274(15): 10557-10565.

Liu, P., M. Arnold, I. Belenkie, J. Howlett, V. Huckell, A. Ignazewski, M. H. LeBlanc, R. McKelvie, J. Niznick, J. D. Parker, V. Rao, H. Ross, D. Roy, S. Smith, B. Sussex, K. Teo, R. Tsuyuki, M. White, D. Beanlands, V. Bernstein, R. Davies, D. Issac, D. Johnstone, H. Lee, G. Moe, G. Newton, P. Pflugfelder, S. Roth, J. Rouleau and S. Yusuf. 2001. The 2001 Canadian Cardiovascular Society consensus guideline update for the management and prevention of heart failure. Can. J. Cardiol. 17 Suppl E: 5E-25E.

Lloyd-Jones, D., R. J. Adams, T. M. Brown, M. Carnethon, S. Dai, G. De Simone, T. B. Ferguson, E. Ford, K. Furie, C. Gillespie, A. Go, K. Greenlund, N. Haase, S. Hailpern, P. M. Ho, V. Howard, B. Kissela, S. Kittner, D. Lackland, L. Lisabeth, A. Marelli, M. M. McDermott, J. Meigs, D. Mozaffarian, M. Mussolino, G. Nichol, V. L. Roger, W. Rosamond, R. Sacco, P. Sorlie, R. Stafford, T. Thom, S. Wasserthiel-Smoller, N. D. Wong and J. Wylie-Rosett. 2010. "Heart disease

and stroke statistics--2010 update: a report from the American Heart Association." Circulation 121(7): e46-e215.

Lõhmussaar, E., Gschwendtner, A., Mueller, J. C., Wichmann, E., Hamann, G., Meitinger, T., & Dichgans, M. (2005). ALOX5AP gene and the PDE4D gene in a central European population of stroke patients. Stroke, 36(4), 731-736.

Lohse, M.J., Engelhardt, & T. Eschenhagen. 2003. What is the role of beta-adrenergic signalling in heart failure. Circ Res 93: 896-906.

Lourenco, C.M., Houle, S., Wilson, A.A., DaSilva, J.N. 2001. Characterization of r-[11C]Rolipram for PET imaging of phosphodiesterase-4: in vivo binding, metabolism, and dosimetry studies in rats. Nucl Med Biol 28(4):347-358.

Lourenco, C.M., Kenk, M., Beanlands, R.S., DaSilva, J.N. 2006. Increasing synaptic noradrenaline, serotonin and histamine enhances in vivo binding of phosphodiesterase-4 inhibitor (R)-[11C]Rolipram in rat brain, lung and heart. Life Sci 79(4):356-364.

Lugnier C., Keravis T., Le Bec A., Pauvert O., Proteau S., Rousseau E. 1999. Characterization of cyclic nucleotide phosphodiesterase isoforms associated to isolated cardiac nuclei. Biochim Biophys Acta 1472:431–46.

Lymperopoulos, A., Rengo, G., and Koch, W.J. 2007. Adrenal adrenoceptors in heart failure: fine-tuning cardiac stimulation. Trends Mol Med 13:503-511.

Lymperopoulos, A., & A. Bathgate. 2012. Pharmacogenomics of the heptahelical receptor regulators G-protein-coupled receptor kinases and arrestins: the known and the unknown. Pharmacogenomics 13:323-341.

Lymperopoulos, A. 2012. Ischemic emergency? Endothelial cells have their own “adrenaline shot” at hand. Hypertension 60:12-14.

Lymperopoulos, A. 2013. Physiology and pharmacology of the cardiovascular adrenergic system. Frontiers in Physiology 4 Article 240.

Mackenzie, S.J., Baillie, G.S., McPhee, I., MacKenzie, C., Seamons, R., McSorely, T., Millen, J., Beard, M.B., van Heeke, G. & M.D. Houslay. 2002. Long PDE4 cAMP specific phosphodiesterases are activated by protein kinase A-mediated phosphorylation of a single serine residue in upstream conserved region 1 (UCR1). Br. J. Pharmacol. 136:421-433.

Malpas, S. 2010. Sympathetic Nervous System Overactivity and Its Role in the Development of Cardiovascular Disease. Physiol Review 90: 513-557.

Manganiello, V. C. and Degerman, E. 1999. Cyclic nucleotide phosphodiesterases

(PDEs): diverse regulators of cyclic nucleotide signals and inviting molecular targets
for novel therapeutic agents. Thromb. Haemostasis 82, 407-411.

Manganiello, V. C., Taira, M., Degerman, E., and Belfrage, P. 1995. Type III cGMP-inhibited cyclic nucleotide phosphodiesterases (PDE 3 gene family). Cell. Signalling 7, 445–455.

Marks, A. R. 2013. Calcium cycling proteins and heart failure: mechanisms and therapeutics. J Clin Invest, 123(1), 46-52.

Martins, T.J., M.C., Mumby, & J.A. Beavo. 1982. Purification and characterization of a cyclic GMP-stimulated cyclic nucleotide phosphodiesterase from bovine tissues. J. Biol. Chem. 257(4): 1973-1979.

Marx, S.O., Reiken, S., Hisamatsu, Y., Jayaraman, T., Burkhoff, D., Rosemblit, N. & A.R. Marks. 2000. PKA phosphorylation dissociates FKBP12.6 from the calcium release channel (Ryanodine receptor): defective regulation in failing hearts. Cell 101: 365-376.

Mathes, P., & Gudbjarnason, S. 1971. Changes in norepinephrine stores in the canine heart following experimental myocardial infarction. American heart journal, 81(2), 211-219.

McCahill A.C., Huston E., Li X., Houslay M.D. 2008. PDE4 associates with different scaffolding proteins: Modulating interactions as treatment for certain diseases. Handb Exp Pharmacol 186:125–166.

Mackasey, K. 2012. Evaluating angiotensin II type 1 receptor changes in post-renal insufficiency and in left anterior descending artery ligation animal models using [11C]Methyl-Candersartan. M.Sc. Thesis. University of Ottawa, Canada.

Manning, C. D., Burman, M., Christensen, S. B., Cieslinski, L. B., Essayan, D. M., Grous, M., ... & Barnette, M. S. (1999). Suppression of human inflammatory cell function by subtype-selective PDE4 inhibitors correlates with inhibition of PDE4A and PDE4B. British journal of pharmacology, 128(7), 1393-1398.

McKay, R.G., Pfeffer, M.A., Pasternak, R.C., Markis, J.E., Come, P.C., Nakao, S., Alderman, J.D., Ferguson, J.J., Safian, R.D. & Grossman W. 1986. Left ventricular remodeling following myocardial infarction: A corollary to infarct expansion. Circulation 74: 693-702.

McMurray, J.J., Petrie, M.C., Murdoch, D.R., & Davie, A.P. 1998. Clinical epidemiology of heart failure: public and private health burden. Eur. Heart. J. 19(Suppl P):9-16.

McMurray, J. J., Adamopoulos, S., Anker, S. D., Auricchio, A., Böhm, M., Dickstein, K., ... & Ben Lamin, H. A. 2012. ESC Guidelines for the diagnosis and treatment of acute and chronic heart failure 2012. European journal of heart failure, 14(8), 803-869.

McMurrary, J.J., & Pfeffer, M.A. 2005. Heart Failure. Lancet 365(9474): 1877-1889.

Mehel H., J.C.V. Emons et al. 2013. Phosphodiesterase-2 is upregulated in human failing hearts and blunts b-adrenergic responses in cardiomyocytes. J Am Coll Cardiol. 62(17): 1596-1606.

Merlet, P., Delforge, J., Syrota, A., Angevin, E., Mazière, B., Crouzel, C., ... & Rande, J. L. 1993. Positron emission tomography with 11C CGP-12177 to assess beta-adrenergic receptor concentration in idiopathic dilated cardiomyopathy. Circulation, 87(4), 1169-1178.

Mitchell PJ, Wang C, Tjian R. 1987. Positive and negative regulation of transcription in vitro: enhancer- binding protein AP-2 is inhibited by SV40 T antigen. Cell 50, 847–861

Molina, C. E., Leroy, J., Richter, W., Xie, M., Scheitrum, C., Lee, I. O., ... & Fischmeister, R. 2012. Cyclic adenosine monophosphate phosphodiesterase type 4 protects against atrial arrhythmias. Journal of the American College of Cardiology, 59(24), 2182-2190.

Moens, A. L., Yang, R., Watts, V. L., & Barouch, L. A. 2010. Beta 3-adrenoreceptor regulation of nitric oxide in the cardiovascular system. Journal of molecular and cellular cardiology, 48(6), 1088-1095.

Mongillo, M., McSorely, T., Evellin, S., Sood, A., Lissandron, V., Terrin, A. Et al. 2004. Fluorescence resonance energy transfer-based analysis of cAMP dynamics in live neonatal rat cardiac myocytes reveals distinct functions of compartmentalized phosphodiesterases. Circ. Res. 95: 67-75.

Moniotte S., Kobzik L., Feron O., Trochu J.N., Gauthier C., Balligand J.L. 2001. Upregulation of beta(3)-adrenoceptors and altered contractile response to inotropic amines in human failing myocardium. Circulation 103:1649–1655.

Montminy M. 1997. Transcriptional regulation by cyclic AMP. Annu Rev Biochem 66, 807–822.

Motomura S., Zerkowski H.R., Daul A. and Brodde O.E. 1990. On the physiologic role of beta-2 adrenoceptors in the human heart: In vitro and in vivo studies. Am Heart J 119:608–619.

Morisco, C., Zebrowski, D. C., Vatner, D. E., Vatner, S. F., & Sadoshima, J. 2001. β-Adrenergic Cardiac Hypertrophy is Mediated Primarily by the β1-Subtype in the Rat Heart. Journal of molecular and cellular cardiology, 33(3), 561-573.

Movsesian, M. A., Smith, C. J., Krall, J., Bristow, M. R., & Manganiello, V. C. 1991. Sarcoplasmic reticulum-associated cyclic adenosine 5'-monophosphate phosphodiesterase activity in normal and failing human hearts. Journal of Clinical Investigation, 88(1), 15-19.

Munch, G., Nguyen, N.T., Nekolla, S. Et al. 2000. Evaluation of sympathetic nerve terminals with [^{11}C]epinephrine and [^{11}C]hydroxyephedrine and positron emission tomography. Circulation 101(5):516-523.

Myslivecek, J. & S. Trojan. 2003. Regulation of adrenoceptors and muscarinic receptors in the heart. Gen. Phsyiol. Biophys. 22(1):3-14.

Nagarakanti, R. & M. Ezekowitz. 2008. Diastolic dysfunction and atrial fibrillation. J Interv Card Electrophysiol 22:111-118.

Nagatsu, T., Levitt, M. & S. Udenfriend. 1964. Tyrosine hydroxylase: the inital step in norepinephrine biosynthesis. J Biol Chem 239:2910-2917.

Nemoz G., Sette C., Conti M. 1997. Selective activation of Rolipram-sensitive, cAMP-specific phosphodiesterase isoforms by phosphatidic acid. Mol Pharmacol 51:242–249.

Nikolaev, V.O., Moshkov, A., Lyon, A.R., Miragoli, M., Novak, P., Paur, H., Lohse, M.J., Korchev, Y.E., Harding, S.E. & Gorelik, J. 2010. Beta2-adrenergic receptor redistribution
in heart failure changes cAMP compartmentation. Science 327, 1653–1657.

Notarius, C.F., Spaak, J., Morris, B.L. et al. 2007. Comparison of muscle sympathetic activity in ischemic and nonischemic heart failure. J Card Fail 13(6): 470-475.

O'Donnell, J. M., & Zhang, H. T. (2004). Antidepressant effects of inhibitors of cAMP phosphodiesterase (PDE4). Trends in pharmacological sciences, 25(3), 158-163.

Okruhlicova, L., Tribulova, N., Eckly, A., Lugnier, C., & J. Slezlak. 1996. Cytochemical distribution of cyclic AMP-dependent 3-5’nucleotide phosphodiesterase in the rat myocardium. Histochem J 28: 165-172.

Ohte, N., Narita, H., Ida, Akihiko, Fukuta, H., Iizuka, N., Hayano, J., Kuge, Y., Tamaki, N. & G. Kimura. 2012. Cardiac β-adrenergic receptor density and myocardial systolic function in the remote noninfarcted reion after prior myocardial infarction with left ventricular remodelling. Eur J Nucl Med Mol Imaging 39: 1246-1253.

Oliveira R.F., Terrin A., Di Benedetto G., Cannon R.C., Koh W., Kim M., Zaccolo M., Blackwell K.T. 2010. The role of type 4 phosphodiesterases in generating microdomains of cAMP: large scale stochastic simulations. PLoS One 5: e11725.

Olsen, A.E. & G.B. Bolger. 2000. Physical mapping and promoter structure of the murine cAMP-specific phosphodiesterase pde4a gene. Mamm. Genome 11 (1) 41-45.

Olson, E.N. 2004. A decade of discoveries in cardiac biology. Nat. Med. 10: 467-474.

Osadchii, O.E. 2007. Myocardial phosphodiesterases and regulation of cardiac contractility in health and cardiac disease. Cardiovasc Drugs Ther 21(3):171-194.

Packer, M. 1996. New concepts in the pathophysiology of heart failure: beneficial and deleterious interaction of endogenous haemodyamic and neurohormonal mechanisms. J Intern Med 239: 327-333.

Pai, R.G., Chandraratna, P.A.N., Varadarajan, P. & S. Malik, Ed. Echocardiography a case studies based approach. Burlington MA: Jones & Bartlett 2013. Print.

Parlmey, W.W. 1989. Pathophysiology and current therapy of congestive heart failure. J. Am. Coll. Cardiol. 13(4): 771-785.

Packer, M. 1992. Pathophysiology of chronic heart failure. Lancet 340:88-92.

Perets T., Blumenstein Y., Shistik E., Lotan I., Dascal N. 1996. A potential site of functional modulation by protein kinase A in the cardiac Ca^{2+} channel α1C subunit. FEBS Lett 384:189–92.

Perry S.J., Baillie G.S., Kohout T.A., McPhee I., Magiera M.M., Ang K.L., Miller W.E., McLean A.J., Conti M., Houslay M.D., Lefkowitz R.J. 2002. Targeting of cyclic AMP degradation to beta 2-adrenergic receptors by beta-arrestins. Science 298: 834–836.

Petch, M.C. & W.G. Nayer. 1979. Uptake of catecholamines by human cardiac muscle in vitro. Br Heart J 41: 336-339.

Petty, M.A., Lukovic, L., Grisar, J.M., Dow, J., Bolkenius, F.N., & W. De Jong. 1994. Myocardial protection by a cardioselective free radical scavenger. European Journal of Pharmacology 255:215-222.

Pfeffer M.A., Pfeffer J.M., Fishbein M.C., Fletcher P.J., Spadaro J., Kloner R.A., et al. 1979. Myocardial infarct size and ventricular function in rats. Circ Res 44:503–12.

Pfeffer, J.M., Pfeffer, M.A. & E. Braunwald. 1985. Influence of chronic captopril therapy on the infarcted left ventricle of the rat. Circ Res 57: 84-95.

Pfeffer, M.A. & E. Braunwald. 1990. Ventricular remodeling after myocardial infarction. Circulation 81(4): 1161-1172.

Pickard, B. S., Thomson, P. A., Christoforou, A., Evans, K. L., Morris, S. W., Porteous, D. J., ... & Muir, W. J. (2007). The PDE4B gene confers sex-specific protection against schizophrenia. Psychiatric genetics, 17(3), 129-133.

Pierpont, G.L., DeMaster, E.G., Reynolds, S., Pdereson, J., and Cohn, J.N. 1985. Ventricular myocardial catecholamines in primates. J. Lab. Clin. Med. 106: 205-210.

Piper, H.M., Garcia-Dorado, D. & Ovize M. 1998. A fresh look at reperfusion injury. Cardiovasc Res 38:291-300.

Pitcher, J.A. et al. 1998. G protein-coupled receptor kinases. Annu Rev Biochem 67:653-692.

Popper, C. W., Chiueh, C. C., & Kopin, I. J. 1977. Plasma catecholamine concentrations in unanesthetized rats during sleep, wakefulness, immobilization and after decapitation. Journal of Pharmacology and Experimental Therapeutics, 202(1), 144-148.

Pride, Y. B., Piccirillo, B. J., & Gibson, C. M. 2013. Prevalence, consequences, and implications for clinical trials of unrecognized myocardial infarction. The American journal of cardiology 111(6): 914-918.

Qin, F., Vulapalli, R. S., Stevens, S. Y., & Liang, C. S. 2002. Loss of cardiac sympathetic neurotransmitters in heart failure and NE infusion is associated with reduced NGF. American Journal of Physiology-Heart and Circulatory Physiology, 282(1): H363-H371.

Ramakrishnan, C., Dani, T., & A. Ramasarma. 2002. A conformational anaylsis of Walker motif A [GXXXXGKT (S)] in nucleotide-binding and other proteins. Protein Eng. 15: 783-798.

Redfield, M.M., Jacobsen, S.J., Burnett Jr., J.C., Mahoney, D.W., Bailey, K.R., & R.J. Rodeheffer. 2003. Burden of systolic and diastolic ventricular dysfunction in the community: Appreciating the scope of the heart failure epidemic. JAMA, 289: 194-202.

Reeves, M.K., Leigh, B.K. & P.J. England. 1987. The identification of a new cyclic neuclotide phosphodiesterase activity in human and guinea-pig cardiac ventricle. Biochem J 241: 535-541.

Reiter, E. & R.J. Lefkowitz. 2006. GRKs and β-arrestins: roles in receptor silencing, trafficking and signaling. Trends in endocrinology and metabolism 17(4): 159-165.

Rena, G., F. Begg, A. Ross, C. MacKenzie, I. McPhee, L. Campbell, E. Huston, M. Sullivan & M. D. Houslay. 2001. Molecular cloning, genomic positioning, promoter identification, and characterization of the novel cyclic amp-specific phosphodiesterase PDE4A10. Mol Pharmacol 59(5): 996-1011.

Richter, W., Jin, J.L.C., & M. Conti. 2005. Splice variants of the cyclic nucleotide phosphodiesterase PDE4D are differentially expressed and regulated in rat tissue. Biochem J 388: 803-811.

Richter, W., Xie, M., Cheitrum, C., Krall, J., Moveseian, M.A. & M. Conti. 2011. Conserved expression and functions of PDE4 in rodent and human heart. Basic Res Cardiol 106: 249-262.

Rischpler, C., Nekolla, S. & Schwaiger, M. 2013. PET and SPECT in Heart Failure. Curr. Cardiol. Rep. 15:1-12.

Rockman, H.A., W.J., Koch, & R.J. Lefkowitz. 2002. Seven transmembrane-spanning receptors and heart function. Nature 415(6868): 206-212.

Roger, V.L., Westson, S.A., Redfield, M.M., et al. 2004. Trends in heart failure incidence and survival in a community-based population. JAMA 292(3):344-350.

Ross, R. 1993. The pathogenesis of atherosclerosis: a perspective for the 1990s. Nature 362: 801-809.

Rubin, C. S. 1994. A kinase anchor proteins and the intracellular targeting of signals carried by cAMP. Biochim. Biophys. Acta 1224, 467-479.

Said M., Mundina-Weilenmann C., Vittone L., Mattiazzi A. 2002. The relative relevance of phosphorylation of the Thr(17) residue of phospholamban is different at different levels of beta-adrenergic stimulation. Pflugers Arch Sep;444(6):801–809.

Sanchez- Mas, J., Lax, A., Asensio- Lopez, M. C., Palacio, F. D., Caballero, L., Santarelli, G., ... & Pascual- Figal, D. A. 2014. Modulation of IL-33/ST2 system in post-infarction heart failure: correlation with cardiac remodeling markers. European journal of clinical investigation 44(7):643-51.

Sassone-Corsi P. 1988. Cyclic AMP induction of early adenovirus promoters involves sequences required for E1A trans-activation. Proc Natl Acad Sci USA 85, 7192–7196.

Saraiva RM, Kanashiro RM, Antonio EL, Campos Fo O, Tucci PJF, Moisés VA. 2007. Rats with high left ventricular end-diastolic pressure can be identified by Doppler echocardiography one week after myocardial infarction. Braz J Med Biol Res. 40 (11): 1557-65.

Sauls, J.L. & T. Rone. 2005. Emerging trends in the management of heart failure: beta blocker therapy. Nurs Clin N Am. 40:135-148.

Schlaich, M.P., Kaye, D.M., Lambert, E., Sommerville, M., Socratous, F. & M.D. Esler. 2003. Relation between cardiac sympathetic activity and hypertensive left ventricular hypertrophy. Circulation 108: 560-565.

Schwaiger, M., Hutchins, G.D., Kalff, V., et al. 1991. Evidence for regional catecholamine uptake and storage sites in the transplanted human heart by positron emission tomography. J. Clin. Invest. 87(5):1681-1690.

Senni, M., Tribouilloy, C.M., Rodeheffer, Jacobsen, S.J., Evans, J.M., Bailey, K.R., et al. 1998. Congestive heart failure in the community: A study of all incident cases in Olmsted Count, Minnesota, in 1991. Circulation 98: 2282-2289.

Serrels, B., Sandilands, E. , Serrels, A., Baillie, G., Houslay, M.D., Brunton, V.G., Canel, M., Machesky, L.M., Anderson, K.I., & M.C. Frame. 2010. A complex between FAK, RACK1, and PDE4D5 controls spreading initiation and cancer cell polarity. Current Biology20, no. 12 : 1086-1092.

Sette, C. & Cont, M. 1996. Phosphorylation and activation of a cAMP-specific in the enzyme activation. J. Biol. Chem. 271: 19677-19534.

Sharma, K. & D.A. Kass. 2014. Heart failure with preserved ejection fraction mechanisms, clinical features, and therapies. Circulation research 115(1): 79-96.

Shen, Y. T., Zhang, H., & Vatner, S. F. 1994. Peripheral vascular effects of beta-3 adrenergic receptor stimulation in conscious dogs. The Journal of Pharmacology and Experimental Therapeutics, 268, 466–473.

Shepherd, M., T. McSorley, A. E. Olsen, L. A. Johnston, N. C. Thomson, G. S. Baillie, M.D. Houslay and G. B. Bolger. 2003. Molecular cloning and subcellular distribution of the novel PDE4B4 cAMP-specific phosphodiesterase isoform. Biochem J 370(Pt 2): 429-38.

Shimizu-Albergine M., Rybalkin S.D., Rybalkina I.G., Feil R., Wolfsgruber W., Hofmann F., Beavo J.A. 2003. Individual cerebellar Purkinje cells express different cGMP phosphodiesterases (PDEs): in vivo phosphorylation of cGMP-specific PDE (PDE5) as an indicator of cGMP-dependent protein kinase (PKG) activation. J Neurosci 23: 6452–6459.

Shen, Y. T., Cervoni, P., Claus, T., et al. 1996. Differences in beta3-adrenergic receptor cardiovascular regulation in conscious primates, rats and dogs. The Journal of Pharmacology and Experimental Therapeutics, 278, 1435–1443.

Skeberdis, V. A., Gendviliene, V., Zablockaite, D., et al. 2008. Beta3-adrenergic receptor activation increases human atrial tissue contractility and stimulates the L-type Ca^{2+} current. The Journal of Clinical Investigation, 118, 3219–3227.

Smith, C.J., Huang, R., Sun, D., Ricketts, S., Hoegler, C., Ding, D-Z, et al. 1997. Development of decompensated dilated cardiomyopathy is associated with decreased gene expression and activity of the milrinone-senestive cAMP phosphodiesterase PDE 3A. Circulation 96: 3116-3123.

Snitker, S., I., Macdonald, E., Ravussin & A. Astrup. 2000. The sympathetic nervous system and obesity: role in aetiology and treatment. Obes. Rev. 1:5-15.

Solaro R.J., Rarick H.M. 1998. Troponin and tropomyosin. Proteins that switch on and tune in the activity of cardiac myofilaments. Circ Res.83: 471–480.

Soldering, S.H. & Beavo J.A. 2000. Regulation of cAMP and cGMP signalling: new phosphodiesterases and new functions. Curr. Opin. Cell Biol. 12: 174-179.

Sopory S., Kaur T., Visweswariah S.S. 2004. The cGMP-binding, cGMP-specific phosphodiesterase (PDE5): intestinal cell expression, regulation and role in fluid secretion. Cell Signal 16: 681–692.

Sonnenburg, W.K., S.D. Rybalkin, K.E., Bornfeldt, K.S., Kwak, I.G., Rybalkina, & J.A. Beavo. 1998. Identification, quantitation, and cellular localization of PDE1 calmodulin-stimulated cyclic nucleotide phosphodiesterases. Methods 14(1): 3-19.

Stangherlin, A., & Zaccolo, M. 2012. Phosphodiesterases and subcellular compartmentalized cAMP signaling in the cardiovascular system. American Journal of Physiology-Heart and Circulatory Physiology, 302(2), H379-H390.

Stelzer, J.E., J.R., Patel, & Moss, R.L. 2006. Protein kinase A-mediated acceleration of the stretch activation response in murine skinned myocardium is eliminated by ablation of cMyBP-C. Integrative Physiology 99: 884-890.

Strulovici, B., Cerione, R. A., Kilpatrick, B. F., Caron, M. G. & Lefkowitz, R. J. 1984. Direct demonstration of impaired functionality of a purified desensitized b-adrenergic receptor in a reconstituted system. Science 225, 837–840.

Tang, T., Lai, N. C., Hammond, H. K., Roth, D. M., Yang, Y., Guo, T., & Gao, M. H. 2010. Adenylyl cyclase 6 deletion reduces left ventricular hypertrophy, dilation, dysfunction, and fibrosis in pressure-overloaded female mice. Journal of the American College of Cardiology, 55(14): 1476-1486.

Taylor, S.S., J.A., Buechler, & W. Yonemoto. 1990. cAMP-dependent protein kinase: framework for a diverse family of regulatory enzymes. Annu. Rev. Biochem. 59: 971-1005.

Taylor, S.S., Keshwani, M.M., Steichen, J.M., & A.P. Kornev. 2012. Evolution of the eukaryotic protein kinases as dynamic molecular switches. Philos. Trans. R. Soc. B 367:2517-2528.

Taylor, S.S., Zhang, P., Stiechen, M.M., Keshwani, & A.P. Kornev. 2013. PKA: Lessons learned after twenty years. Biochimica et Biosphysica Acta 1834: 1271-1278.

Tayyabi, E. 2014. Cardiac Tissue Norepinephrine at 3-Weeks Post Ischemia/Reperfusion and 8-Weeks Post-Myocardial Infarction in Rats Measured via Column-Switch HPLC. Honours Thesis. University of Ottawa, Canada.

Thackeray, J. T., Beanlands, R. S., & DaSilva, J. N. 2013. Insulin restores myocardial presynaptic sympathetic neuronal integrity in insulin-resistant diabetic rats. Journal of Nuclear Cardiology, 20(5), 845-856.

Theroux, P., Ross J. Jr., Franklin, D., Covell, J.W., Bloor, C.M. & S. Sasayama. 1977. Regional myocardial function and dimensions early and late after myocardial infarction in the unanesthetized dog. Circ Res 40: 158-165.

Thomas, J.D. 1994. Doppler echocardiography and left ventricular diastolic dysfunction. In: Gasch W.H., LeWinter, M.M., Eds. Left ventricular diastolic dysfunction and heart failure. Philadelphia PA: Lea and Febiger 192-218.

Thomas, A.J., DaSilva, J.N., Lortie, M., Renaud, J.M., Kenk, M., Beanlands, R.S., deKemp, R.A. 2011. PET of (R)-11C-Rolipram binding to phosphodiesterase-4 is reproducible and sensitive to increased norepinephrine in the rat heart. J Nucl Med. 52(2):263-269.

Thompson, W. J., & M. M. Appleman. 1971. Cyclic Nucleotide Phosphodiesterase And Cyclic Amp. Annals of the New York Academy of Sciences 185(1): 36-41.

Thompson W.J. 1994. Cyclic nucleotide phosphodiesterases: pharmacology, biochemistry and function. Pharmacol. Ther. 51: 13-33.

Thorn, S., MacKasey, K., Ismail, B., Renaud, J., Klein, R., Kolajova, M., de Kemp, R., Beanlands, R. & J.N. DaSilva. Coronary Artery Ligation/Reperfusion Induces Increase in Cardiac AT1R Binding Independent of Myocardial Blood Flow. *Unpublished* .

Thum, T. Galuppo, P., Wolf, C., Fiedler, J., Kneitz, S., van Laake, L.W. et al. 2007.Micrornans in the human heart: a clue to fetal gene reprogramming in heart failure. Circulation 116: 258-267.

Thygesen, K., Alpert, J.S., White, H.D., Joint ESC/ACCF/AHA/WHF Task Force for the Redefinition of Myocardial Infarction. 2007. Universal definition of myocardial infarction. J Am Coll Cardiol 50: 2173-2195.

Torphy, T.J. 1998. Phosphodiesterase isozymes: molecular targets for novel antiasthma agents. Am. J. Respir. Crit. Care Med. 157(2): 351-370.

Tavernier, G., Galitzky, J., Bousquet-Melou, A., et al. 1992. The positive chronotropic effect induced by BRL 37344 and CGP 12177, two beta-3 adrenergic agonists, does not involve cardiac beta adrenoceptors but baroreflex mechanisms. The Journal of Pharmacology and Experimental Therapeutics, 263, 1083–1090.

Triposkiadis, F., Karayannis, G., Giamousiz, G., Skoularigis, J., Louridas, G., & Butler, J. 2009. They sympathetic nervous system in heart failure physiology, pathophysiology, and clinical implications. JACC 54: 1747-1762.

Tsai L.L., Shimizu-Albergine M., Beavo J.A. 2011. The high affinity cAMP-specific phosphodiesterase 8B controls steroidogenesis in the mouse adrenal gland. Mol Pharmacol 79: 639–648.

Tucci, P. J. (2011). Pathophysiological characteristics of the post-myocardial infarction heart failure model in rats. Arquivos brasileiros de cardiologia, 96(5), 420-424.

Ungerer, M., Böhm, M., Elce, J. S., Erdmann, E., & Lohse, M. J. 1993. Altered expression of beta-adrenergic receptor kinase and beta 1-adrenergic receptors in the failing human heart. Circulation 87(2), 454-463.

Van der Heyden M.A.G., Wijnhoven T.J.M., Opthof T. 2005. Molecular aspects of adrenergic modulation of cardiac L-type Ca2+ channels. Cardiovasc Res 65:28–39.

Watchel, H.1983. Neurotropic effects of the optical isomers of the selective adenosine cyclic 3',5'-monophosphate phosphodiesterase inhibitor Rolipram in rats in-vivo. J. Pharm. Pharmacol. 35:440-444.

Vasan, R.S., Benjamin, E.J., & D. Levy. 1995. Prevalence , clinical features and prognosis of diastolic heart failure: an epidemiological perspective. JACC 26: 1565-1574.

Vasta V., Shimizu-Albergine M., Beavo J.A. 2006. Modulation of Leydig cell function by cyclic nucleotide phosphodiesterase 8A. Proc Natl Acad Sci U S A, 103, 52.

Verde I., Pahlke G., Salanova M., Zhang G., Wang S., Coletti D., Onuffer J., Jin S.L., Conti M. 2001. Myomegalin is a novel protein of the golgi/centrosome that interacts with a cyclic nucleotide phosphodiesterase. J Biol Chem 276: 11189–11198.

Verghese, M. W., R.T., McConnell, J.M., Kenhard, L. Hamacher. & S.L.C. Jin. 1995. Regulation of distinct cyclic AMP-specific phosphodiesterase (phosphodiesterase type 4) isozymes in human monocytic cells. Mol. Pharmacol. 47: 1164-1171.

Von Euler, U.S. 1946. A specific sympathomimetic ergone in adrenergic nerve fibres (sympathin(and its relations to adrenaline and noradrenaline. Acta Physiol Scand 12: 73-96.

Wachtel, H. 1982. Characteristic behavioural alterations in rats induced by Rolipram and other selective cAMP phosphodiesterases inhibitors. Psychopharmacology 77: 309-314.

Wachtel, H. 1983. Potential antidepressant activity of Rolipram and other selective cyclic adenosine 3′, 5′-monophosphate phosphodiesterase inhibitors.Neuropharmacology, 22(3), 267-272.

Wahl, R.L., Ed. Principles and Practice of PET and PET/CT. 2nd ed. Philadelphia PA: Lippincott Williams & Wilkens 2009. Print.

Walsh D.A . & Van Patten S.M. 1994. Multiple pathway signal transduction by the cAMP-dependent protein kinase. FASEB J 8:1227–1236.

Wehrens X.H., Lehnart S.E., Huang F., et al. 2003. FKBP12.6 deficiency and defective calcium release channel (Ryanodine receptor) function linked to exercise-induced sudden cardiac death. Cell. 113:829–840.

Weishaar, R. E., Cain, M. H., and Bristol, J. A. 1985. A new generation of phosphodiesterase inhibitors: multiple molecular forms of phosphodiesterase and the potential for drug selectivity J. Med. Chem. 28,537–545.

Weishaar, R.E., Kobylarz-Singer, D.C., Steggen, R.P., & H.R. Kaplan. 1987. Subclasses of cyclic AMP-specific phosphodiesterase in left ventricular muscle and their involvement in regulating myocardial contractility. Circ Res 61: 539-547.

Wilden U. 1995. Duration and amplitude of the light-induced cGMP hydrolysis in vertebrate photoreceptors are regulated by multiple phosphorylation of rhodopsin and by arrestin binding. Biochemistry 34:1446–1454.

Williams, S. G., Jackson, M., Cooke, G. A., Barker, D., Patwala, A., Wright, D. J. & Tan, L. B. 2005. How do different indicators of cardiac pump function impact upon the long-term prognosis of patients with chronic heart failure? American heart journal, 150(5): 983e1-983e6.

Willoughby D., Wong W., Schaack J., Scott J.D., Cooper D.M. 2006. An anchored PKA and PDE4 complex regulates subplasmalemmal cAMP dynamics. EMBO J 25: 2051–2061.

Winten-Johansen, J. 2004. Involvement of neutrophils in the pathogenesis of lethal myocardial reperfusion injury. Cardiovasc Res 61:481-497.

Xiang, Y., Naro, F., Zoudilova, M., Jin, S. L. C., Conti, M., & Kobilka, B. 2005. Phosphodiesterase 4D is required for β2 adrenoceptor subtype-specific signaling in cardiac myocytes. Proceedings of the National Academy of Sciences of the United States of America, 102(3), 909-914.

Xiao, R., Ji, X. & Lakatta, E. G. 1995. Functional coupling of the b2-adrenoceptor to a pertussis toxinsensitive G protein in cardiac myocytes. Mol. Pharmacol. 47, 322–329.

Xu, R.X. et al. 2000. Atomic structure of PDE4: insights into phosphodiesterase mechanism and specificity. Science 288: 1822-1825.

Yan, C., J.K., Bentley, W.K. Sonnenburg, & J.A. Beavo. 1994. Differential expression of the 61 kDa and 63 kDa calmodulin-dependent phosphodiesterases in the mouse brain. J. Neurosci 14(3 pt 1): 973-984.

Yarwood S.J., Steele M.R., Scotland G., Houslay M.D., Bolger G.B. 1999. The RACK1 signaling scaffold protein selectively interacts with the cAMP-specific phosphodiesterase PDE4D5 isoform. J Biol Chem 274: 14909–14917.

Yellon, D.M. & D.J. Hausenloy. 2007. Myocardial Reperfusion injury. N. Engl. J. Med. 357(11): 1121-1135.

Yusuf, S., Reddy, S., Ôunpuu, S., & Anand, S. 2001. Global burden of cardiovascular diseases part I: general considerations, the epidemiologic transition, risk factors, and impact of urbanization. Circulation, 104(22), 2746-2753.

Zeller, E., H.J. Stief, B. Pflug & M. Sastre-y-Hernandez. 1984. Results of phase II study of the antidepressant effect of Rolipram. Pharmacopsychiatry 17: 188-190.

Zhang, Y., Ruel, R., Beanlands, R.S.B., deKemp, R.A., Suuronen, E.J. & J.N. DaSilva. 2008. Tracking stem cell therapy in the myocardium: applications of positron emission tomography. Current Pharmaceutical design 14: 3835-3853.

Zhang, D. Y., & Anderson, A. S. 2014. The Sympathetic Nervous System and Heart Failure. Cardiology clinics, 32(1), 33-45.

Zhao,M., Hagler, H. K., & Muntz, K. H. 1996. Regulation of alpha 1-, beta 1-, and beta 2-adrenergic receptors in rat heart by norepinephrine. American Journal of Physiology-Heart and Circulatory Physiology, 271(5), H1762-H1768.

Zhu B, Strada S, & Stevens T. 2005. Cyclic GMP-specific phosphodiesterase 5 regulates growth and apoptosis in pulmonary endothelial cells. Am J Physiol Lung Cell Mol Physiol 289: L196–L206.

Zweier, J.L., Flaherty, J.T., & M.L. Weisfeldt. 1987. Direct measurement of free radical generation following reperfusion of ischemic myocardium. Proceedings of the National Academy of Sciences of the United States of America 84: 1404-1407.

Zweier, J.L. 1988. Measurement of superoxide-derived free radicals in the reperfused heart: evidence for a free radical mechanism of reperfusion injury. J Biol Chem 263:1353-1357.

Zweier, J.L, & Talukder, M.A. 2006. The role of oxidants and free radicals in reperfusion injury. Cardiovascular Res 70: 181-90.